Technical Report No. 183

3674-12-T

UNDERWATER SOUND PROPAGATION IN THE STRAITS OF FLORIDA: THE MIMI EXPERIMENT OF 3 AND 4 FEBRUARY 1965

by

R. Unger
R. Veenkant

Approved by: Theodore G. Birdsall

T. G. Birdsall

for

COOLEY ELECTRONICS LABORATORY

Department of Electrical Engineering
The University of Michigan
Ann Arbor

Contract No. Nonr-1224(36)
Office of Naval Research
Department of the Navy
Washington 25, D. C.

May 1967

ABSTRACT

An experiment was conducted on 3 and 4 February 1965 as a part of the study of underwater sound propagation in the Straits of Florida, called Project MIMI. A special pseudo-random modulation of a 420 Hz carrier was used to probe one-way multipath propagation. The non-modulated carrier was used for continuous-wave analysis. This report describes the experiments and the data processing, and presents the results of these analyses in photographical form.

ACKNOWLEDGMENTS

The work described in this report is the result of cooperative research. The overall project, MIMI, is sponsored by the Acoustics Programs, Code 468 of the Office of Naval Research. It is a joint effort of the Acoustics Group, Institute of Marine Sciences (IMS), The University of Miami, Florida, under the direction of Dr. J. C. Steinberg, and the Stochastic Signal Processing Program of Cooley Electronics Laboratory (CEL), The University of Michigan, under the direction of Dr. T. G. Birdsall. This CEL program also utilizes the talent and facilities of other CEL programs and of the various support offices of The University of Michigan. The authors wish to acknowledge the roles played by so many in this work.

The enthusiastic cooperation and support of the sponsor and of the I. M. S. Acoustics Group, and especially the instrumentation and operation of equipment by the latter, made possible the successful performance of the experiment.

In the development of the data processing system the designs and many helpful suggestions of Mr. J. Daws of the CEL Communications Program, in logic circuitry for the digital recording and playback instrumentation, were gratefully accepted.

An important contribution to the MIMI work was made by Mr. W. Goodale and Mr. B. Lastinger of the Publications Department of The University of Michigan's Willow Run facility in developing a permanent system for processing and duplication of any amount of photographed data.

The earlier work, mainly by Mr. C. V. Kimball, on computer analysis techniques, in particular the complete CW1, MCOR1, and POLAR routines, was used in the design of the total computer program. A small group of students was involved in the development of the processing system. T. Lipps assisted in computer work, N. Hatter built the external circuitry for synchronization of playback system and camera, and together with E. Tury, performed the patient job of photographing the results.

The authors wish to express their gratitude to Mrs. Carol Wray for her patience and work in typing the rough draft and the final copy of this report.

TABLE OF CONTENTS

LIST OF ILLUSTRATIONS

CHAPTER I

Introduction

1.1. General Information

Relationships between variations in sound propagation and variations in environmental factors are under study in the Straits of Florida by means of a fixed sound course off Miami and fixed receiving hydrophones off Bimini, Bahamas. The project, dubbed MIMI, is carried on by members of the Acoustics Group of the Institute of Marine Science of the University of Miami, Florida and the Cooley Electronics Laboratory of the Electrical Engineering Department of The University of Michigan. MIMI is envisioned as a continuing program of measurements of several years' duration. The 43 mile expanse of the Straits affords a variety of sound propagation conditions, in which periodic variation and variations associated with storms and weather changes occur. The repeatability of signal afforded by a fixed system is an important requirement for studying the effect of the varying environment of sound propagation over long periods of time.

The background information on the initial tests and installation of the sound source and environmental factors was reported in the Journal of the Acoustical Society [Ref. 1]. Figures 1 and 2, taken from that article, show the geographic location of the sound projector and the receiving hydrophone and the bottom profile between transmitter and receiving hydrophones. The source projector is at a depth of 24 meters. The maximum depth of the water is approximately 800 meters. The sound velocity decreases monotonely with depth, leading to sharply downward refracting sound propagation. (See Appendix C and Ref. 1) The expected propagation will therefore almost entirely be refracted bottom-reflected mode or surface-reflected bottom-reflected mode.

The carrier frequency of the source is 420 Hz. Continuing measurements of pure sine wave (CW) are demodulated at Bimini in a coherent demodulator, yielding measurements of the received amplitude and phase. Environmental measurements are made at both the transmitting and receiving sites and recorded there. The multipath structure cannot be

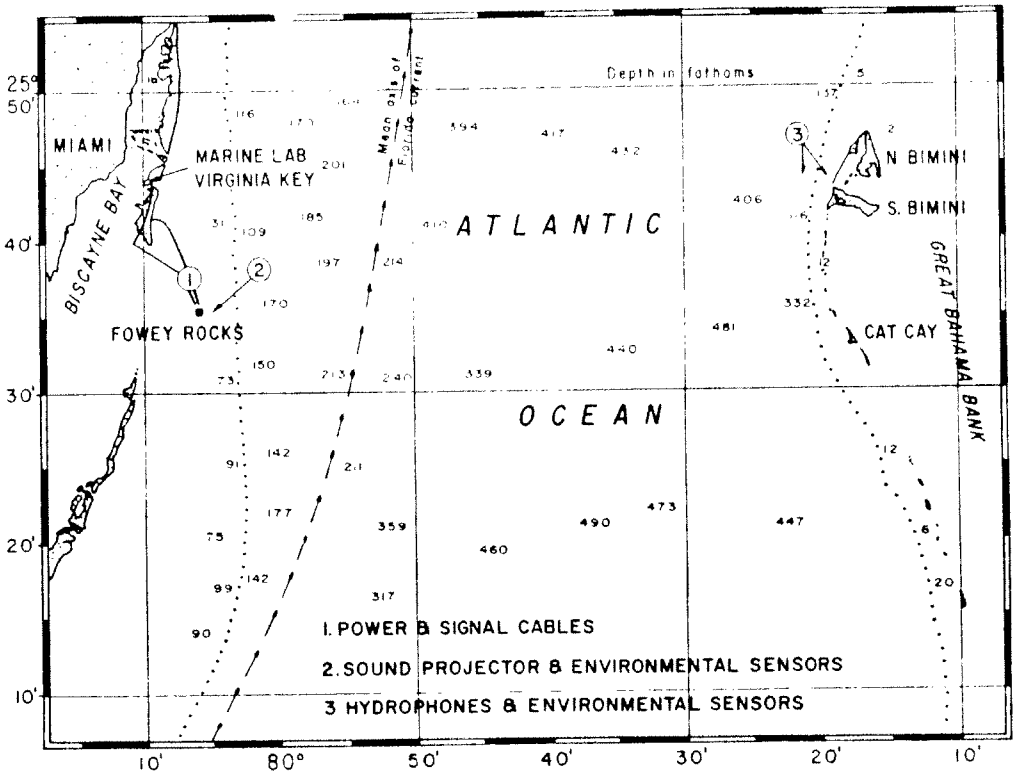

FIG. 1. Straits of Florida, Miami to Bimini.

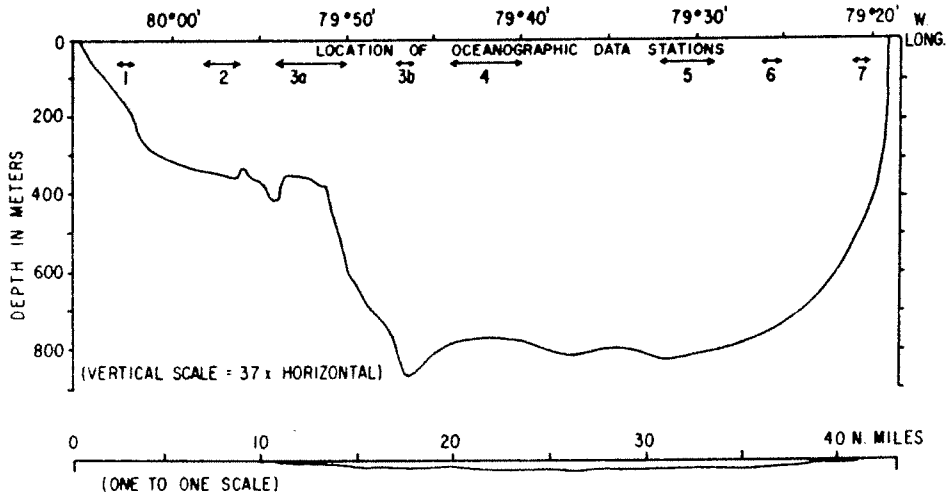

FIG. 2. Bottom profile, Fowey Rocks to Bimini.

resolved by CW transmission; however, the stability of the path structure can be implied by the stability of the resultant CW transmission. The multipath structure is probed by using signals with as sharp a time resolution as is permitted by the 100 Hz bandwidth of the source projector. MIMI uses a pseudo-random sequence modulation to obtain a high average power, sharp autocorrelation signal to probe the multipath structure.

1.2. Purpose of the Experiment

Previous experiments demonstrated that the pseudo-random sequence modulation afforded the expected multipath resolution. These previous experiments included transmission of short bursts of a few periods of the sequence, and signal processing integration times of a single period of the sequence (0.6, 0.9, and 1.2 seconds). The purpose of the experiment of 3 and 4 February 1965 was to investigate the feasibility of longer integration times to obtain higher processing gains, and a cleaner picture of the multipath structure. The transmission used 250 periods of a 1.2 second period sequence, occupying 5 minutes of transmission at intervals over the 2 day period.

During 1965 intensive study was made of one of these 5 minute transmissions. The results of this intensive study were summarized in the article in the Journal of the Acoustical Society [Ref. 1], and at the U. S. Navy Underwater Sound Symposium in November in 1965 [Ref. 2]. As a result of these intensive studies a particular processing procedure was developed and used on all of the receptions. This standardized processing and the resulting analyses are the topic of this present report.

CHAPTER II

Transmission and Reception: MIMI-A to MIMI-B

2.1. Transmission

The control of the source and the modulated signal is at the laboratory of the Acoustics Group, Institute of Marine Sciences, on Virginia Key, Miami, nicknamed MIMI-A. Two types of signal were transmitted during these experiments.

1. A continuous sine wave of 420 Hz, in a 25 seconds on, 5 seconds off mode, which we call CW 25/5.

2. A pseudo-random sequence, double sideband suppressed carrier ("phase flip") modulation of the 420 Hz sine wave carrier, which we call BMSEQ for bi-phase modulated by sequence. One period of BMSEQ consists of 63 digits, each digit containing 8 carrier cycles. A digit is called positive when the signals before and after modulation are in phase and negative when the signals have opposite phase. The duration of one BMSEQ period is exactly 1.2 seconds, one digit is $19\frac{1}{21}$ msec.

Both signals are derived from the Miami 1680 Hz precision oscillator. At intervals of one-half hour to two hours, 5 minutes of BMSEQ transmission replaced the CW 25/5 transmission. The source level referenced to one meter was 103 dbμb during CW transmission with a transducer applied voltage of 1000 volts.

The entire real time operation of the experiment is conducted by the Acoustics Group. CW and environmental data collected and analyzed by the Acoustics Group is not included in this present report.

2.2. Reception

The control, amplification, and filtering of the receptions and control of all auxiliary and recording takes place at the Bimini laboratory, nicknamed MIMI-B. MIMI-B is staffed and operated by the Acoustics Group.

During the experiment reported here, analog recordings of seven or eight minutes' duration were made of the signals received by one deep and one shallow hydrophone. The

deep phone is located in 330 meters of water about two miles west of Bimini, the shallow phone is in 20 meters of water about one mile west of Bimini. The recordings included the 5 minute BMSEQ signal, preceded and terminated with CW 25/5. The first recording contains a calibration tone (CAL) of -15 dbμb in the second part of CW 25/5. CAL is a 420 Hz noise-free sine wave, derived from the MIMI-B 1680 Hz precision oscillator. Both the MIMI-A and the MIMI-B precision oscillators have a stability of about one part in 10^{10} and are checked against each other periodically.

Recordings were made on an Ampex SP300 4-track analog tape recorder, at a speed of 3.75 ips. Channel 1 contained the shallow "A-2" hydrophone, Channel 2 the deep "B-1" hydrophone signal, and Channel 4 the reference 1680 Hz sine wave from the MIMI-B precision oscillator. Channel 3 was not used. Before recording, the hydrophone signals were amplified, and filtered through a fixed bandpass set at 420 ± 50 Hz.

CHAPTER III

The Data Processing System at MIMI-C

The actual demodulation and data processing to obtain an analysis of the multipath propagation is accomplished at the University of Michigan Cooley Electronics Laboratory, nicknamed MIMI-C. In Section 3. 1 a particular data handling technique which is the basis for the coherent signal processing will be explained. In Section 3. 2 the general processing system will be outlined, followed by three sections describing the three major parts of the system; the analog-digital recording system, the computer system, and the final recording system for the results.

3. 1. Coherent Sampling Technique

All of the MIMI phase-coherent signal processing makes use of a reference frequency oscillator whose frequency is precisely four times the carrier frequency of the transmission. This technique is based on some rather elementary theoretical considerations, and has practical implications for both the digital processing, and the analog tape recording. Let us first consider the theoretical use of digital sampling using a reference at four times carrier frequency. We may represent the received bandpass signal, in a band not extending down to DC and about a carrier frequency f_0, as is shown in Eq. 3. 1.

$$r(t) = x(t) \cos 2\pi f_0 t + y(t) \sin 2\pi f_0 t \tag{3. 1}$$

Both x(t) and y(t) will be low pass waveforms. This reception could be equally well represented as shown in Eq. 3. 2.

$$r(t) = R(t) \cos [2\pi f_0 t - \theta(t)] \tag{3. 2}$$

by use of the usual trigonometric identities. x(t) and y(t) are referred to as the Cartesian components of the reception while R(t) and $\theta(t)$ are referred to as the polar coordinates of the reception. The usual Cartesian to polar relations are shown for identification in Fig. 3.

Many readers may be familiar with a caution which is related to Eq. 3. 2, namely, that it applies for a narrow band signal. Indeed, if one wishes to obtain the value of R(t)

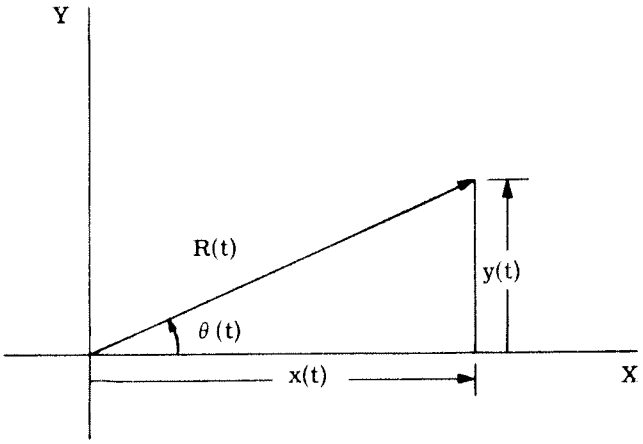

Fig. 3. Cartesian to polar conversion.

by use of a simple rectifier-filter envelope detector the quality of this system will depend upon the relative narrowness of the band of reception of r(t). On the other hand, the representations of Eqs. 3. 1 and 3. 2 are rigorously valid so long as the reception does not extend down to zero frequency.

In the present MIMI receptions the carrier frequency is 420 Hz and the receiving bandwidth is 100 Hz centered around 420 Hz. In the digital processing of the reception the reference frequency of 1680 Hz, four times the carrier frequency, is used to synchronize a sampling circuit. The sampling times are therefore at a spacing of $1/4f_0$ as indicated by Eq. 3. 3.

$$t_k = k/4f_0 \qquad k = 0,\ 1, \ldots \tag{3. 3}$$

Inserting Eq. 3. 3 into Eq. 3. 1, one writes that the sample values of the reception are related to the Cartesian coordinates of the reception in a very simple manner.

$$r(t_k) = x(t_k) \cos\left(k \frac{\pi}{2}\right) + y(t_k) \sin\left(k \frac{\pi}{2}\right) \tag{3. 4}$$

When the sampling time corresponds to an even sample the sine value will be zero and the sample value of the reception will be a sample value of the Cartesian x component. Similarly, the odd numbered samples of the reception will be samples of the Cartesian y component. Since the sign of the trigonometric function alternates, the sampling values will alternate between plus and minus samples of the Cartesian components as shown in Eq. 3. 5.

$$
\begin{aligned}
r(t_k) &= x(t_k) && k = 0,\ 4,\ 8, \ldots \\
r(t_k) &= y(t_k) && k = 1,\ 5,\ 9, \ldots \\
r(t_k) &= -x(t_k) && k = 2,\ 6,\ 10, \ldots \\
r(t_k) &= -y(t_k) && k = 3,\ 7,\ 11, \ldots
\end{aligned}
\tag{3.5}
$$

Use of a sampling technique at four times carrier frequency thus allows one to take alternate samples of the Cartesian coordinates. Since both Cartesian coordinates are not sampled at precisely the same time, corresponding samples of the polar coordinates are not rigorously possible. Now the restriction of a relatively narrow band comes into play. If the band is relatively narrow compared to the carrier frequency, the Cartesian coordinate values will not change significantly between sample values, and local average values of these Cartesian coordinates can be used to determine the polar coordinates, if one so desires. This restriction is not important in the present MIMI processing, which processes the Cartesian components directly and does not operate with the polar coordinate components.

A primary consideration in using analog tape recording in processing real data is the problem of compensation for wow, flutter, and slew in recording. Wow and flutter refer to the nonuniform speed of the tape in the recording and playback processes; slew refers to the differential motion of the various parts of the magnetic tape that pass across the parallel heads of a multihead tape recorder. In the MIMI processing the reference signal, the 1680 Hz signal, is recorded simultaneously with the raw data. Any nonuniform motion, or change of speed of the tapes crossing the head will result in a very minor time-varying gain of the signal recording and playback system. However, sampling time derived from the coherency signal will be aligned with very great accuracy with the sampling time that would have occurred had there been no wow and flutter. The slew problem is not eliminated by the use of the four times carrier reference signal. However, the present MIMI experiments use instrument quality tape recorders with closely spaced heads and quarter-inch tape, minimizing the slew problem.

In order to maintain the proper sampling time, it is necessary that the reference signal be tracked, but it is not necessary that the playback tape speed be the same as the recording tape speed. In practice, the playback speed is higher than the recording speed, to reduce the necessary analysis time.

3. 2. General Processing System

Three major blocks of operations constitute the processing system used in this present experiment. The first block consists of converting the analog recordings to digital recordings that may be used as the computer input. The second major block is the processing which goes on in the IBM 7090 digital computer. The output of this second block is a pair of digital recordings, one with the results of the CW analysis, and the other with the results of the analysis of the BMSEQ processing. The third block consists of the transferral of the results from the digital tapes to a permanent form. At present, this permanent form consists of 35 mm pictures taken from an oscilloscope display of the digital output. Each of these three major blocks will be discussed in the following sections.

3. 3. Analog Recording to Digital Recording

See Figure 4. On the MIMI-C SP 300 the analog tapes are played back at a speed of 4 x 3.75 = 15 ips. The signal from Channel 1 or 2 is attenuated with a calibrated attenuator so that only occasional clipping of high amplitude occurs, filtered in a Kronhite bandpass filter set at 4 x (420 Hz ± 100 Hz) and fed into the A/D converter. In 10-bit A/D conversion the originally bipolar signal is described unipolarly by 1024 levels. In the process a bias of 512 levels, representing the original zero voltage, is added to the signal. The reference signal, now 6720 Hz, synchronizes a phase-lock oscillator which generates a square-wave of 6720 Hz. The square-wave is used as an external sampling clock for the A/D converter and determines the sampling times. Since the clock signal follows

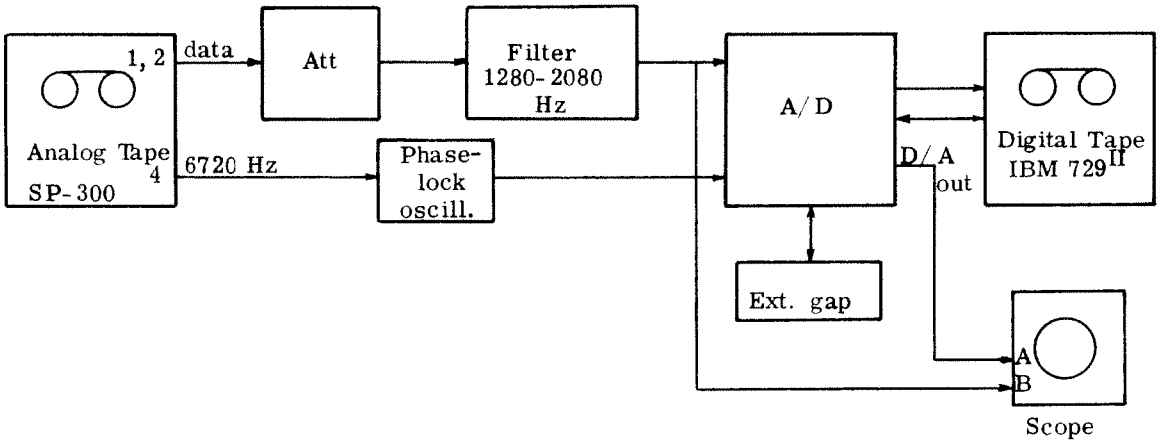

Fig. 4. A-D conversion and digital recording.

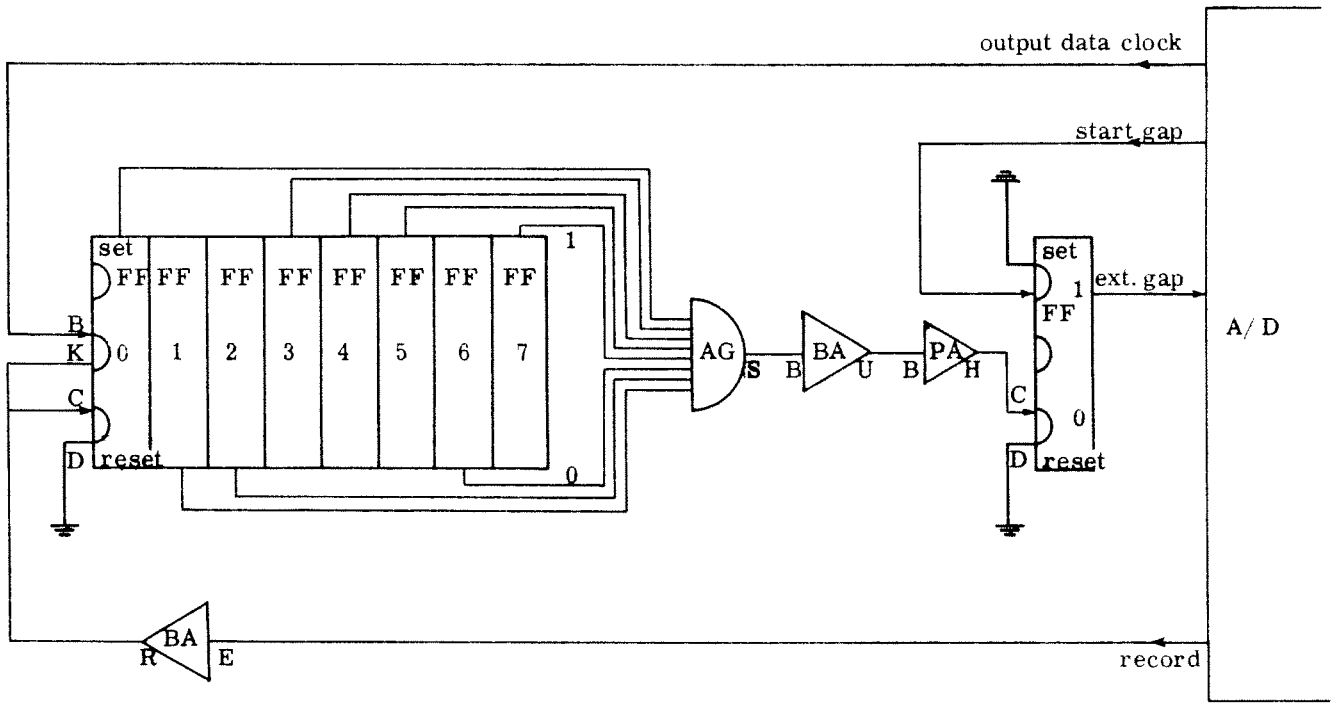

key: FF flip flop
AG AND gate
BA buffer amplifier
PA pulse amplifier

Fig. 5. External record gap timing circuit.

the data, phase-coherent sampling and demodulation of the data is obtained at a rate of four samples per carrier cycle of the transmitted signal.

The digital recordings are made with an IBM 729^{II} digital tape unit, controlled by the Raytheon A/D converter and format generator in low density (L. D.) of 200 bytes per inch. One byte contains 6 binary digits plus parity; each 10-bit sample requires two bytes. The standard L. D. (low density) writing frequency is 15, 000 bytes per second or 7500 10-bit samples per second. The sampling frequency of 6720 Hz is within the permissible range of writing frequencies for L. D. Each 7 - 8 minute portion of data is recorded as a "file" of data. In turn, each file of analog data is split up into digital records. Except for a loss of data in the header and in the record gap between two records each record contains 30 seconds of original recording or 25 1. 2 sec periods. The duration of the record gap is 13. 8 msec (55. 2 msec original analog recording time) determined by an external logical circuit (Fig. 5). This logic causes 186 write pulses, the equivalent of 93 samples, to be omitted in each record. Together with the IBM word (equivalent to 3 samples) taken by the header, a consistent number of 96 samples is omitted from each record. Because of this consistency, phase-coherent processing of all records in one file can be achieved.

Summarizing, one record contains 4 samples per carrier cycle, 8 x 4 = 32 samples per digit, 63 x 32 = 2016 samples per 1. 2 second period and 25 x 2016 - 96 = 50, 304 samples total.

3. 4. Computer Program

Because of the relatively large amounts of data processed, the computer program used on the IBM 7090 consists of a main program, written in the MAD language, which calls UMAP subroutines to perform special functions with high efficiency. The basic flow of processing is outlined below.

1. Complete the demodulation into Cartesian components (CMPRES)
2. Pass each Cartesian "waveform" through a 1. 2 second matched filter to obtain the carrier component (CW1)
3. Convert these Cartesian results to polar form (POLAR)
4. Prepare the results in proper form for the output tape (JR1PAC)

This completes the CW analysis.

5. Form two representative periods from the CMPRES results by means of circulating averaging (CIRAV)

6. Crosscorrelate the representative periods with a stored reference-period of pseudo-random sequence (MCOR1)

7. Convert these Cartesian results into polar form (POLAR)

8. Prepare the results for output tape (JR1PAC)

This completes sequence analysis. These subroutines and the auxiliary subroutine CKBYTE are explained below.

3.4.1. CMPRES. After reading in a record of 16,769 words (16,768 words of data, 3 samples/word, plus the one word header),the program calls the subroutine CMPRES. The function of this subroutine is threefold: (1) to unpack the data from three samples/word to one sample/word, (2) to complete demodulation, and (3) to average the data for a reduction by a factor of four. All three functions are performed simultaneously in the following way. Eight words (three samples/word) are unpacked into a temporary list (one sample/word). Call these unpacked samples T(I) where $1 \leq I \leq 24$. Then six average samples are computed from the 24 in the temporary list.

$$\begin{aligned} S(1) &= T(1) - T(3) + T(5) - T(7) \\ S(2) &= T(2) - T(4) + T(6) - T(8) \\ S(3) &= T(9) - T(11) + T(13) - T(15) \\ &\vdots \\ S(6) &= T(18) - T(20) + T(22) - T(24) \end{aligned} \tag{3.6}$$

The output from this subroutine is a list of 12,576 samples (one per IBM word) which replaces the original list:

$$16,768 \text{ words} \times \frac{3 \text{ samples}}{\text{word}} \times \frac{1 \text{ averaged sample}}{4 \text{ original samples}} = 12,576 \text{ averaged samples or words}$$

Hereafter, these averaged samples will be called samples.

Although it also removes the 512 bias and any other dc level from the signal, the basic purpose of this program is to reduce data storage; it does not improve the signal-to-noise ratio.

3. 4. 2. CW1. The subroutine CW1 processes the list S(1)... S(12, 576). It is a 1. 2 second filter matched to CW, or a crosscorrelation process between m(t), the carrier modulating signal, and the low pass Cartesian modulation components x(t) and y(t) of the received signal r(t). In the case of CW transmission the modulating signal is constant, m(t) = 1. In equation form the desired filter output is

$$\begin{aligned} \phi_x(\tau) &= \int_0^T m(t)\, x(t+\tau)\, dt = \int_0^T x(t+\tau)\, dt \\ \phi_y(\tau) &= \int_0^T m(t)\, y(t+\tau)\, dt = \int_0^T y(t+\tau)\, dt \end{aligned} \tag{3.7}$$

where the integration time T = 1. 2 seconds.

1. 2 seconds of signal is equivalent to 504 data samples, where the Cartesian components appear interlaced; that is, x(n) = S(2n - 1) and y(n) = S(2n). The integrals $\phi_x(\tau)$ and $\phi_y(\tau)$ convert into summations with $\tau = 2P$, P = 0, 1, 2, 3,..., 6035.

$$\begin{aligned} \phi_x(P) &= \sum_{n=1}^{252} S(2n - 1 + 2P) \\ \phi_y(P) &= \sum_{n=1}^{252} S(2n + 2P) \end{aligned} \tag{3.8}$$

CW1 computes these two summations, using a simple differencing technique after an initial summation.

$$\phi_x(0) = \sum_{n=1}^{252} S(2n - 1) \tag{3.9}$$

$$\phi_x(P) = \phi_x(P - 1) + S(503 + 2P) - S(2P - 1), \quad 1 \leq P \leq 6035 \tag{3.10}$$

and similarly

$$\phi_y(0) = \sum_{n=1}^{252} S(2n) \tag{3.11}$$

$$\phi_y(P) = \phi_y(P - 1) + S(504 + 2P) - S(2P), \qquad 1 \leq P \leq 6035 \tag{3.12}$$

The initializing sums require 502 add operations and two stores, while the rest of the processing requires 12, 070 add, subtract and store sequences. On the IBM 7090 this is a total of 122, 712 cycles, including indexing, or . 268 seconds with the 7090 cycle time of 2. 18 μsec.

3. 4. 3. POLAR. The subroutine POLAR converts Cartesian coordinates x and y into polar coordinates R and θ. In this program it is applied to convert the Cartesian correlation results $\phi_x(\tau)$ and $\phi_y(\tau)$ from CW1 and MCOR1 into amplitude and phase values $R(\tau)$ and $\theta(\tau)$. Instead of the conventional process

$$R = (x^2 + y^2)^{\frac{1}{2}}, \quad \theta = \tan^{-1} \frac{y}{x} \tag{3. 13}$$

a faster method was developed using linear equations to approximate R and θ, with a modest sacrifice in accuracy. The usual conversion of Eq. 3. 13 is based on a circle. One may view the approximation by linear segments geometrically as replacing the circle by an octagon. This geometric relation is illustrated in Fig. 6. The maximum percentage error in R of this approximation is less than four degrees. The errors are known in each, and a correction could be applied if necessary. For present purposes, however, the non-corrected approximation is sufficiently accurate.

The chords C_i, i = 1, 2, . . . , 8 of the octagon are described by equations of the form

$$\begin{aligned} y &= \pm mx \pm R, \text{ in octant 2, 3, 6, or 7, or } |x| \leq |y| \\ x &= \pm my \pm R, \text{ in octant 1, 4, 5, or 8, or } |y| \leq |x| \end{aligned} \tag{3. 14}$$

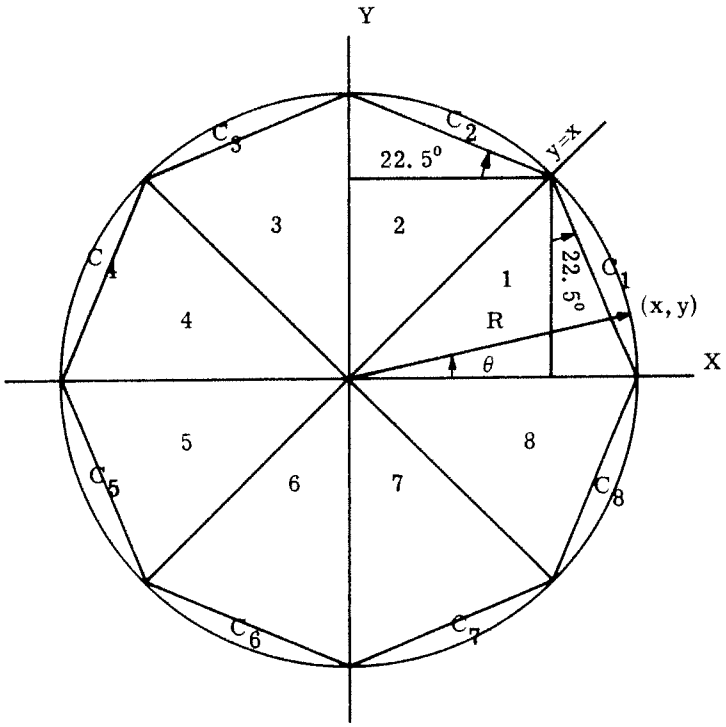

Fig. 6. POLAR: approximation of R, θ.

where $m = \tan 22.5^{\circ} = .4142$ and in which the signs depend upon the octant concerned. From these equations the R value can be derived:

$$\begin{aligned} R &= \pm\, y \mp mx \qquad |x| \leq |y| \\ R &= \pm\, x \mp my \qquad |y| \leq |x| \end{aligned} \tag{3.15}$$

By applying the equations in each octant, the minus signs in the equations will be compensated by the minus signs of x or y in the octant concerned, so that

$$\begin{aligned} R &= |y| + m|x| \qquad |x| \leq |y| \\ R &= |x| + m|y| \qquad |y| \leq |x| \end{aligned} \tag{3.16}$$

The maximum percentage error for R in this case, occurring whenever $\theta = 22.5^{\circ} \pm n\,45^{\circ}$, is (see Fig. 7)

$$\epsilon_{R_{max}} = 1 - \cos 22.5^{\circ} = .0761 \tag{3.17}$$

By shifting the chords outwards over the distance $R\epsilon_{R_{max}}(c_i - c_i')$, this error can be halved. The R value then becomes

$$\begin{aligned} R &= .9582\,|y| + .3971\,|x|, \quad |x| \leq |y| \\ R &= .9582\,|x| + .3971\,|y|, \quad |y| \leq |x| \end{aligned} \tag{3.18}$$

The phase angle θ is approximated by linearization of the curves $\tan^{-1}\frac{y}{x}$ and $\tan^{-1}\frac{x}{y}$ in the interval $-45^{\circ} \leq \tan^{-1}\frac{y}{x} \leq 45^{\circ}$ and $-45^{\circ} \leq \tan^{-1}\frac{x}{y} \leq +45^{\circ}$, see Fig. 8. The θ value in degrees then is found from one of the equations

$$\theta = \pm(90 - 45\,\tfrac{x}{y}), \qquad \theta = 45\,\tfrac{x}{y}, \quad \text{or} \quad \theta = \pm(180 + 45\,\tfrac{y}{x}) \tag{3.19}$$

according to the octant in which (x, y) is contained. The phase angle is expressed in values between -180° and $+180^{\circ}$. The correction curve is shown in Fig. 9.

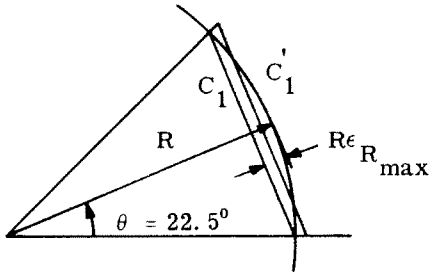

Fig. 7. Error in R.

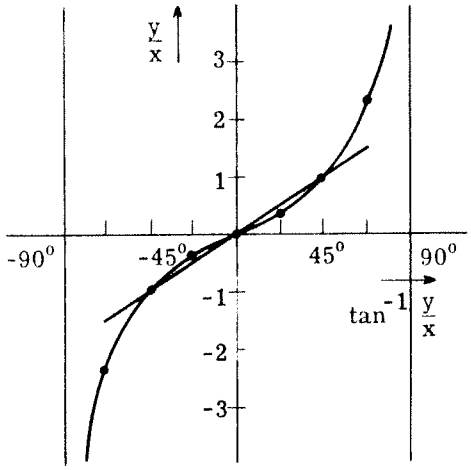

Fig. 8. Linearisation of $\tan^{-1}\frac{y}{x}$ in the interval $-45^{\circ} \leq \tan^{-1}\frac{y}{x} \leq 45^{\circ}$.

In a modification of MAD the basic program is as follows.

```
WHENEVER |X|.<. |Y|
   θ=Y. SM. 90-(45*X)/ Y
   R=(9582*|Y|+3971*|X|)/ 10,000
OTHERWISE
   R=(9582*|X|+3971*|Y|)/ 10,000
   WHENEVER X. ≥.0
   θ=(45*Y)/ X
   OTHERWISE
   θ=Y. SM. 180+(45*Y)/ X
END OF CONDITIONAL
```

where the instruction . SM. in C = A. SM. B denotes that C has the sign of A, magnitude of B, or

$$C = \frac{A}{|A|} * |B| \tag{3.20}$$

3.4.4. JR1PAC. Before the R, θ results are written onto tape, the R values are scaled down so that $R < 2^{10}$ (10-bit mode for D/A conversion), a bias of 512_{10} is added to θ (unipolar playback system), and R's and θ's are packed 3/IBM word into separate lists by JR1PAC. In the processing of the files III, IV, V and VI, the scaling factor, 2^{RS}, RS = number of right shifts, is determined by the magnitude of the correlation results. In order to make the outputs comparable in magnitude, a constant scaling factor of 2^{10} was used for

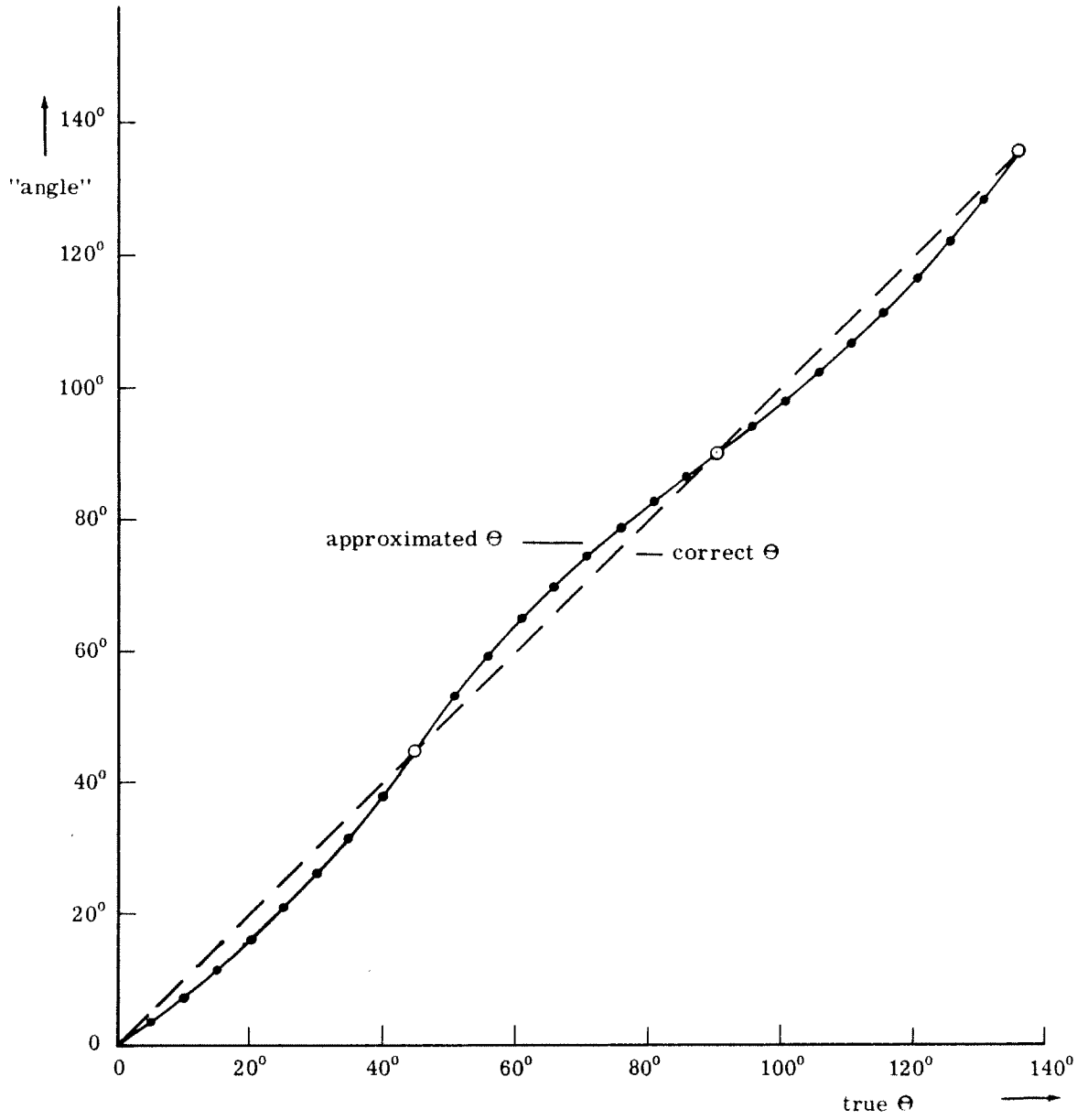

Fig. 9. Phase-angle correction curve.

the processing of all other files.

3.4.5. CIRAV. Before the CMPRES results are destroyed by CW analysis they are prepared for sequence analysis by a circulating average routine, CIRAV. The first 28.8 sec (24 periods of sequence) of the data is split into two groups of 12 periods each. The last partial period, shortened by the record-gap and header, is omitted in the sequence analysis. Each of these 12 period sections is averaged to give one resultant representative

period. Since there are 504 samples/period after CMPRES, the circulating average looks like the following in equation form

$$L(I) = \sum_{J=0}^{11} S(I + 504 * J), \qquad 1 \leq I \leq 504 \tag{3.21}$$

This routine returns two representative periods to be used in sequence analysis.

3.4.6. Sequence Analysis. After the CW1 R and θ are written onto tape, sequence analysis of the CIRAV output begins. Each representative period, CIRAV output L(I), ... L(504), is duplicated after itself in core,

$$L(I + 504) = L(I), \quad 1 \leq I \leq 504 \tag{3.22}$$

The list becomes 1008 entries long to facilitate more efficeint correlation of the entire 504 original entries.

MCOR1 performs the correlations (sequence matched filter)

$$\begin{aligned} \phi_x(\tau) &= \int_0^T m(t)\, x(t + \tau)\, dt \\ \phi_y(\tau) &= \int_0^T m(t)\, y(t + \tau)\, dt \end{aligned} \tag{3.23}$$

where m(t) is the stored version of the sequence modulation and T = 1.2 sec., the duration of one period of pseudo-random sequence. These two integrals are computed simultaneously as discrete summations, using interlaced lists:

$$\begin{aligned} \phi_x(P) &= \sum_{n=1}^{252} M(2n - 1)\, L(2n - 1 + 2P) \\ \phi_y(P) &= \sum_{n=1}^{252} M(2n)\, L(2n + 2P) \end{aligned} \tag{3.24}$$

where 2P digits replace the time displacement τ,

$$P = 0,\ 1,\ 2,\ 3, \ldots,\ 251$$

The subscripts in n replace the variable t and refer to addresses in the 1008 entry list.

For purposes of computation speed, MCOR1 does not perform the above summations directly. A shortcut using partial sums is applied. Since the duration of one value of m(t), or 1 digit, equals the duration of four pairs of x and y values, we can proceed as follows.

The summation index n is replaced by a double index I, J;

$$n = 4J - I, \qquad 0 \leq I \leq 3, \qquad 1 \leq J \leq 63 \tag{3.25}$$

which cover the range $1 < n < 252$. As M is constant for blocks of four pairs of samples the values

and

$$\begin{aligned} M(2n - 1) &= M(8J - 2I - 1) \\ M(2n) &= M(8J - 2I) \end{aligned} \tag{3.26}$$

do not change while incrementing I. Thus, in double index summation, M depends only on J. The correlations can now be written as

$$\begin{aligned} \phi_x(P) &= \sum_{I=0}^{3} \sum_{J=1}^{63} M(8J)\ L(8J - 2I - 1 + 2P) \\ \phi_y(P) &= \sum_{I=0}^{3} \sum_{J=1}^{63} M(8J)\ L(8J - 2I + 2P) \end{aligned} \tag{3.27}$$

From these equations it can be seen that incrementing P is equivalent to decrementing I. Therefore, using partial sums

$$S(K) = \sum_{J=1}^{63} M(8J)\ L(8J + K) \qquad -7 \leq K \leq 504 \tag{3.28}$$

each result of S(K) for $1 \leq K \leq 504$ can be used four times in the computation of $\phi_x(P)$ or $\phi_y(P)$:

$$\begin{aligned} \phi_x(P) &= \sum_{I=0}^{3} S(2P - 2I - 1) \\ \phi_y(P) &= \sum_{I=0}^{3} S(2P - 2I), \qquad 0 \leq P \leq 251 \end{aligned} \tag{3.29}$$

To bypass the relatively slow process of multiplication in these summations, a stored set of 32 ADD and 31 SUBTRACT instructions represents the 63 digit bi-phase sequence modulation M. ADD corresponds to multiplication by +1 (positive digit), SUBTRACT to multiplication by -1 (negative digit).

In principle MCOR1 has to perform 504 summations per increment P. With 2 x 252 increments the total number of summations would be $2 \times 252^2 = 127,008$. By using each of the 512 partial sums four times, the actual total number of summations performed in MCOR1 is

$$63 \times 512 + 252 \times 4 \times 2 = 34,\ 280$$

The Cartesian results from MCOR1 are converted to polar values R and θ by again calling the subroutine POLAR. The subroutine JR1PAC is used again for scaling and preparation for tape-writing.

3.4.7. CKBYTE. In Section 3.3 it was noted that the standard low density writing frequency is 7500 10-bit samples/second. However, in using the external clock, the writing frequency is 6720 samples/second. This frequency is permissible although it sometimes causes difficulty in reading the tape into the computer. The slower writing rate leaves more space between bytes on the tape than the normal rate. From several observations it was noted that the majority of reading errors were erroneously inserted bytes caused by anomalies between written bytes being read as true bytes. Each sample of data consists of two bytes, a high order byte, and a low order byte; a byte error then will result in misinterpretation of this ordering, thus completely destroying the data values from the point of error to the end of the record.

It was also discovered that this added byte usually contained only one one bit and five zeros. Our 10-bit samples use two 6 bit bytes with two unused bits in every other byte. Therefore any disruption in this format, 0 0 X X X X, X X X X X X, can be easily detected. Using the above information (added bytes, a single one bit in an added byte, and the 0 0 X X X X, X X X X X X format) a program called "check byte" (CKBYTE) was written to check the data and to correct it if necessary. The routine is called only if the computer detects a parity error while reading a record.

3.5. Playback System

(See Fig. 10). The CW and SEQ output tapes written by the computer are played back on the IBM 729^{II}, and the digital values converted to analog levels in 10-bit mode. The D/A output is connected to the dual trace of a Tektronix 545A oscilloscope (P-2 tube), set in "alternate" mode. Using the record gaps as an external triggering the R records are then displayed through Channel 1 and the θ records through Channel 2 of the oscilloscope.

The HD (high density) CW output tape contains 6036 values per record; the playback frequency is 20850 samples per second. Thus the sweep duration of one record is 294.4 ms. The LD (low density) SEQ tape contains 252 values per record, which with a playback frequency of 7500 samples/second results in a sweep duration of 33.6 ms. To avoid the influence of the two percent byte position jitter in the computer written records, an external digital time base

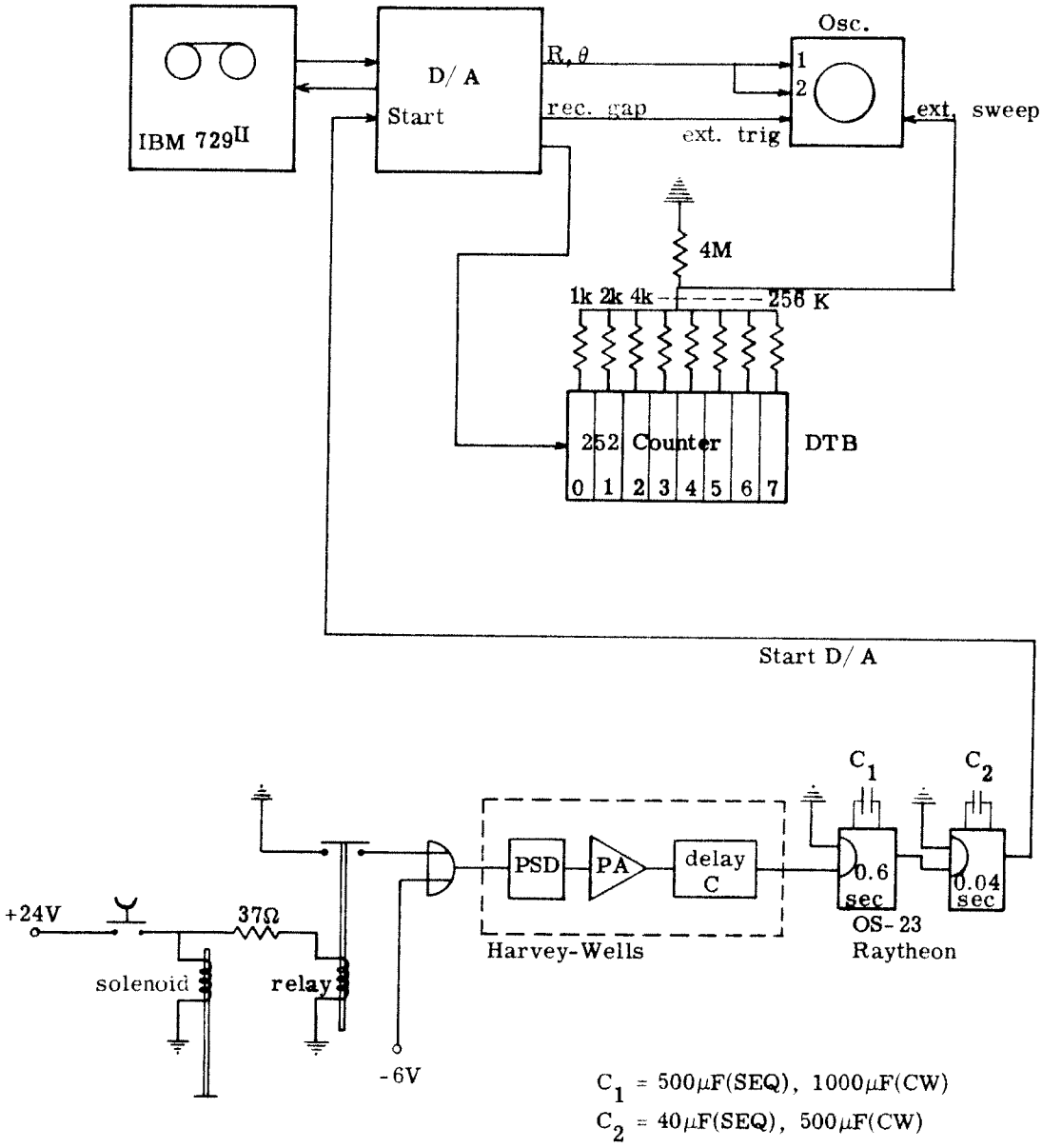

Fig. 10. Play-back system.

(DTB) is utilized.[1] The DTB generator uses the playback clock pulse from the D/A converter as an input to a 252 digit counter built from Harvey Wells logics. The outputs of the seven stages are fed into a resistor summing circuit, which results in a 252 level staircase voltage. For alternating the dual trace channels, the internal time base set for a 33.6 msec sweep and triggered externally by the record gap has to be used in combination with the external sweep. CW records are displayed using the internal time-base in combination with the external triggering by the record gaps.

The images are photographed with a Fairchild 35 mm oscilloscope camera, solenoid activated and using a dichroic mirror for simultaneous recording of written data. One frame normally contains one R record and one θ record; some sequence pictures however are multiple (composite) exposures of several records, showing consistency of amplitude and phase pattern. The settings used are f5.6, 1/4 sec for SEQ single exposures; f16, "B" for SEQ composite exposures, and f11, "B" for CW, using Kodak Panatomic X film. The solenoid switch also causes the triggering of the D/A converter for playback of one R, θ record pair utilizing Harvey Wells and Raytheon logics.

[1] Designed by J. Daws, Cooley Electronics Laboratory.

CHAPTER IV

Mathematical Analysis of the Computer Program

In this chapter the mathematical background and physical significance of the computer program are analyzed. In the first section it is shown that the continuous-wave analysis, CW1, and the sequence analysis, the combination of CIRAV and MCOR1, are equivalent to filters matched to the transmitted modulations of the 420 Hz carrier.

The second section illustrates the correlation techniques used in sequence analysis and its significance for detection of multipath sound arrivals.

The third section describes the validity of the applied sampling and demodulation method and emphasizes the fact that this method yields both the amplitude and the phase information. Therefore, filtering the demodulated received signal at d. c., matched to the transmitted modulation, is equivalent to filtering the non-demodulated received signal at carrier frequency, matched to the modulated transmission. Filter characteristics or transfer functions are derived for the routines CMPRES, CW1, and CIRAV, by Fourier transformation of their similar (digital) impulse response. The magnitude of the MCOR1 transfer function is found by Fourier transformation of a single sequence pulse. Because of the applied method of digital demodulation, the frequency band centered around the carrier frequency may be transferred to a band around d. c. Thus the derived transfer functions concerning the processing after CMPRES apply to the low pass components of the received signal.

Finally, Section 4. 4 is dedicated to the processing gain obtained, for matched filtering being the 2WT product.

4. 1. Matched Filters

In a linear system the time response of a filter to its input is given by the convolution integral

$$\phi(\tau) = h(\tau) * g(\tau) = \int_{-\infty}^{\infty} h(\lambda)\, g(\tau - \lambda)\, d\lambda \qquad (4.1)$$

where

$h(\tau)$ = impulse response of the filter

$g(\tau)$ = filter input

$\phi(\tau)$ = filter output

A filter matched to a given waveform has as its impulse response the time-reversal of that waveform, suitably delayed to allow the filter to be realizible. To match to a waveform, $m(\tau)$, with duration T, let the impulse response be

$$\begin{aligned} h(\lambda) &= m(T - \lambda) && 0 < \lambda < T \\ &= 0 && \text{otherwise} \end{aligned} \tag{4.2}$$

The filter output is determined by substituting Eq. 4.2 into Eq. 4.1

$$\phi(\tau) = \int_0^T m(T - \lambda)\, g(\tau - \lambda)\, d\lambda \tag{4.3}$$

The substitution $t = T - \lambda$ yields

$$\phi(\tau) = \int_0^T m(t)\, g(t - T + \tau) dt \tag{4.4}$$

or

$$\phi(\tau + T) = \int_0^T m(t)\, g(t + \tau) dt \tag{4.5}$$

Thus the output of the matched filter is the correlation between the given waveform m(t) and the most recent T seconds of the filter input, g(t). This result was to be expected since two folding back operations in time are involved in this process, one because of the convolution, and one because of the matched filter.

In our processing system of CW and SEQ analysis the waveform to be matched is the transmitted modulation m(t) of the 420 Hz carrier. In CW transmission the modulation is constant, $m(t) = 1$; the duration is $T = 1.2$ sec. Therefore, with Eq. 4.4 our CW 1.2 sec matched filter output is

$$\phi(\tau) = \int_0^{1.2} g(t - 1.2 + \tau)\, dt \tag{4.6}$$

The integral is computed as a discrete summation in the program CW1, see Section 3.4.2. Since the filter has to be "loaded" with one period T of data, it shows a 1.2 sec ramp step-response, see Fig. 11. The time-shifting process in this correlation is illustrated in Fig. 12.

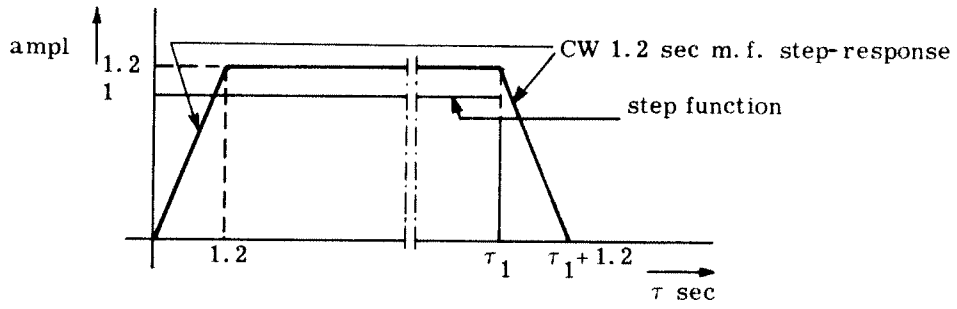

Fig. 11. Step function response of CW 1.2 sec. matched filter.

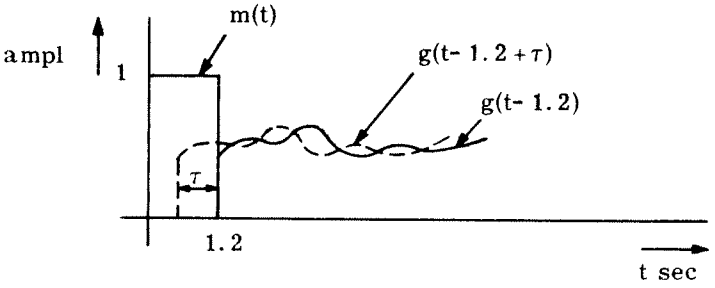

Fig. 12. Illustration of time displacement in CW analysis.

In sequence analysis the waveform to be matched is the bi-phase pseudo-random sequence modulation with period 1.2 sec. In our processing the duration of m(t) was chosen as 12 periods of sequence, T = 14.4 sec. According to Eq. 4.5 the correlation to be performed then is

$$\phi(\tau + 14.4) = \int_0^{14.4} m(t)\, f(t + \tau)\, dt \qquad (4.7)$$

or, because of the periodicity of m(t)

$$\phi(\tau + 14.4) = \int_0^{1.2} m(t) \sum_{n=0}^{11} g(t + n\,1.2 + \tau)\, dt \qquad (4.8)$$

Substituting

$$G(t) = \sum_{n=0}^{11} g(t + n1.2), \qquad 0 < t \leq 1.2 \text{ sec} \qquad (4.9)$$

in Eq. 4. 8 yields

$$\phi(\tau + 14.4) = \int_0^{1.2} m(t)\, G(t + \tau)\, dt \qquad (4.10)$$

The summation of Eq. 4. 9 is performed in the subroutine CIRAV (section 3. 4. 5) in digital form, resulting in a representative 1. 2 sec period G(t) consisting of 252 Cartesian digit pairs. This data G(t) is duplicated to form a 2-period list:

$$G(t + 1.2) = G(t) \quad , \quad 0 \leq t < 1.2 \text{ sec} \qquad (4.11)$$

whereafter the subroutine MCOR1 performs the correlation in Eq. 4. 10 in digital form. Figure 13 illustrates the time displacements involved.

4. 2. Significance of the Correlation in Sequence Analysis

For graphical interpretation of the correlation used in sequence analysis let us assume the transmitted signal to be a simple periodic pulse function s(t) with pulse height = 1, pulse width = b, and with period = T. See Fig. 14. Let us assume further that the received signal r(t) is identical to the transmitted signal except for a time-delay d in the signal arrival.

$$r(t) = s(t - d) \qquad (4.12)$$

To perform the correlation

$$\phi(\tau) = \int_0^T s(t)\, r(t + \tau)\, dt \qquad (4.13)$$

we have to displace the received signal over a time τ, multiply the corresponding instantaneous values of s(t) and r(t + τ) and integrate the obtained products over a period T. For each displacement τ, $0 \leq \tau \leq T$, a new value of $\phi(\tau)$ is found. The result of this correlation

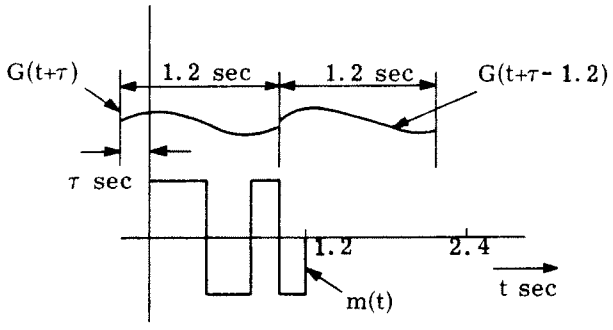

Fig. 13. Illustration of time displacements in sequence analysis.

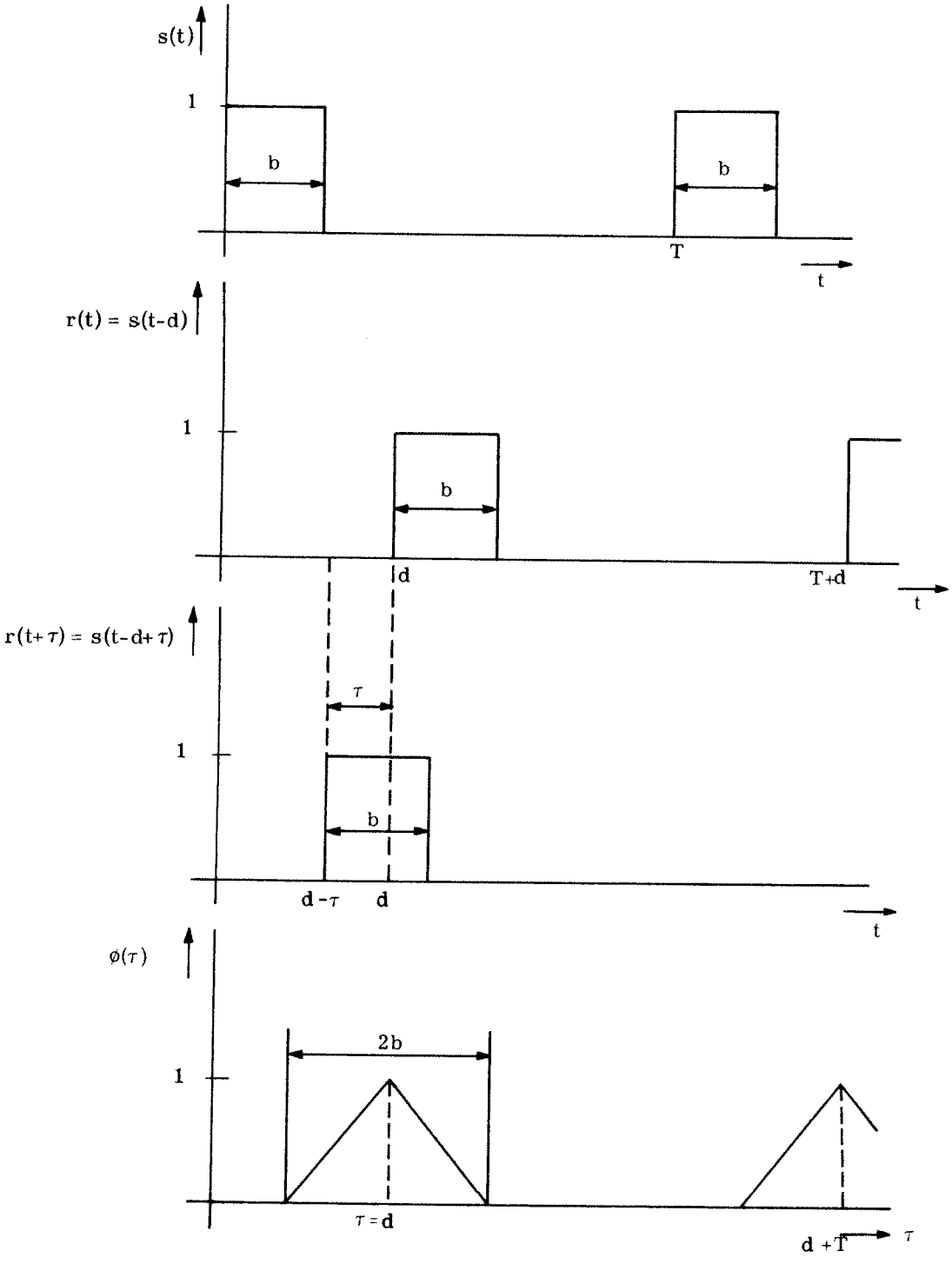

Fig. 14. Correlation of single-pulse signals.

is a "triangular peak" with base = 2b and its peak occurring at τ = d; that is, when the transmitted signal and the displaced received signal coincide. Outside the interval $d - b \leq \tau \leq d + b$ the correlation function equals zero, $\phi(\tau) = 0$.

The correlation of pseudo-random sequences yields a similar result. To illustrate this, let us correlate a seven digit "maximal" sequence "transmission" and its delayed "arrival" at reception; the sequence consists of four +1 digits and three -1 digits. The "transmitted" and displaced "received" signals are as follows:

+ + + - - + -	s(t), "transmitted" sequence
- - + - + + +	r(t), "received" sequence with 4-digit delay, $\tau = 0$
- + - + + + -	r(t + 1), r(t) displaced over τ = 1 digit
+ - + + + - -	r(t + 2) , r(t) displaced over τ = 2 digits

To compute the correlation function we count the number of algebraic agreements between s(t) and r(t + τ) and subtract the number of algebraic disagreements, after each displacement τ = 1 digit. Thus we obtain

$$\phi(4) = +7$$

$$\phi(0) = \phi(1) = \phi(2) = \phi(3) = \phi(5) = \phi(6) = -1$$

See Fig. 15. When all digits of s(t) and r(t + τ) coincide, i. e., when the time displacement equals the time delay, τ = d = 4 digits, the triangular peak occurs. The maximum equals the sequence duration or length L digits, $\phi(\tau)_{max}$ = L. Thus the occurrence of the peak indicates the time delay of the received signal. Outside the arrival interval $\tau = d \pm b$, which as in the case of the simple pulse, is two digits wide, the correlation function has the value -1.

The [6, 5, 0] sequence applied in our experiments has a duration L = 63 digits and consists of 32 plus ones and 31 minus ones. A single-path, non-attenuated signal arrival would result in a peak height of $\phi(\tau)_{max}$ = +63 occuring when τ equals the delay d of the signal arrival.

In our processing system we obtain four Cartesian sample pairs per digit of 8

carrier cycles after CMPRES. Separate x and y correlation each using 252 digital displacements ($0 \leq \tau < T$) are performed on this data and the results converted into polar coordinates, $R(\tau)$, $\theta(\tau)$. Thus a single arrival peak in $\phi_x(\tau)$, $\phi_y(\tau)$, $R(\tau)$, consists of 8 samples, 4 upslope and 4 downslope. Since $R(\tau)$ is expressed as a magnitude

$$R(\tau) = |\phi(\tau)| \tag{4.14}$$

the function will be positive and equals zero at the skirts of the peak. As both $\phi_x(\tau)$ and $\phi_y(\tau)$ increase and decrease linearly in their correlation peak, in general with different slopes,

$$\phi_x(\tau) = m_1\tau \quad , \quad \phi_y(\tau) = m_2\tau \tag{4.15}$$

the peak angle

$$\theta(\tau)_{\text{peak}} = \tan^{-1}\frac{\phi_y(\tau)}{\phi_x(\tau)} = \tan^{-1}\frac{m_2}{m_1} \tag{4.16}$$

is constant during the entire triangular peak. Since also $\phi_x(\tau)$ and $\phi_y(\tau)$ have constant values outside the peak interval, there $\theta(\tau)$ will also be constant, although different from $\theta(\tau)_{\text{peak}}$ However, the amount of signal power present outside the peak interval is only $(\frac{1}{63})^2$ times the power at $R(\tau)_{\max}$ and the values of $R(\tau)$ and $\theta(\tau)$ can be easily destroyed by noise, yielding a random phase-pattern outside the peak interval.

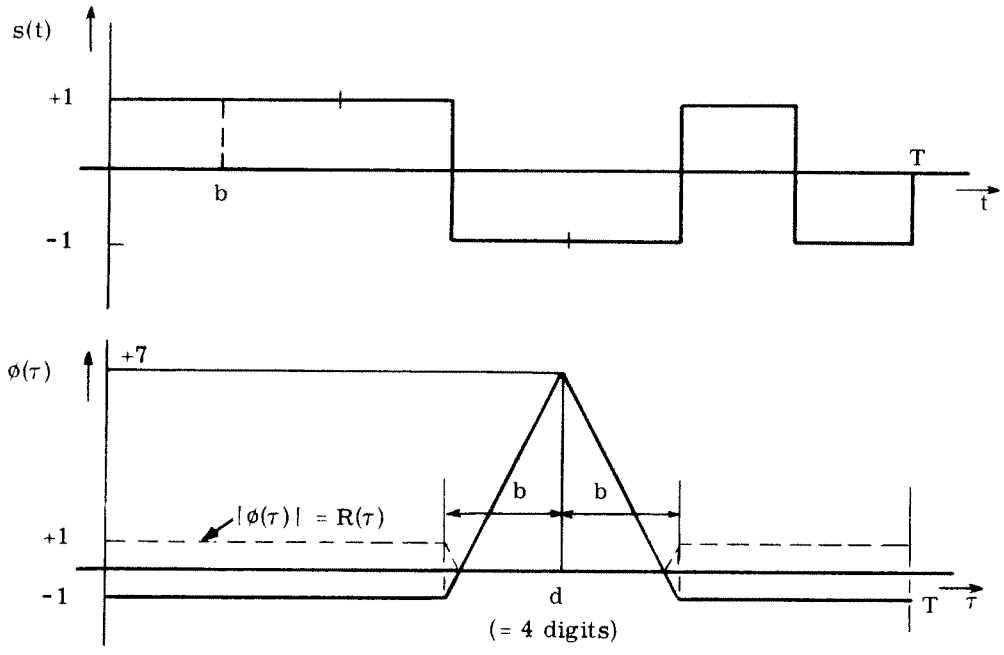

Fig. 15. Correlation of 7-digit sequences.

4.3. Demodulation and Filter Characteristics

4.3.1. Demodulation, CMPRES. The waveforms subject to processing are the output of an analog filter of nominal bandpass 370 Hz to 470 Hz with 18 db/octave skirts outside this band. The sampling with a frequency of 1680 Hz adequately describes any waveform bandlimited (from d. c. to) 840 Hz. The only possible error in the representation of the analog waveform therefore comes from whatever small amount of energy passing the analog filter in frequencies higher than 840 Hz. We will proceed without regard to this energy.

Using the phase-coherent sampling technique as described in Section 3. 1, we obtain the lowpass Cartesian components x(t), y(t) of the filtered received signal. By processing the x and y data separately all phase information is being preserved and is expressed as the phase angle $\theta(\tau)$ at the end of the processing procedure.

The program CMPRES completes the digital demodulation by averaging blocks of four x or four y samples and thus smooths out the effect of the difference in sampling time of x and y samples. In this averaging process it compensates for the sign changes due to the 180° phase difference between subsequent x or subsequent y samples in a carrier cycle. Taking a block of 4 samples for one of the coordinates can be described as a digital filter with impulse response

$$h(t) = \sum_{n=0}^{3} (-1)^n \delta(t - nT), \quad 0 \leq t \leq 4T \tag{4.17}$$

where $T = \frac{1}{840}$ sec, the time-difference between samples for one coordinate. See Fig. 16.

To obtain the frequency characteristic, we Fourier transform Eq. 4.17 into the frequency domain:

$$H(\omega) = \int_0^{4T} \sum_{n=0}^{3} (-1)^n \delta(t - nT)\, e^{-j\omega t} dt \tag{4.18}$$

or

$$H(\omega) = \sum_{n=0}^{3} (-1)^n e^{-jn\omega T}$$

$$= \sum_{n=0}^{3} (-e^{-j\omega T})^n \tag{4.19}$$

Using the algebraic identity

$$1 + x + x^2 + \ldots + x^n \equiv \frac{1 - x^{n+1}}{1 - x} \qquad x \neq 1 \tag{4.20}$$

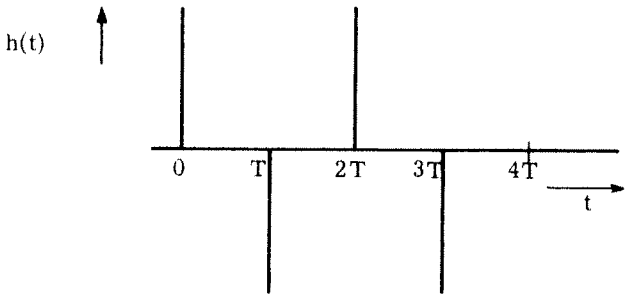

Fig. 16. Impulse response of CMPRES.

it follows that

$$H(\omega) = \frac{1 - e^{-j4\omega T}}{1 + e^{-j\omega T}} \tag{4.21}$$

or

$$H(\omega) = e^{-j\frac{3\omega t}{2}} \frac{e^{j2\omega T} - e^{-j2\omega T}}{e^{j\frac{\omega T}{2}} + e^{-j\frac{\omega T}{2}}} \tag{4.22}$$

With $\omega = 2\pi f$ we obtain

$$H(f) = je^{-j2\pi fT} \frac{\sin 4\pi fT}{\cos \pi ft} \tag{4.23}$$

$$|H(f)| = \frac{|\sin 4\pi fT|}{|\cos \pi ft|} \tag{4.24}$$

The frequency of the numerator sine-wave is four times the frequency of the denominator cosine wave. Zero-magnitudes occur every 210 Hz, except where both numerator and denominator equal zero, that is, at 420 and 1260 Hz. There the magnitude has a maximum equal to four, the relative maxima between the zeros are 12 db down. The magnitude spectrum and the functions of the numerator and the denominator are shown in Fig. 17. Although the magnitude spectrum is periodic in frequency with period 840 Hz, its main effect is in the passband of the fixed analog filter, also indicated in the figure. As mentioned in Section 3.4.1, any d.c. level, including the 512_{10} bias necessary for unipolar A/D conversion, and a possible d.c. misalignment between Kronhite filter and A/D converter, are removed by CMPRES. This is illustrated by the zero magnitude at 0 Hz. The effect of crosstalk from the 1680 Hz reference channel to the data channel on the analog recording, which has already been reduced to a minimum after the Kronhite analog filter, is also completely eliminated because of the zero magnitude at 1680 Hz in the CMPRES transfer characteristic.

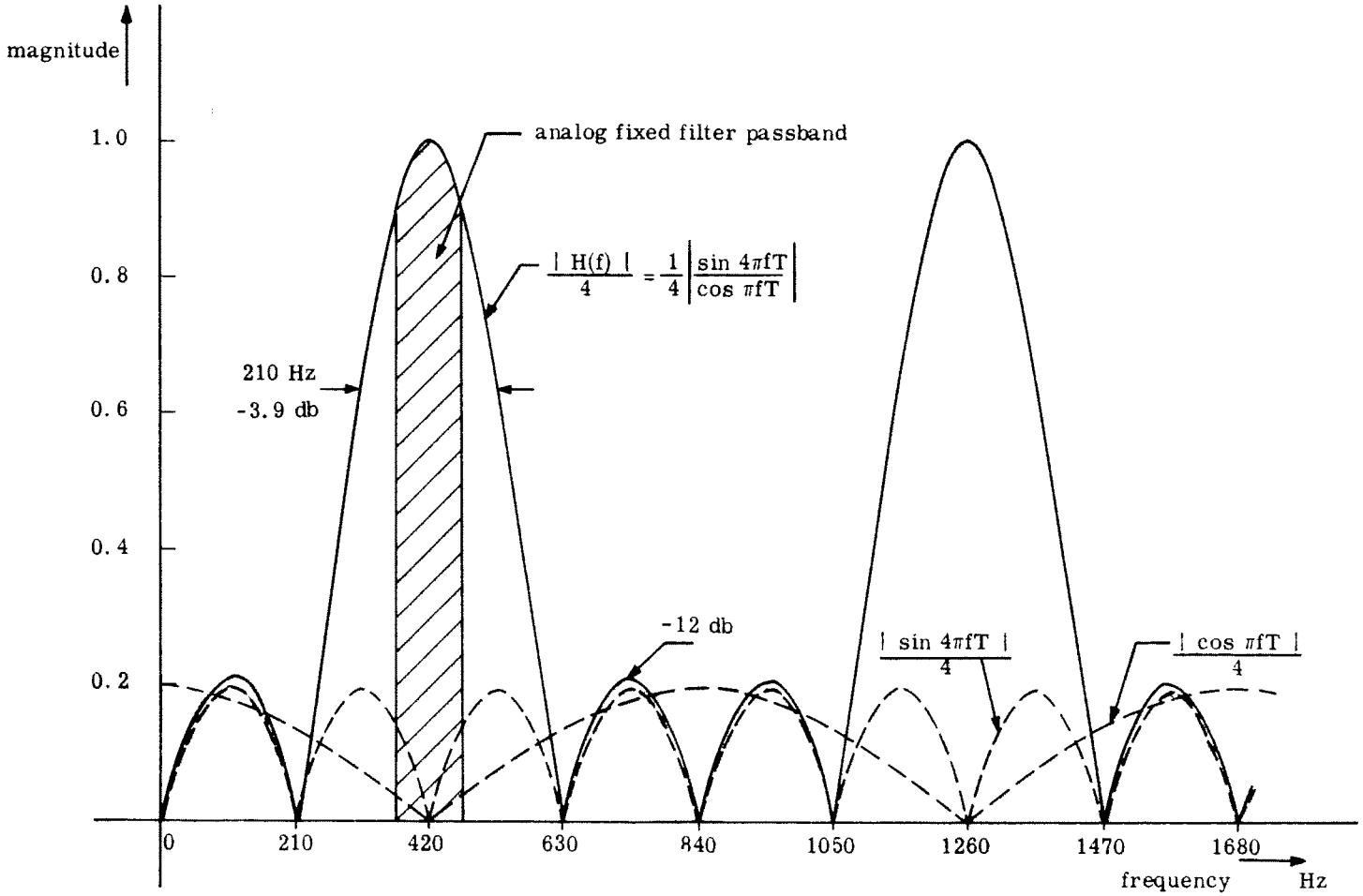

Fig. 17. Normalized low frequency part of CMPRES RMS spectrum.

Also indicated in the figure is the 210 Hz passband around the carrier, its ± 105 Hz points being at a -3.9 db power level from the maximum.

4.3.2. CW1. The program CW1 correlates the compressed samples representing the received signal r(t) with the modulation m(t) = 1 of the 420 Hz carrier in CW transmission. A similar digital filter as in CMPRES describes this operation

$$h(t) = \sum_{n=0}^{N-1} \delta(t - nT) \tag{4.25}$$

where N = 252, the total number of samples in a 1.2 sec period (for one coordinate) and $T = \frac{1.2}{N} = \frac{1}{210}$ sec, the time interval between samples, see Fig. 18.

As in CMPRES, we find the frequency characteristic by Fourier transformation of Eq. 4.25 resulting in

$$H(\omega) = \sum_{n=0}^{N-1} e^{-jn\omega T} \tag{4.26}$$

$$H(\omega)\, e^{-(N-1)\frac{\omega T}{2}} \frac{\sin N \frac{\omega T}{2}}{\sin \frac{\omega T}{2}} \tag{4.27}$$

and thus

$$|H(f)| = \frac{|\sin N\pi f T|}{|\sin \pi f T|} \tag{4.28}$$

The normalized spectrum (maximum magnitude = 1) is shown in Fig. 19. The frequency of the numerator sine wave is N times the frequency of the denominator sine wave. Spectral zeros occur at the frequencies $f = \frac{k}{NT}$, k = 1, 2, 3, . . . , N-1, N+1, . . . , that is, every $\frac{1}{1.2}$ Hz except at zero, $\frac{N}{1.2}$, $\frac{2N}{1.2}$ Hz, etc. At these frequencies, spaced 210 Hz, both the numerator and the denominator are zero and the CW1 transfer function has its maximum magnitude

$$|H(f)|_{max} = N = 252 \tag{4.29}$$

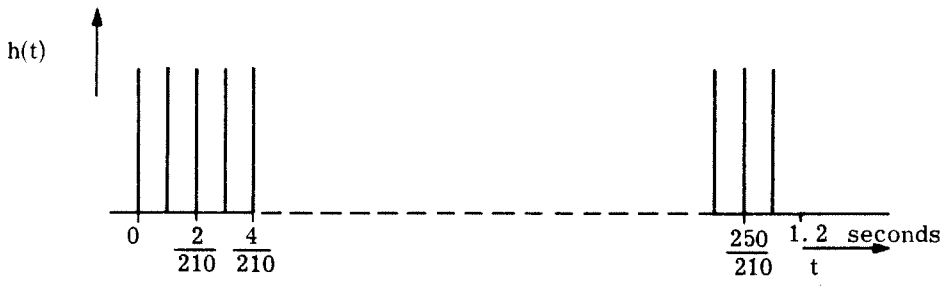

Fig. 18. CW1 impulse response.

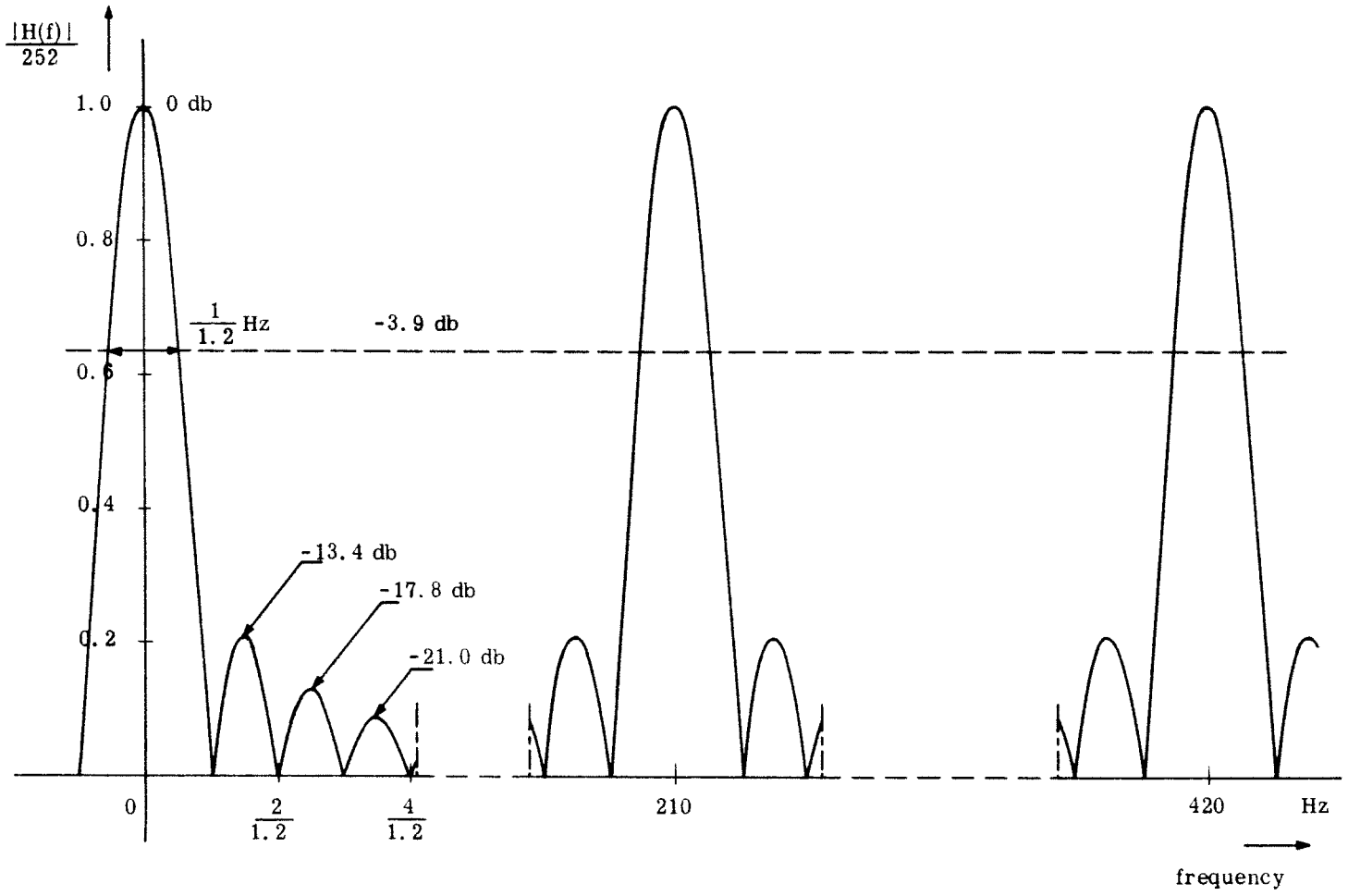

Fig. 19. Details of CW1 normalized magnitude spectrum.

Relative maxima in these 210 Hz intervals are more than 12 db down.

Transferring the center frequency of the CMPRES transfer function from carrier to d. c., it is seen that the combination of CMPRES and CW1 yields a transfer function with its main lobes around 0 Hz, 840 Hz, etc. The CW1 lobes at k210 Hz between these maxima are made zero by CMPRES. Together with the passband of the analog filter, only the lobe around d. c. becomes of interest. As a result the combination of analog filter, CMPRES, and CW1 forms a narrowband filter with zero magnitude bandwidth $\pm \frac{1}{1.2} = \pm .83$ Hz centered around d. c., or transferred back to the carrier frequency, centered around 420 Hz. The .83 Hz effective bandwidth between -3.9 db points, in which most of the power is contained, is indicated in the figure.

4. 3. 3. CIRAV. To average the data in preparation for sequence analysis, corresponding samples from twelve 1. 2 sec periods, one sample per period, are added together. To describe this process we use the same impulse response as in CW1, but with different values for N and T:

$$h(t) = \sum_{n=0}^{N-1} \delta(t - nT) \tag{4.30}$$

where now N = 12 and T = 1. 2 sec (see Fig. 20). Fourier transformation of Eq. 4. 30 results in

$$|H(f)| = \frac{|\sin N\pi fT|}{|\sin \pi ft|} = \frac{|\sin \pi f\ 14.4|}{|\sin \pi f\ 1.2|} \tag{4.31}$$

The CIRAV transfer function has spectral zeros at $f = \frac{k}{14.4}$ Hz, k = 1, 2, 3,..., 11, 13,..., and maximum magnitude = 12 at f = 0, $\frac{1}{1.2}$, $\frac{2}{1.2}$, $\frac{3}{1.2}$, etc. The normalized magnitude spectrum is shown in Fig. 21. Relative maxima are more than 13 db down.

It should be noted that the period, or frequency interval between the main lobes is only determined by the time interval T between samples. Thus, with a 1. 2 sec sequence,

Fig. 20. CIRAV impulse response.

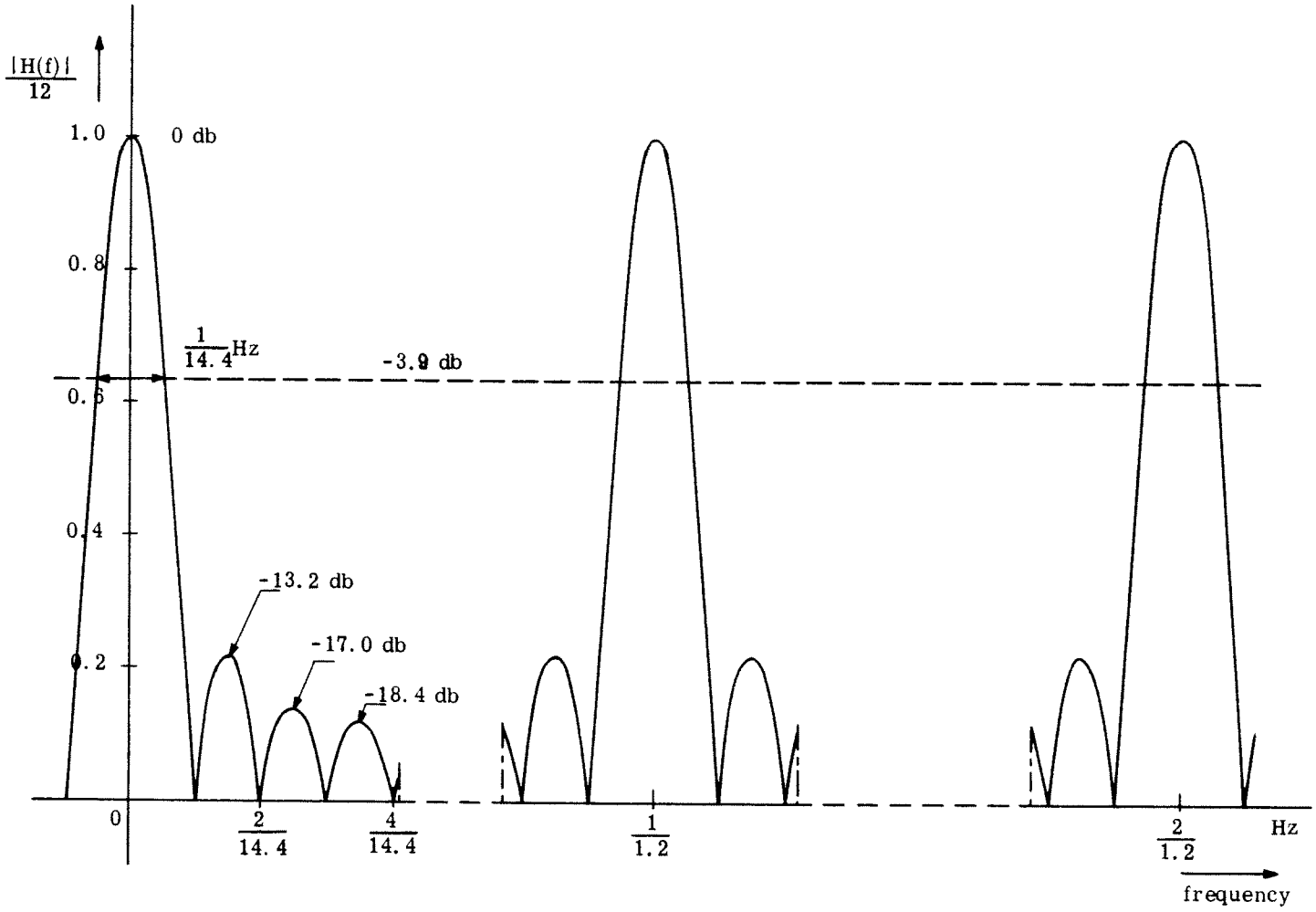

Fig. 21. Details of CIRAV normalized magnitude spectrum.

the spectral maxima will always occur at frequencies equal to an integer number times $\frac{1}{1.2}$ Hz, and this occurrence will be independent of the number of averaged periods N. This number N only determines the number of spectral zeros between the main lobes and with that, the bandwidth of each main lobe, equal to $\pm \frac{1}{N\ 1.2}$ Hz. In this case of 12 averaged periods, this bandwidth is ± .07 Hz.

4.3.4. MCOR1. As described in Section 4.1, the program MCOR1 performs in digital form the correlation

$$\phi(\tau + 14.4) = \int_0^{1.2} m(t)\ G(t + \tau)\ dt \qquad (4.32)$$

where m(t) is the digitally stored version of the biphase sequence modulation, and G(t) is the representative digital 1.2 sec period of the received signal, obtained in CIRAV. The correlation of Eq. 4.32 is the equivalent of the convolution

$$G(\tau) * m(T - \tau) \qquad (4.33)$$

where T is the 1.2 sec sequence period and $m(T - \tau)$ is the time reversal of the sequence. In this convolution $m(T - \tau)$ is the impulse response of the filter MCOR1. The MCOR1 transfer function could be obtained by Fourier transformation of $m(T - \tau)$ resulting in $M^*(\omega)$, the complex conjugate of the sequence frequency spectrum $M(\omega)$. However, to find only the magnitude spectrum

$$|M(\omega)| = |M^*(\omega)| \qquad (4.34)$$

we can bypass the complicated and laborious Fourier transformation of the sequence by making use of the correlation theorem. This theorem states that the autocorrelation function and the power density function are a Fourier transform pair. Except for a scaling factor equal to the digital length L of the sequence, and a difference in the d.c. component, the autocorrelation functions of a sequence and of a single pulse from that sequence are identical. Since the power density spectrum is the square of the magnitude spectrum, the latter is determined by the Fourier transformation of one sequence pulse. This process does not yield the phase information of the complex spectrum of MCOR1.

The single sequence pulse is described by

$$\begin{aligned} h(t) &= 1 \qquad 0 \leq t < b \\ h(t) &= 0 \qquad b \leq t < T \end{aligned} \qquad (4.35)$$

where T = sequence period = 1.2 sec, and b = pulse width = $\frac{T}{L} = \frac{1.2}{63}$ sec, see Fig. 22.

Fourier transformation of Eq. 4.35 yields

$$H(\omega) = \int_0^b e^{-j\omega t}\, dt$$

$$= be^{-j\frac{\omega b}{2}} \frac{e^{j\frac{\omega b}{2}} - e^{-j\frac{\omega b}{2}}}{2j\frac{\omega b}{2}}$$

$$= be^{-j\frac{\omega b}{2}} \frac{\sin\frac{\omega b}{2}}{\frac{\omega b}{2}} \qquad (4.36)$$

With $\omega = 2\pi f$ the magnitude spectrum of the single pulse becomes

$$|H(f)| = b \left| \frac{\sin \pi f b}{\pi f b} \right| \qquad (4.37)$$

the familiar $\left| \frac{\sin x}{x} \right|$ type function.

The spectral power of the sequence is approximately 63 times that of the single pulse, but this fact does not change the normalized magnitude spectrum. However, the d.c. power of the sequence is equal to that of the single pulse. Therefore in the normalized magnitude spectrum the line at 0 Hz has the magnitude $\frac{1}{\sqrt{63}}$ rather than 1 and is 18 db down. In the actual transmission of bi-phase sequence modulation, 32 digits have positive phase, and 31 digits have negative phase; the carrier power then is $(\frac{1}{63})^2$ of the total transmitted power.

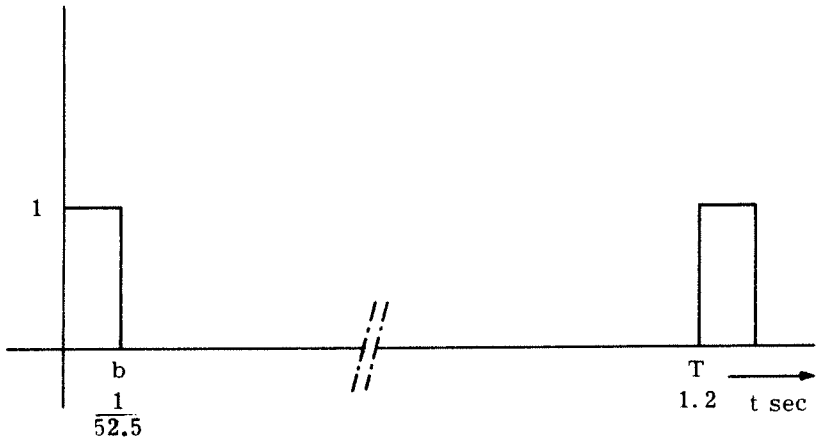

Fig. 22. Single pulse from 1.2 sec sequence.

In writing $b = \frac{T}{L} = \frac{1}{f_c}$, f_c = clock frequency of the single pulse (8 carrier cycles) = 52.5 Hz, the MCOR1 normalized magnitude spectrum becomes:

$$|M(f)| = \left| \frac{\sin(\pi f / f_c)}{\pi f / f_c} \right| = \frac{\sin(\pi f / 52.5)}{\pi f / 52.5}, \qquad f \neq 0$$

and

$$|M(0)| = \frac{1}{L} = \frac{1}{\sqrt{63}} \tag{4.38}$$

This magnitude spectrum is shown in Fig. 23. Because the time function is periodic with period T = 1.2 sec, the complex spectrum M(f) is a line spectrum, the lines being spaced with $\frac{1}{1.2}$ Hz, and thus coincides with the main lobes of CIRAV. Because of the analog filter passband transferred to d. c., the main interest is in the ± 50 Hz interval around d. c., containing 60 spectral lines to each side. The 63rd line at each side, corresponding to ±52.5 Hz, is essentially zero.

4.4. Signal to Noise Ratio Gain

The signal to noise ratio gain obtained in a matched filter is 2WT, where

W = bandwidth of input to matched filter

T = integration time of matched filter

The routine CMPRES does not change the bandwidth of the analog fixed filter output and does not improve the snr. Therefore, the input to the CW and BMSEQ matched filters has a bandwidth equal to the passband of the fixed filter, W = 100 Hz. The integration times of the CW and BMSEQ filters are 1.2 sec and 14.4 sec respectively. The processing gain in these filters then is

snr gain CW matched filter = 2 x 100 x 1.2 = 240 or 23.8 db

snr gain BMSEQ matched filter = 2 x 100 x 14.4 = 2880 or 34.6 db

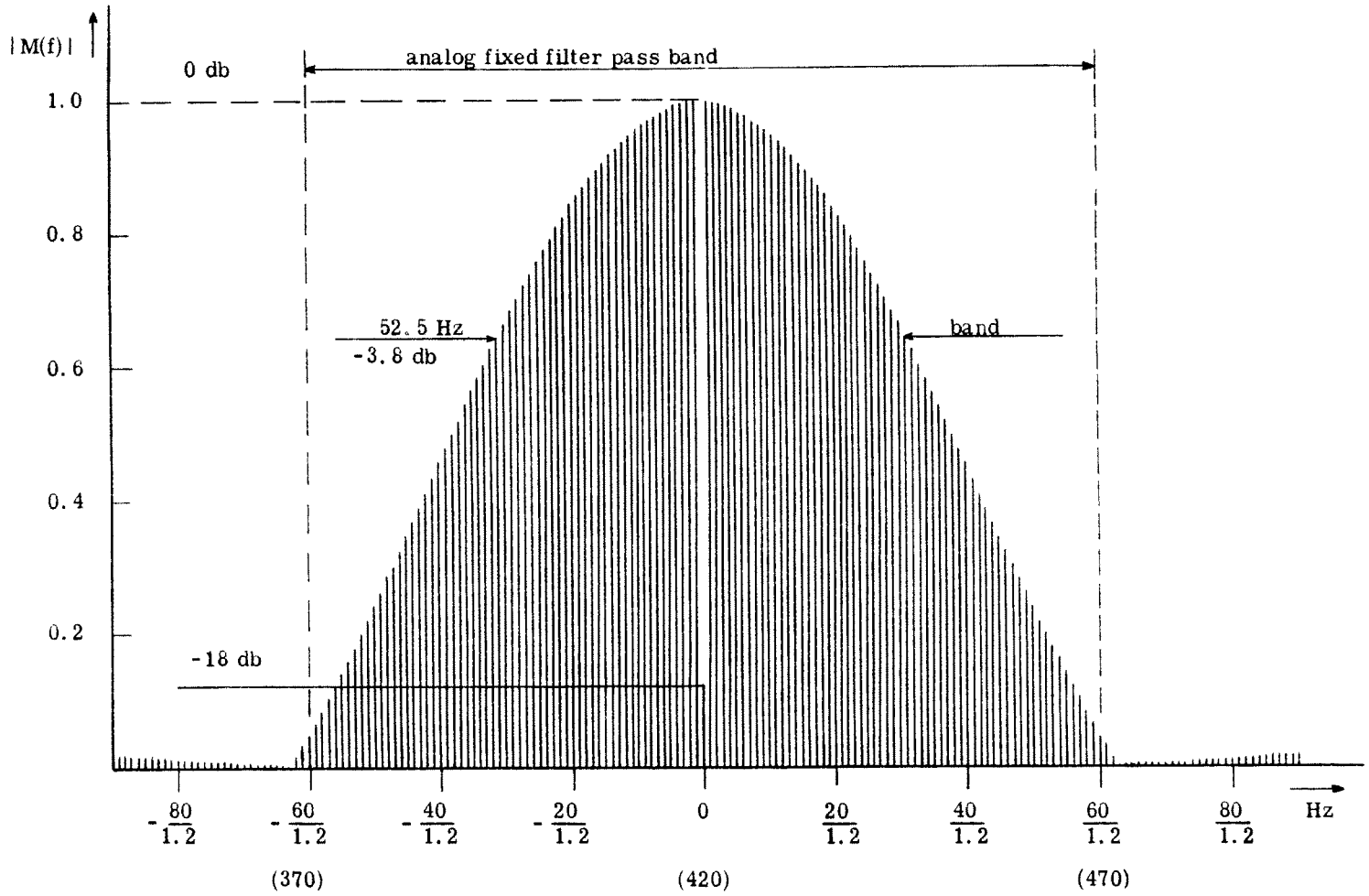

Fig. 23. MCOR1 normalized magnitude spectrum.

CHAPTER V

Results

The sections in this chapter describe the presentation of the results obtained by CW and sequence analysis, summarize the process of these analyses, and discuss the interpretation of the results shown, on the ground of the processing technique applied.

5. 1. Presentation of CW Analysis and Sequence Analysis Results.

In the appendices the photographed results are reproduced as obtained from CW and sequence analysis. These results are on 35 mm microfilm from which duplicates and enlargements can be made. Because of the consistency of the sequence analysis results, it was possible to make composite pictures by exposing one film frame to a number of records from one file. The enlargements of these exposures are printed together with the 35mm strip prints of the sequence single exposures such that complete files can be viewed on a double page. The sequence results are followed by the CW results reproduced as 35 mm strip prints and two enlargements.

In each file are indicated the time of reception, the kind (deep - shallow) of reception, the attenuation in db used for digital recording, and the sensitivities of the amplitude display on the oscilloscope. Since the scaling factor used in JR1PAC is not consistent for the files III, IV, V and VI, this factor, expressed as the power of 2 or the number of right shifts (RS), is also indicated; RS = 10 (factor 2^{10}) for all other files. The attenuation and sensitivity settings and this scaling factor are given solely for comparison of the signal strengths in the different files, the amplitude voltage should not be taken as an absolute measure.

The phase angle is expressed as between -180^{o} and $+180^{o}$, the total range of 360^{o} taking 1. 8 cm on the oscilloscope screen. In this mode $+180^{o}$ is equivalent to -180^{o} and an angle of, for example, 200^{o} is seen as -160^{o}. Thus the phase angle values can be interpreted as ranging either through one, or through several cycles of 360^{o}.

Both CW analysis and sequence analysis are performed on the same data. Since the

only component that the CW and sequence signals have in common is the 420 Hz carrier, and since in sequence the 420 Hz spectral line has a very small magnitude, CW correlation with sequence reception and sequence correlation with CW reception will both result in low magnitude, random phase output. Except for frame 1 of File I (sequence), records consisting of only such low magnitude outputs have not been photographed. Records containing both CW and sequence reception result in low magnitude peaks in sequence analysis and in CW pictures showing the transition from one type of transmission to the other.

5. 2. Resume of CW and Sequence Analysis.

For convenience of the discussion of the results, the essential parts of the processing system are summarized in this section. The received signal, expressed as

$$r(t) = R(t) \cos[\omega_0 t - \theta(t)]$$

is demodulated digitally and phase-coherently into the lowpass Cartesian components, resulting in 252 x and 252 y values per 1. 2 sec period. In this process the data is split into 30 sec records. After this demodulation, the processing continues separately on each Cartesian component, the data being processed by filters matched to the transmitted modulation.

In CW analysis the 1. 2 sec matched filtering process is equivalent to averaging the data over a 1. 2 sec period. The cartesian results, 6036 values $\phi_x(\tau)$ and 6036 values $\phi_y(\tau)$ are converted into polar coordinates, $R(\tau)$ and $\theta(\tau)$, the amplitude and phase of the matched filter output, or the low pass polar components of the received signal. The bandwidth between spectral zeros centered around the carrier frequency is $\pm$. 83 Hz, and the process yields information about the low frequency modulation of the 420 Hz carrier by the ocean. The processing gain is in the order of 24 db. The duration of the filter output for one input record is approximately 28. 8 sec, displayed on a 10 cm wide oscilloscope. In the CW pictures, therefore, the time displacement per cm is $\tau = 2.88$ sec/ cm.

In sequence analysis the 14. 4 sec matched filter is obtained by averaging in CIRAV two groups of twelve 1. 2 sec periods, 252 samples per period per Cartesian component, and correlating each of the representative periods with the stored digital version of one period of the 63 digit bi-phase sequence. The 252 $\phi_x(\tau)$ and 252 $\phi_y(\tau)$ values obtained in each correlation are converted into the polar correlation results $R(\tau)$ and $\theta(\tau)$, the amplitude and phase of the 14. 4 sec SEQ matched filter output. The time displacement τ ranges from 0 to

1.2 sec in 252 steps of $\frac{1}{210}$ sec; four steps form the duration of one sequence digit ($\frac{1}{52.5}$ sec). Sequence analysis returns two 1.2 sec outputs for each 30 sec input record, τ = 120 msec/cm in each sequence picture. The frequency characteristic of the sequence matched filter is a $\frac{\sin x}{x}$ spectrum, with a zero magnitude bandwidth of ± 52.5 Hz (the clock frequency of the sequence generator) centered around carrier. The CIRAV routine determines the "bandwidth" around each spectral line, ± .07 Hz. The magnitude of the carrier spectral line is 18 db down from the maximum $\frac{\sin x}{x}$ value. The processing gain is in the order of 34 db.

5.3. Sequence Analysis Results. (Appendix A).

As explained in Section 4.2, the sequence correlation results yield information about signal arrivals. A single arrival would result in a triangular peak in $R(\tau)$, 4 digital values ("dots") upslope and 4 dots downslope, and a constant phase during this 8 dot interval. A single arrival interval has the duration of two digits of sequence, $38\frac{2}{21}$ msec or .32 cm on the oscilloscope screen. However, the pictures show a more complicated structure containing several peaks and indicating a combination of several arrivals, supposedly caused by propagation along physically different paths.

Although recording and processing in each file is phase coherent, there is no absolute reference for the delay of a sound arrival. A delay, indicated by the time displacement τ of a correlation peak, depends upon the actual moment of sound arrival, as well as upon the moment where the analog to digital recording was started. Therefore, no relation exists between arrival times in different files, the correlation peaks do not indicate any absolute arrival time, and delays or arrival times are to be compared only within a file.

The most striking feature in these results is probably the great consistency within each 5 minutes of sequence reception. Only minor changes in amplitude and phase occur as is illustrated in the multiple exposures. The sudden "shifts" of the correlation peak over parts of the 1.2 sec τ interval are due to transients causing shifts of several digits in the MIMI-A sequence generator. The digital time base enables exact time reproduction of the corresponding dots from each record; variations in amplitude and phase of different records are thus seen as dots in 252 vertical lines in the composite exposures. The oscilloscope display was focused in the center of the image, dots at the sides of the screen unfortunately are somewhat blurred.

Of particular interest is the structure of the phase patterns. Several patterns contain a linear phase sweep through several cycles of 360°, most of them at a rate of $\frac{d\theta(\tau)}{d\tau} = 32\pi$ rad/sec or, expressed as a frequency, f = 16 Hz. Other noticeable points are the small parabolic curves, and phase "jumps" ranging from 90° to 180°. Small intervals of almost constant phase are sometimes present and coincide with high resolution peaks, indicating a distinguished single arrival. The phase duration of the main arrivals seems to be better observable in the phase pattern than in the amplitude graph. The main arrival durations are roughly 300-500 msec.

A point of discussion is the weak consistency in phase patterns outside the main arrival interval. This may be either caused by extended sound arrivals, or by the d. c. value of the correlation function outside the peak. As mentioned in Section 4. 2, constant $\phi_x(\tau)$ and $\phi_y(\tau)$ will cause the phase angle

$$\theta(\tau) = \tan^{-1} \frac{\phi_y(\tau)}{\phi_x(\tau)}$$

to be constant too. Since the magnitudes of $\phi_x(\tau)$ and $\phi_y(\tau)$ are small in that range, they can be easily scattered by noise, resulting in a random phase. The above also is valid for a multipath structure yielding a resultant phase angle. In weak sound arrivals this phase consistency outside the main arrivals will be difficult to recognize. In order to probe arrivals extending longer than 1. 2 sec, experiments using sequences of longer duration will have to be taken. Because of the periodicity of the sequence correlation, the extension of arrivals around τ = 1. 2 sec is seen around τ = 0.

Most of the phase patterns show a phase drift during the 5 minute reception which agrees with the phase difference in the CW results of records at the beginning and at the end of a file.

Because of the different scaling factors used in JR1PAC for the files III, IV, V and VI, the composite pictures of these files show a less consistent amplitude pattern than the other files. The phase pattern is not affected by this scaling. The table below shows the combination of V/cm, attenuation, RS number, maximum amplitude in cm, and the derived db levels taking the magnitude of file I as a 0 db reference, for comparison of signal strengths. Both shallow receptions seem stronger than the deep receptions recorded 5 minutes or 1/2 hour earlier and later.

Reception Time (3 Feb 65)	File	Osc. V/cm	Att. db	Scaling RS	Mag. cm	Level db	Reception
15:45-15:50	I	2.0	4	10	2.0	0	deep
15:55-16:00	II	2.0	7	10	2.0	+3	shallow
17:30-17:35	III	2.0	0	9	2.0	-10	deep
18:00-18:05	IV	2.0	0	9	1.5	-12	deep
18:30-18:35	V	2.0	0	9	1.5	-12	deep
19:00-19:05	VI	2.0	0	9	1.5	-12	deep
19:30-19:35	VII	1.0	0	10	2.0	-10	deep
20:00-20:05	VIII	0.5	0	10	1.5	-18	deep
20:30-20:35	IX	1.0	7	10	2.0	-3	shallow
21:00-21:05	X	0.5	0	10	2.5	-14	deep
10:00-10:05 (4 Feb 65)	XI	0.5	0	10	2.5	-14	deep

Table of magnitude levels in sequence reception.

Some details of the sequence results are discussed per file below. The crude main arrival durations are measured from the phase patterns in the composite exposures.

File I: Arrival duration 360 msec, the linear sweep covers 4 cycles of 360^0 over a 250 msec interval, that is, $\frac{d\theta(\tau)}{d\tau} = 32\,\pi$ rad/sec. The main peak is 3 sequence digits wide and apparently does not represent a single arrival. The phase pattern contains parabolic and constant phase parts as well as 90^0 to 180^0 jumps.

File II: Main arrival duration 240 msec, possibly extended up to 500 msec. The picture shows two main peaks, no parabolic or constant phase, and a linear phase sweep of 32 π rad/sec. The double peak in frame 6 indicates a sequence generator shift at MIMI-A during this 14.4 sec period of sequence transmission.

File III: Arrival duration 480 msec, the picture shows three main peaks later changing into two. No strong linear phase sweep, but phase jumps and some constant phase are present. The pattern has a relatively strong consistency outside the main arrival.

File IV: Arrival duration 420 msec, the amplitude graph contains two to three main peaks

with low resolution. The phase pattern contains jumps, small parts of linear sweep, and some parabolic curves, and has little consistency outside the main arrival interval.

File V: Arrival duration 240 to 360 msec, the amplitude peaks have little resolution. The partial overlap of frames 13 and 14 shows one of the malfunctions of the Fairchild camera. The first multiple exposure contains a peakshift which destroys some of the consistency, in the second one the oscilloscope image was drifted horizontally losing some information in the arrival interval.

File VI: The arrival duration is 360 msec, the picture contains three arrival peaks with reasonable resolution. The highest one even indicates a single arrival according to the eight point peak and the constant phase in this interval. Phase jumps are observed, there is no linear phase sweep. Because of the different scaling in JR1PAC the amplitudes in the two composite pictures differ by a factor of two. The first (small) peak disappears gradually, the later arrivals increase in resolution during the reception period.

File VII: The arrival duration is 420 msec, the main arrival shows two to three major peaks. The phase picture contains the linear sweep and a parabolic curve, the phase seems random outside the arrival interval.

File VIII: contains the lowest measured peaks of the experiment. The arrival duration is 240 msec, the phase is somewhat consistent outside this interval. It is possible that this reception contained a number of arrivals with rather high resolutions, according to the pieces of constant phase in the composite pictures, and according to the peak pattern. The total transmitted energy is then distributed over a number of paths while each arrival contains relatively little energy.

File IX: The second shallow phone reception, with strong, high resolution arrivals. Notice the pieces of constant phase and especially the much later occurring linear sweep plus small peak, the total arrivals extending over about 700 msec. The peak height is at the same level as in File I.

File X: Contains a pronounced arrival duration of 400 msec and at least two arrivals with rather high resolution. In the file a sudden phase change over the entire 1. 2 sec interval is observed at frame 16, also noticeable in the second composite exposure. This is possibly due

to a one-time insufficient phase-locking causing an interchange of x and y samples, or a phase change of 90^{o} from that moment.

File XI: The only reception on 4 February, deep phone. The arrival duration is again roughly 360 msec, some phase consistency can also be distinguished in the rest of the 1. 2 sec interval, especially in the second portion (frames 9 - 16) of this sequence reception. The pictures show several pieces of constant phase, each piece having a different value (phase jumps). There is no linear sweep.

5. 4. CW Analysis Results (Appendix B).

Where separation of the files was not always possible in the analog data, the CW results of most files were combined. A continuous numbering of the frames is used, except where files were clearly separated. The table below, similar to that of the sequence analysis, enables comparison of signal strengths in the different reception intervals of the experiment.

File	Osc. V/ cm	Att. db	Scaling RS	Mag. cm	Level db	Reception
I	0. 5	4	10	1. 5 → 1	0 → -4	deep
II	0. 5	7	10	1	-4	shallow
III	2. 0	0	8	1. 5	-4	deep
IV	2. 0	0	8	1 → . 25	-4 → -16	deep
V	2. 0	0	6	1	-16	deep
VI	2. 0	0	7	1	-10	deep
VII	0. 2	0	10	2	-6	deep
VIII	0. 2	0	10	1	-12	deep
IX	0. 5	7	10	1	-4	shallow
X	0. 2	0	10	1. 5	-8	deep
XI	0. 5	0	10	1	-4	deep

Table of magnitude levels in CW reception.

File I in this table is again taken as a reference of 0 db, this level has no relation to the peak magnitude of the sequence analysis. Comparing this table with the db levels from the sequence analysis results we observe that File I contains the strongest signal in both CW and sequence reception. The relation in signal strength between CW and sequence reception of the other files is rather vague. The weakest sequence signal is found in File VIII whereas the weakest CW signal is in File V. Also, in CW the shallow reception is not obviously stronger than the deep reception, as was the case in sequence reception. The shallow CW signal in File II is up to 4 db lower than the deep CW signal in File I, whereas in sequence the shallow signal II is 3 db higher than the deep signal I.

The pictures show the modulation of the 420 Hz carrier by the ocean within the band of 420 ± . 42 Hz, this being the "effective" passband of the CW 1. 2 sec matched filter, through which most of the power is passed. The amplitude modulation apparently changes considerably in magnitude, and ranges in frequency approximately from . 1 to . 3 Hz. Except in the very weak signals where noise scatters the phase values, the phase shows great stability. As far as can be determined in the CW reception interrupted by 5 minute sequence intervals, the phase drift agrees with the measurements in other CW tests as described in Ref. 1 and with the phase drift noticed in sequence analysis, at a maximum rate of 5^0 - 15^0 per min. Although in other experiments the signal was phase coherently demodulated by analog equipment, the results are comparable with respect to the bandwidth applied.

Where the reception consisted of sequence, a zero magnitude and random phase are observed. At the moment of change in the reception into sequence, the amplitude rises with a 1. 2 sec ramp function step-response to the CW correlation value. The same effect is seen during the 5 second "off" period in CW 25/5 reception. The phase resumes its original value since an integer number of carrier cycles would fit in the 5 second "off" period, and because the demodulation is phase coherent.

CHAPTER VI

Conclusion

The CW 25/5 transmission and 1.2 sec matched filtering at reception yields information about the low frequency modulations of the 420 Hz carrierwave by the ocean. Amplitude modulation with frequencies between .1 Hz and .3 Hz, and with a variety of modulation depths are observed. In agreement with other MIMI CW experiments the phase is found to be very stable with maximum drifts of 5^0 - 15^0/min and very small short term variations in the .83- Hz lowpass band of the CW matched filter. The received signals vary in strength from approximately -15 dbμb to -31 dbμb. With the originally transmitted power of 103 dbμb this means propagation losses of 118 db to 134 db in the 43 mile expanse of the Straits of Florida.

Modulation of the carrier by a 1.2 sec, 63 digit, bi-phase pseudo random sequence and analysis of the received signal by means of a 14.4 sec matched filter or correlation, shows the multipath sound propagation. The major sound arrivals, with durations of 300 - 500 msec, have a great consistency in amplitude and phase. Some receptions contain extended sound arrivals with total durations up to 700 msec. These extended arrivals are particular noticeable in the phase pattern of the composite pictures in which a number of correlation outputs is exposed to one frame. Of special interest is the linear phase sweep observed in several of the sequence analysis results, all of them at a rate approximately $\frac{d\theta(\tau)}{d\tau} = 32\pi$ rad/sec. Since θ has been defined as the lagging phase in $\cos(\omega_0 t - \theta(t))$, this corresponds to a frequency of -16 Hz measured from carrier frequency.

A complete physical explanation for the phenomena observed is beyond the scope of this report. It merely serves to supply the oceanography and underwater acoustics researcher with a set of results from which further studies may be undertaken.

As future experiments are planned a 24-hour continuous sequence transmission, and a 24-hour CW transmission interrupted by periods of sequence transmission. Processing of the received signal will be done phase coherently over the entire data period. These tests will be followed by a complete lunar cycle with 30 days of CW transmission interrupted by

sequence "samples", and phase coherent processing of the received data. During the tests environmental measurements are taken by the Miami Acoustics Group for correlation with the sound propagation results.

Other experiments may involve the use of sequences of longer duration for study of extended multipath sound arrivals. With the development of fast computer programs for Fourier transformation it may be possible to study the obtained results in the frequency domain, yielding information about the ocean transfer characteristic for frequencies around 420 Hz.

The experiment and its data processing system described in this report form a base for further studies and experiments.

APPENDIX A

SEQ Analysis Results

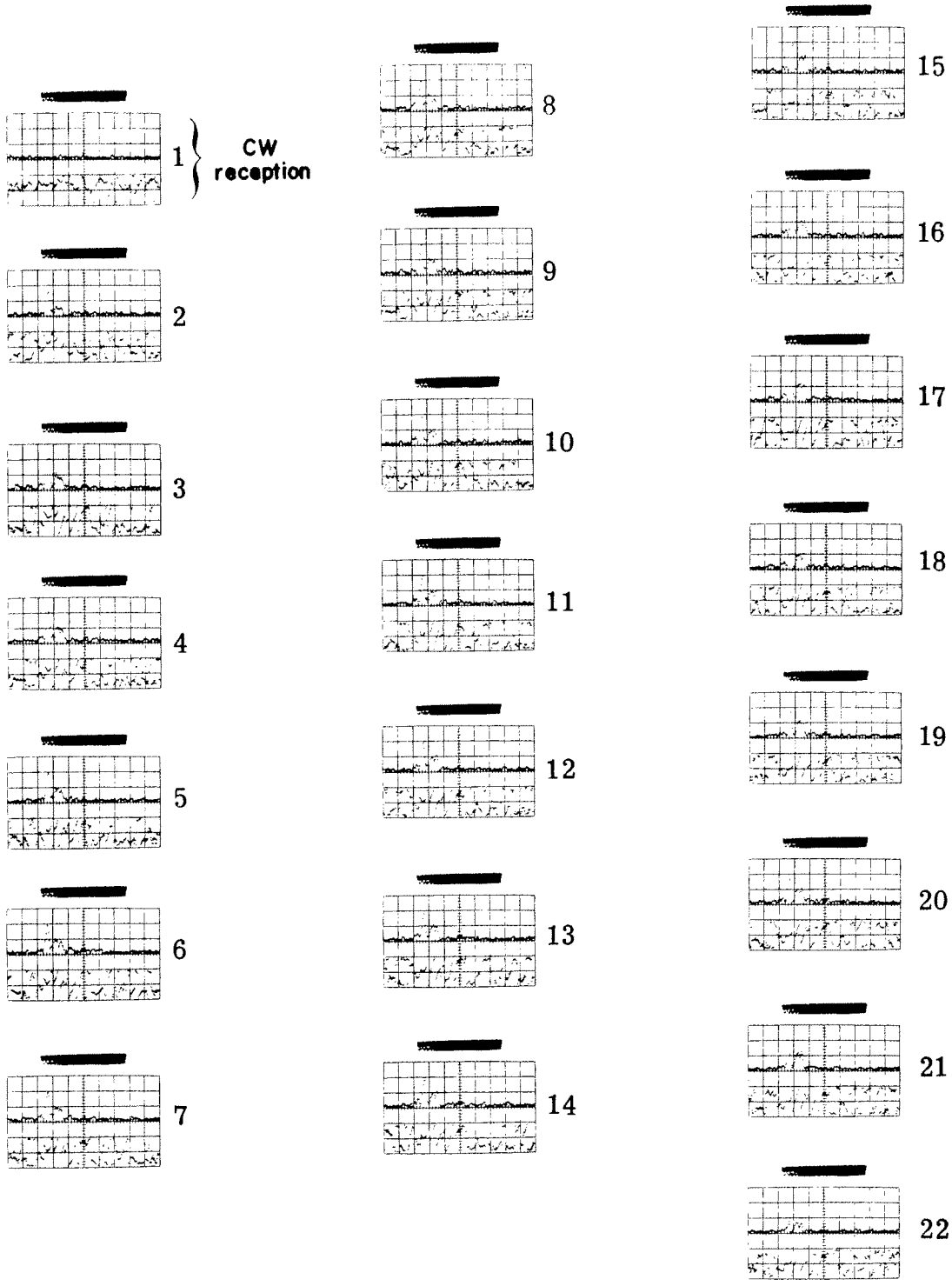

File I. BMSEQ, 3 February 1965, 15:45-15:50 h. reception deep, R = 2 V/cm, att = 4 db, RS = 10.

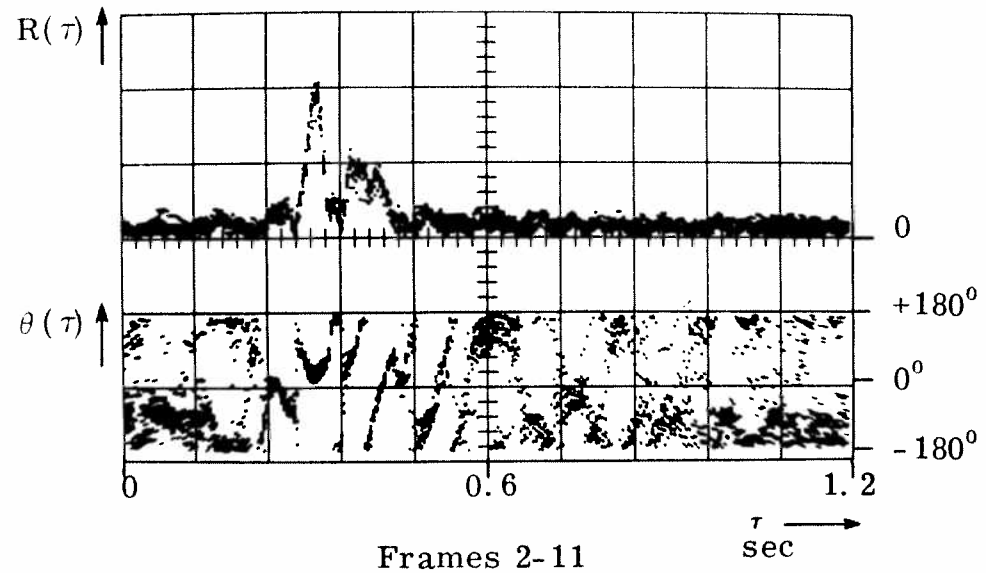

Frames 2-11

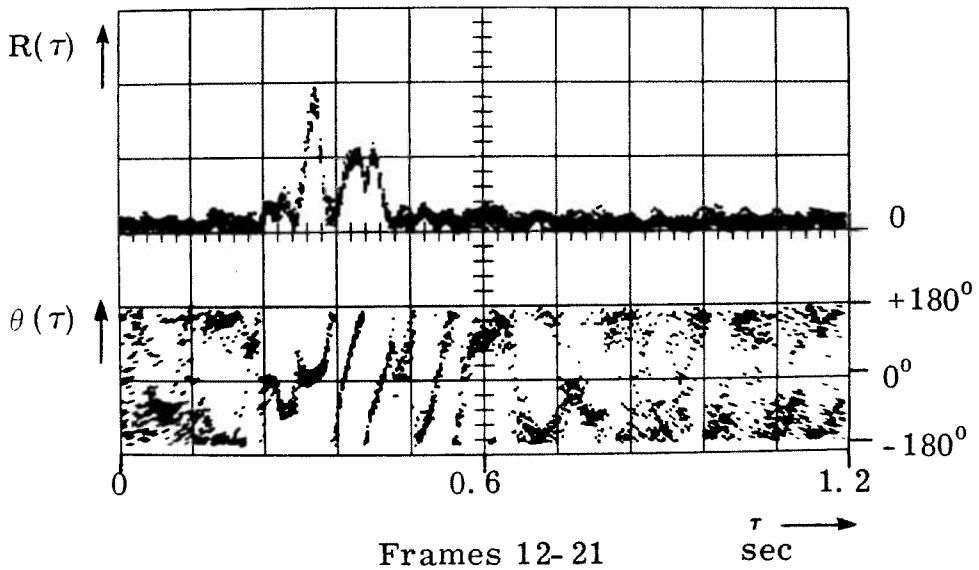

Frames 12-21

File I

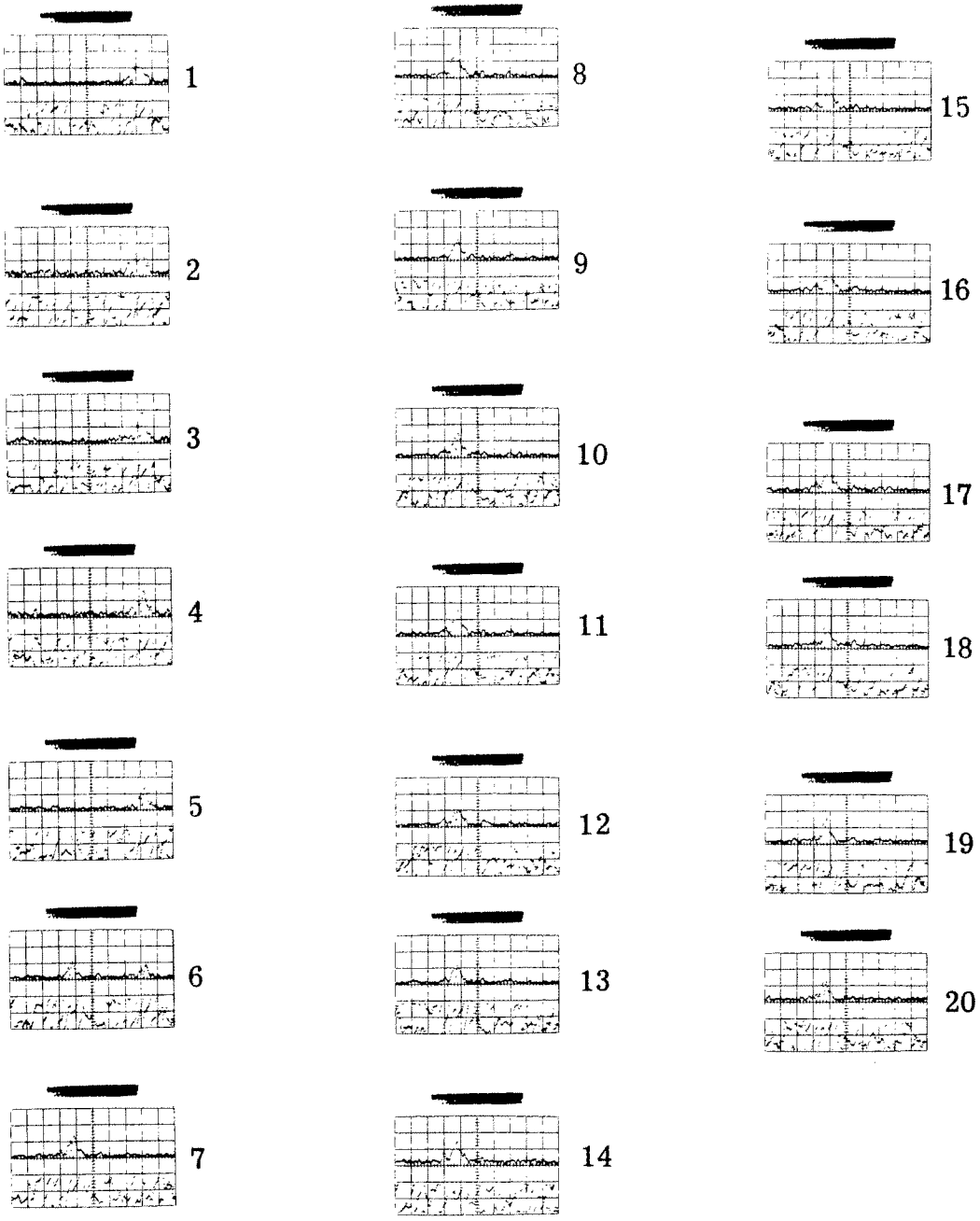

File II. BMSEQ, 3 February 1965, 15:55-16:00 h reception shallow. R = 2 V/cm, att = 7 db, RS = 10.

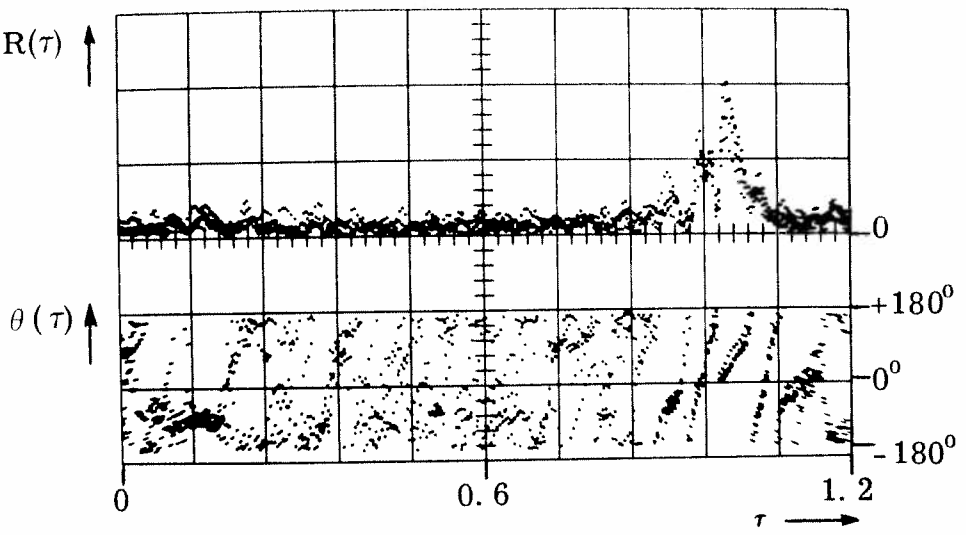

Frames 1-5

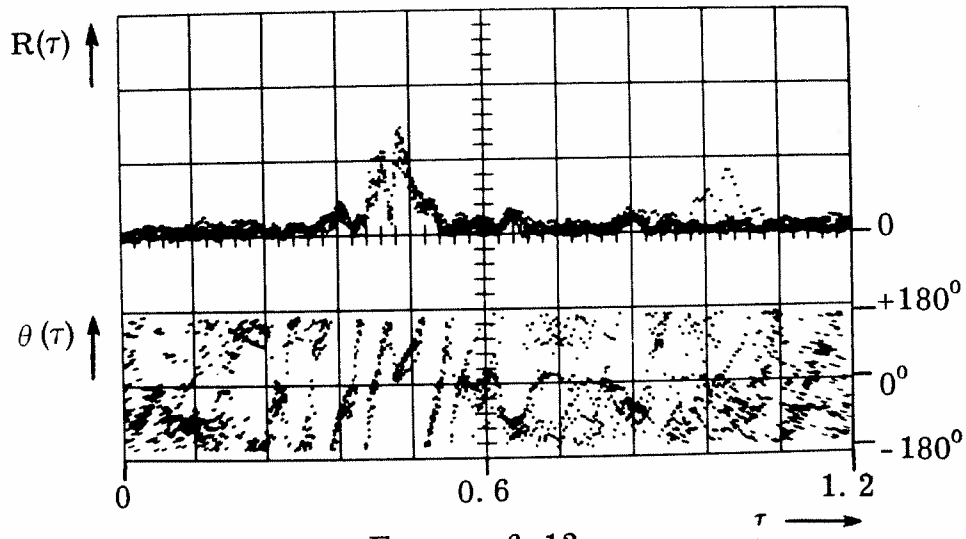

Frames 6-12

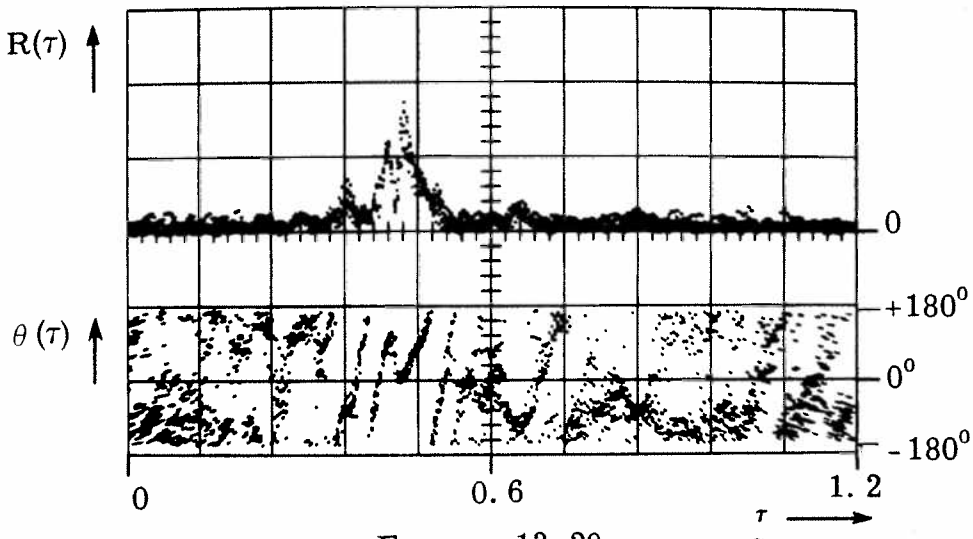

Frames 13-20

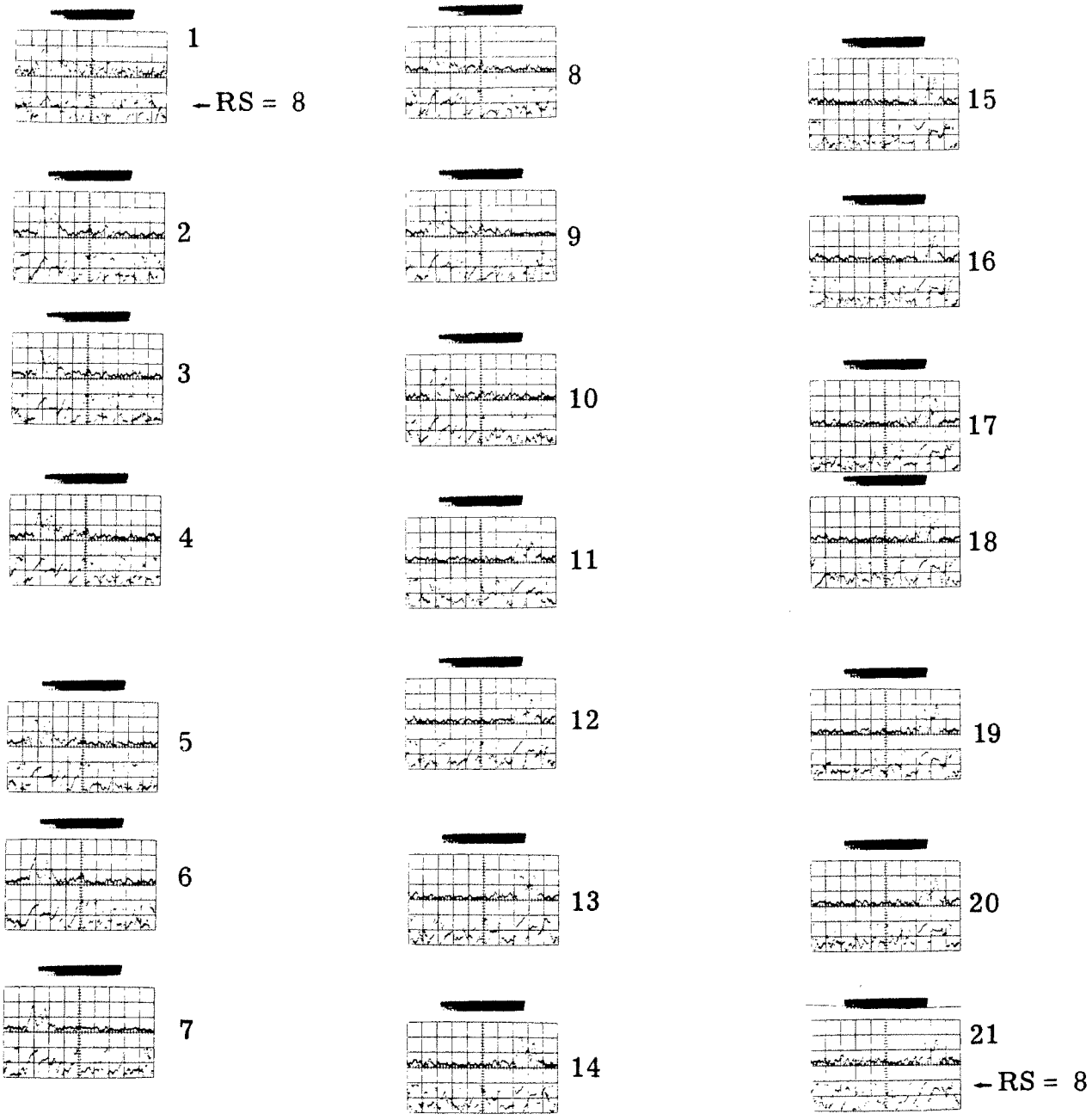

File III. BMSEQ, 3 February 1965, 17:30-17:35 h. reception deep. R = 2V/cm, att = 0 db, RS = 9 unless otherwise indicated.

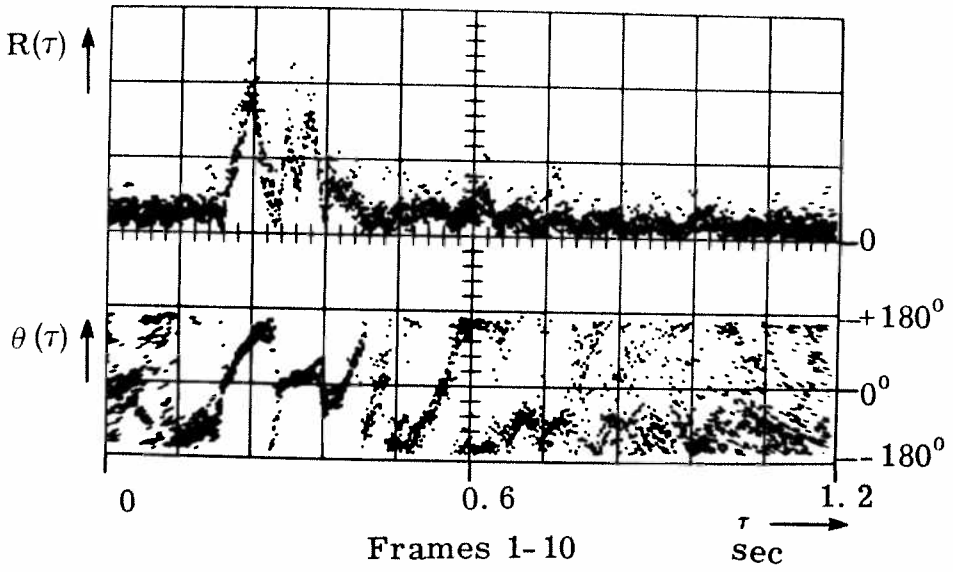

Frames 1-10

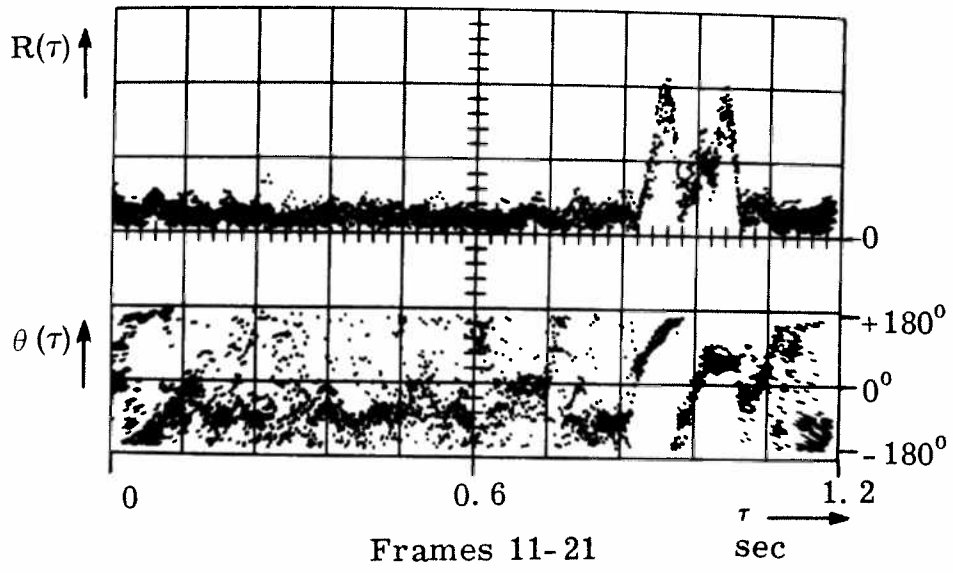

Frames 11-21

File III

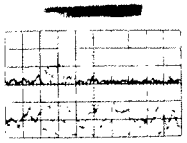

1

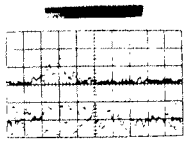

2

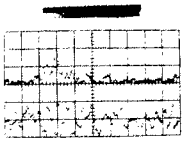

3

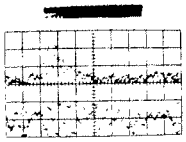

4
← RS = 8

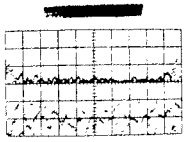

5

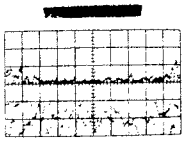

6

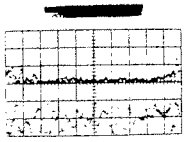

7

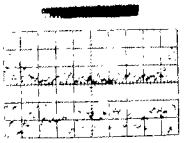

8
← RS = 8

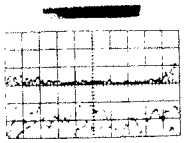

9

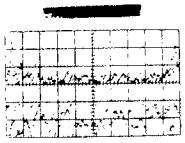

10
← RS = 8

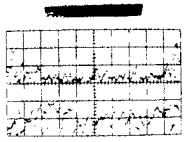

11
← RS = 8

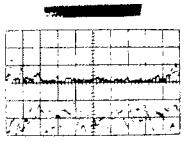

12

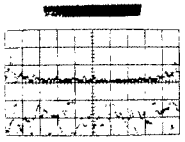

13

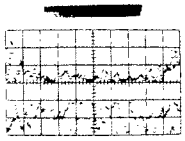

14
← RS = 8

File IV. BMSEQ, 3 February 1965, 18:00-18:05 h. reception deep. R = 2V/cm, att = 0 db, RS = 9 unless otherwise indicated.

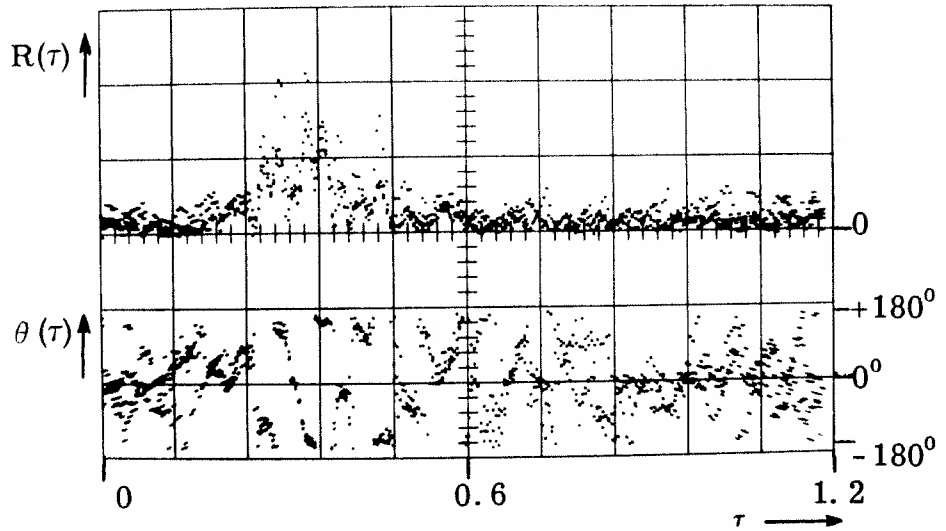

Frames 1-4

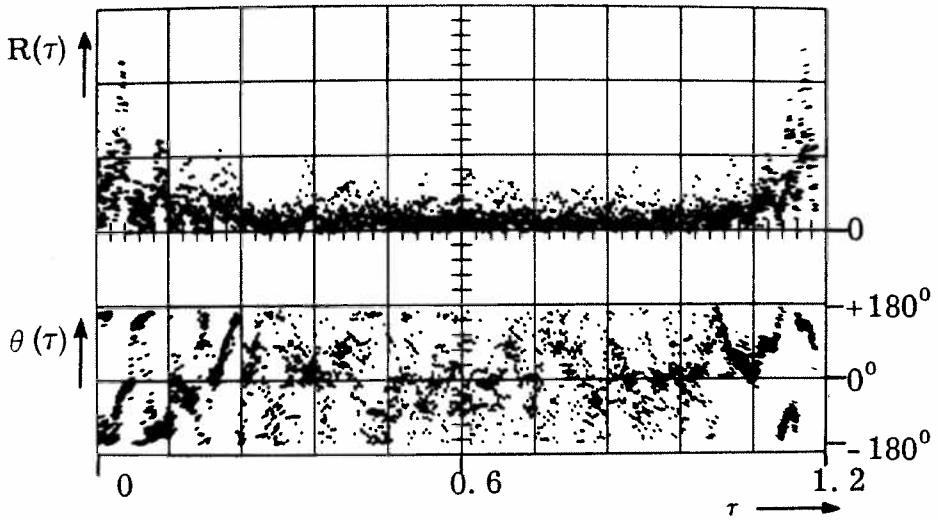

Frames 5-14

File IV

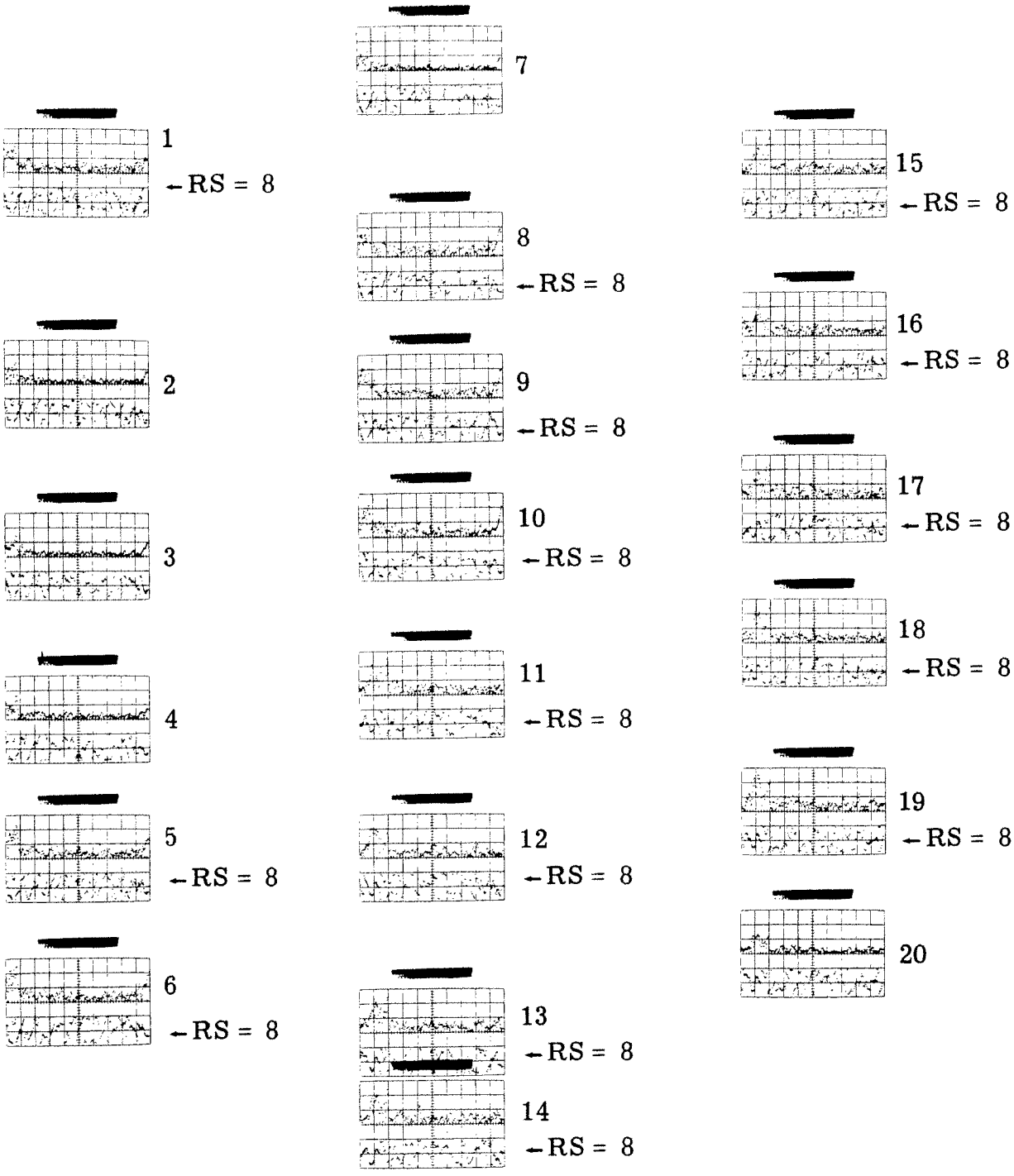

File V. BMSEQ, 3 February 1965, 18:30-18:35 h. reception deep. R = 2V/cm, att = 0 db; RS = 9 unless otherwise indicated.

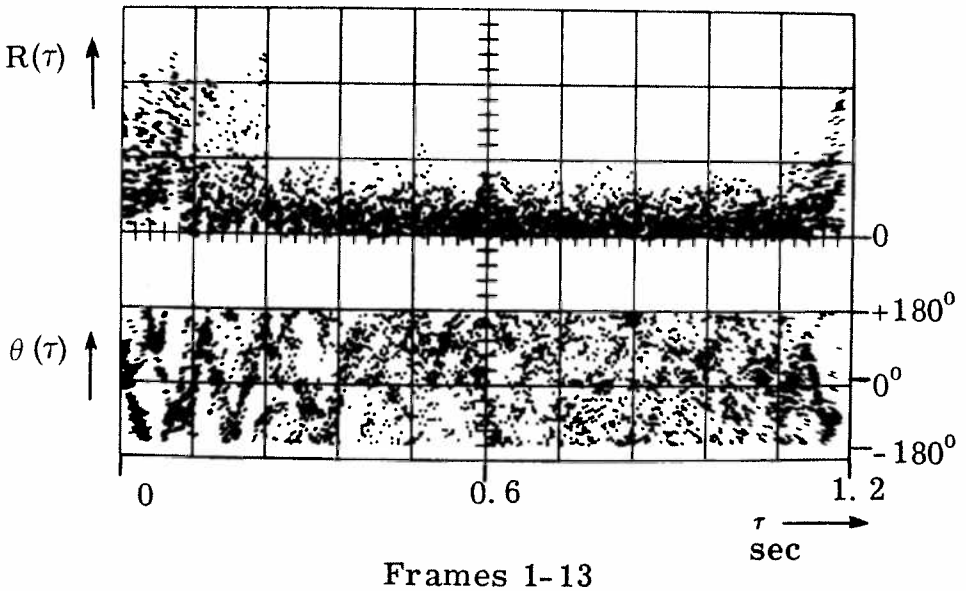

Frames 1-13

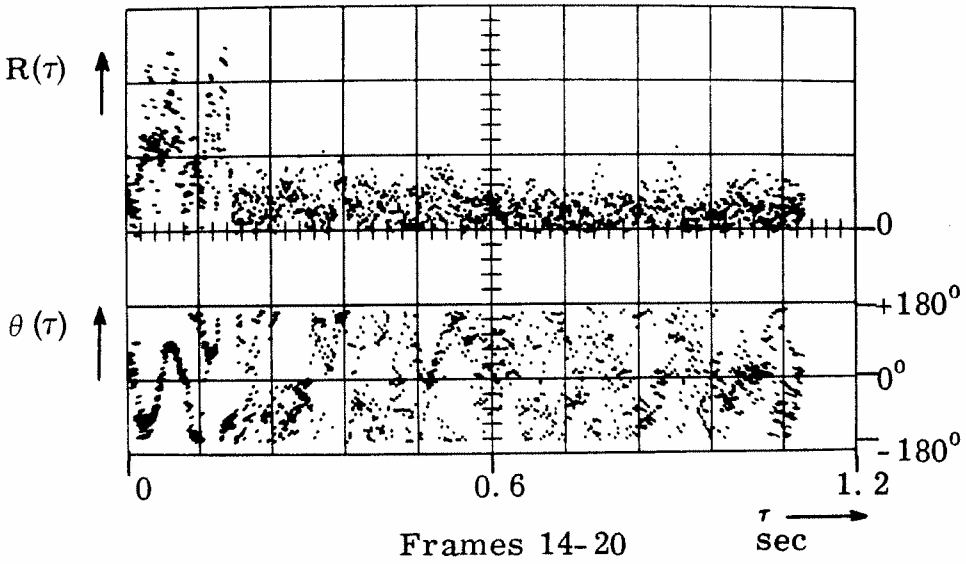

Frames 14-20

File V

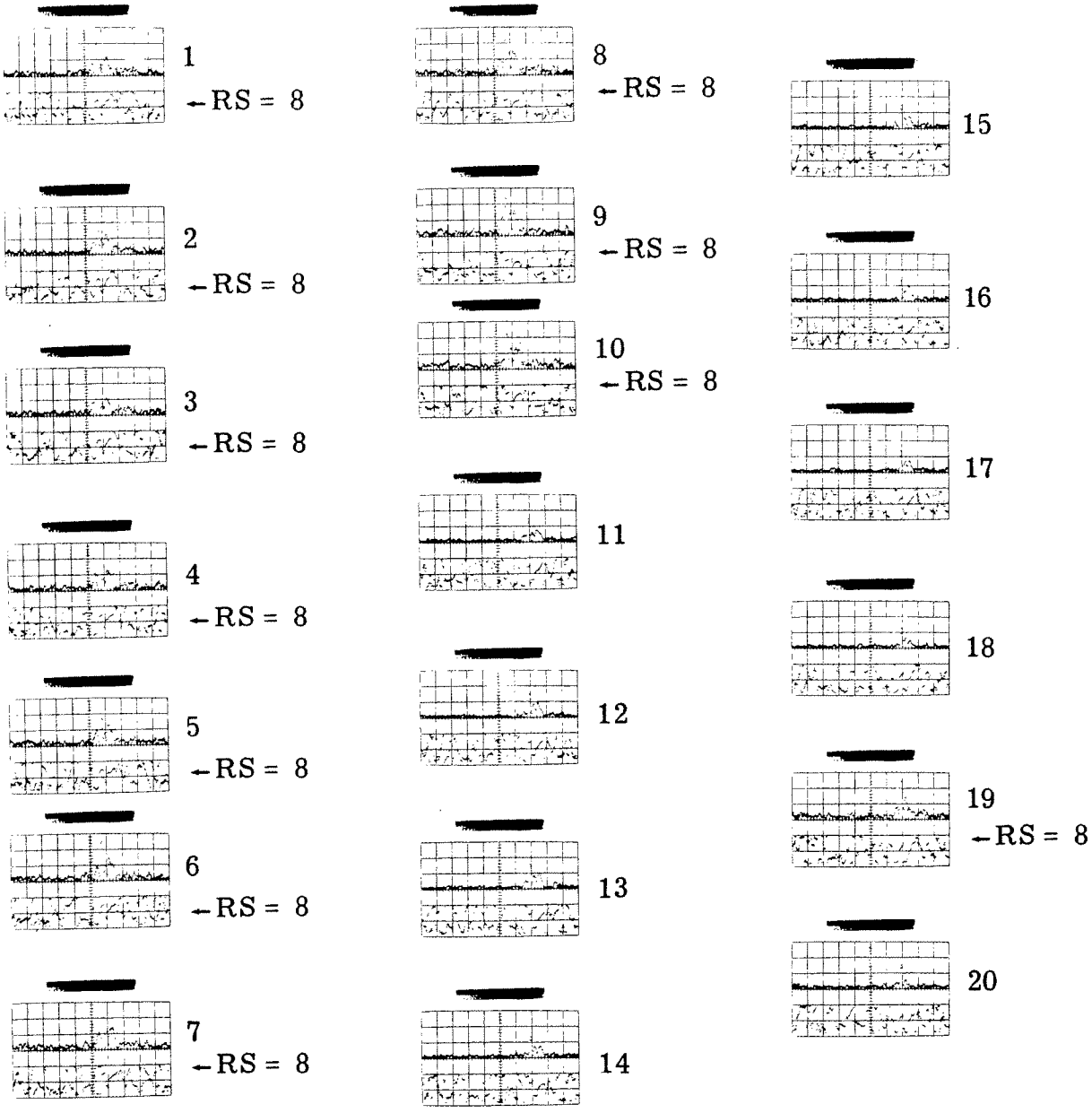

File VI. BMSEQ, 3 February 1965, 19:00-19:05 h.
reception deep, R = 2V/ cm, att = 0 db,
RS = 9 unless otherwise indicated.

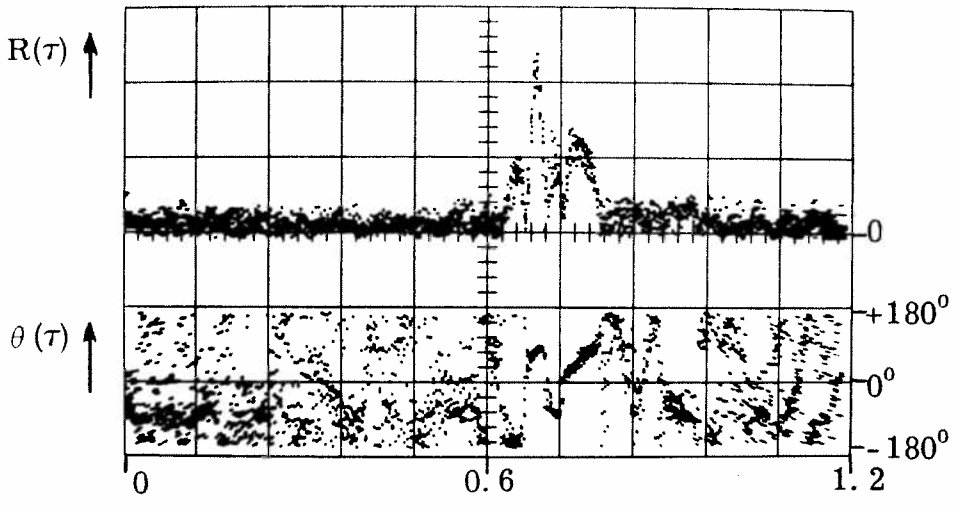

Frames 1-10

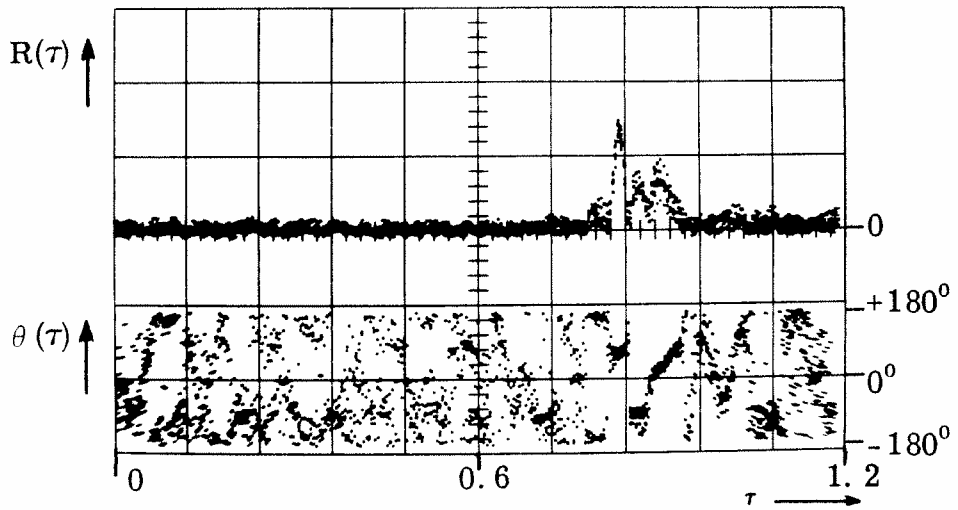

Frames 11-18

File VI

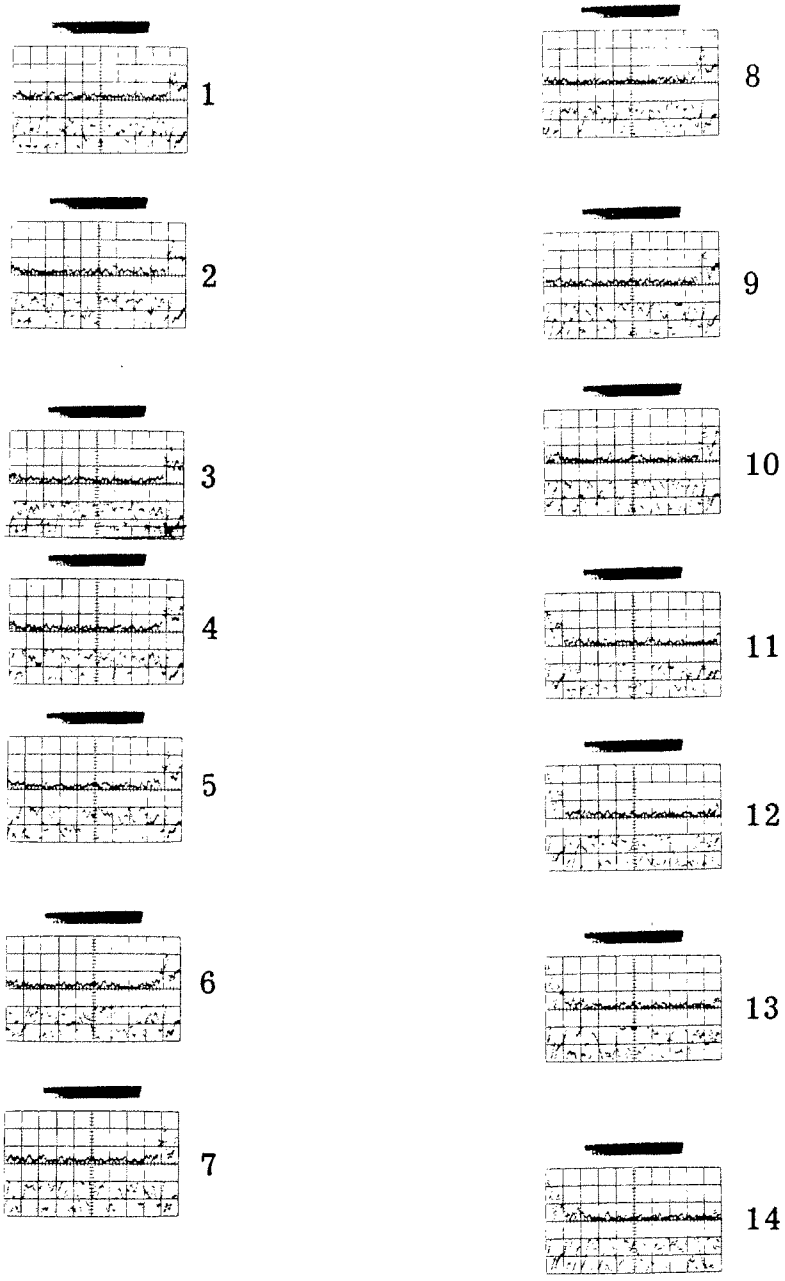

File VII. BMSEQ, 3 February 1965, 19:30-19:35 h. reception deep. R = 1V/cm, att = 0 db, RS = 10.

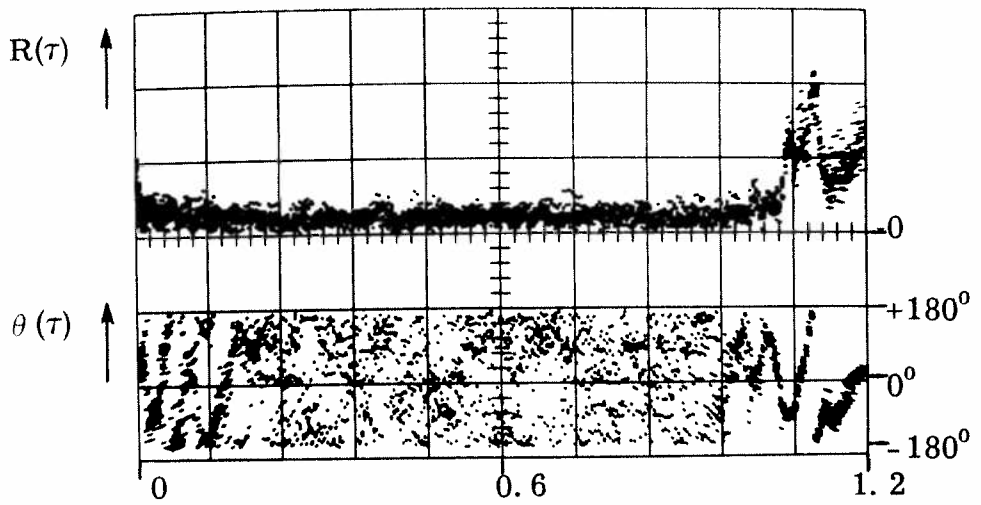

Frames 1-10

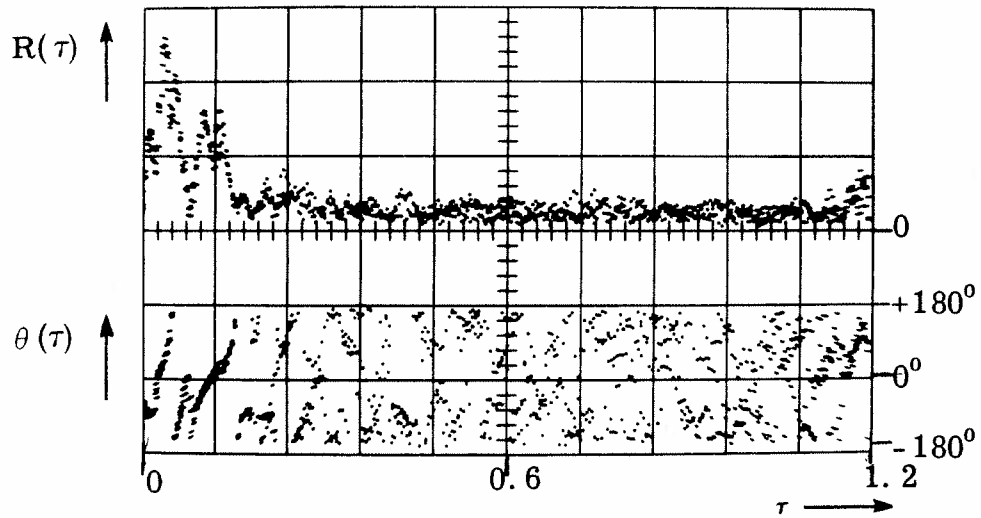

Frames 11-14

File VII

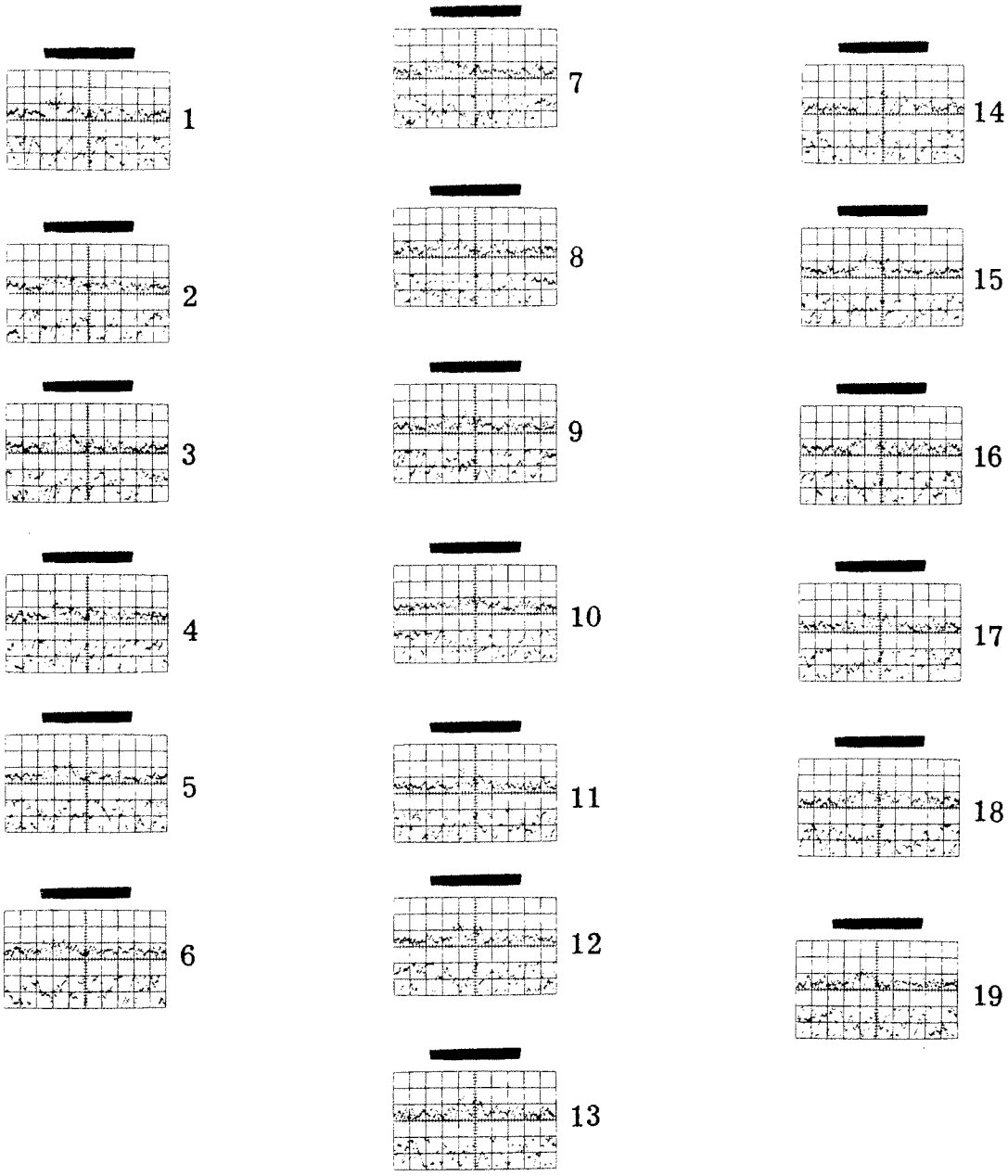

File VIII. BMSEQ, 3 February 1965, 20:00-20:05 h. reception deep. R = 0. 5 V/ cm, att = 0 db, RS = 10.

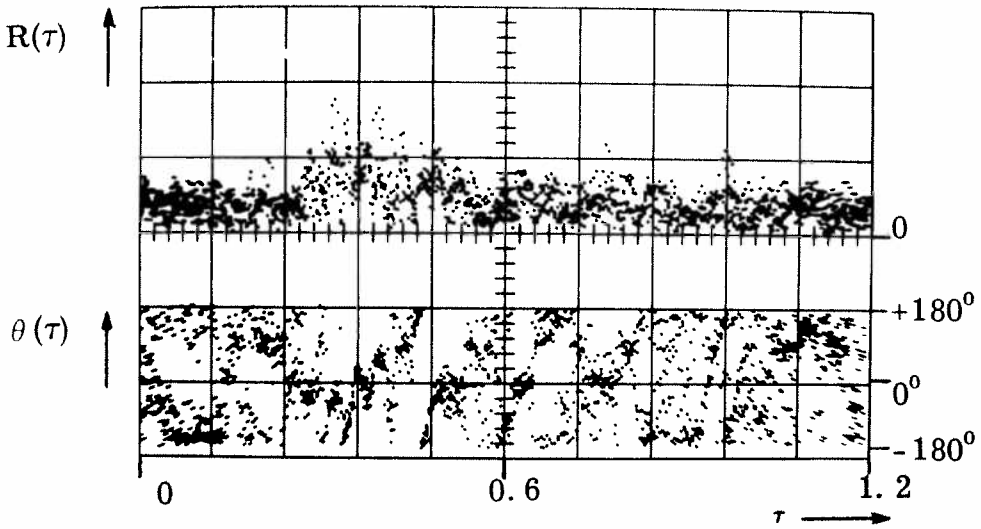

Frames 1-7

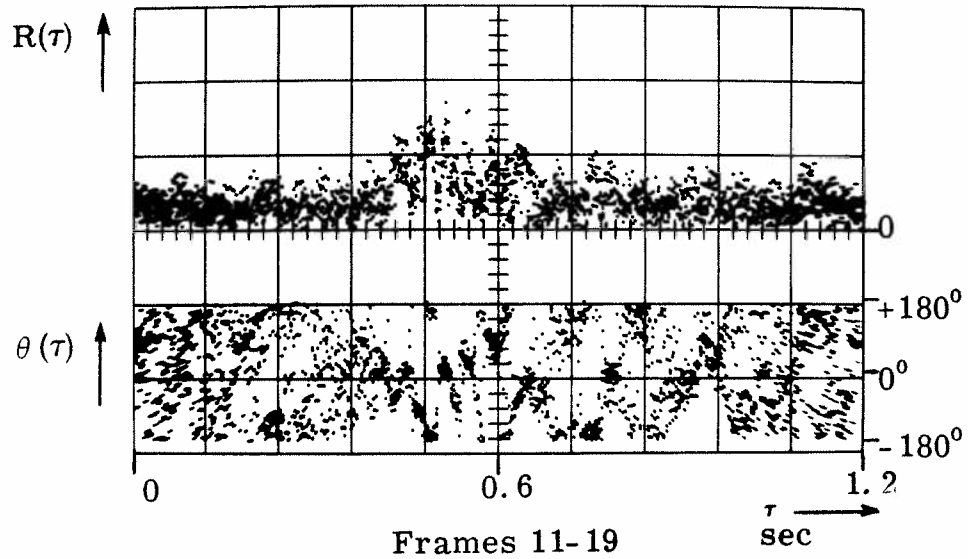

Frames 11-19

File VIII

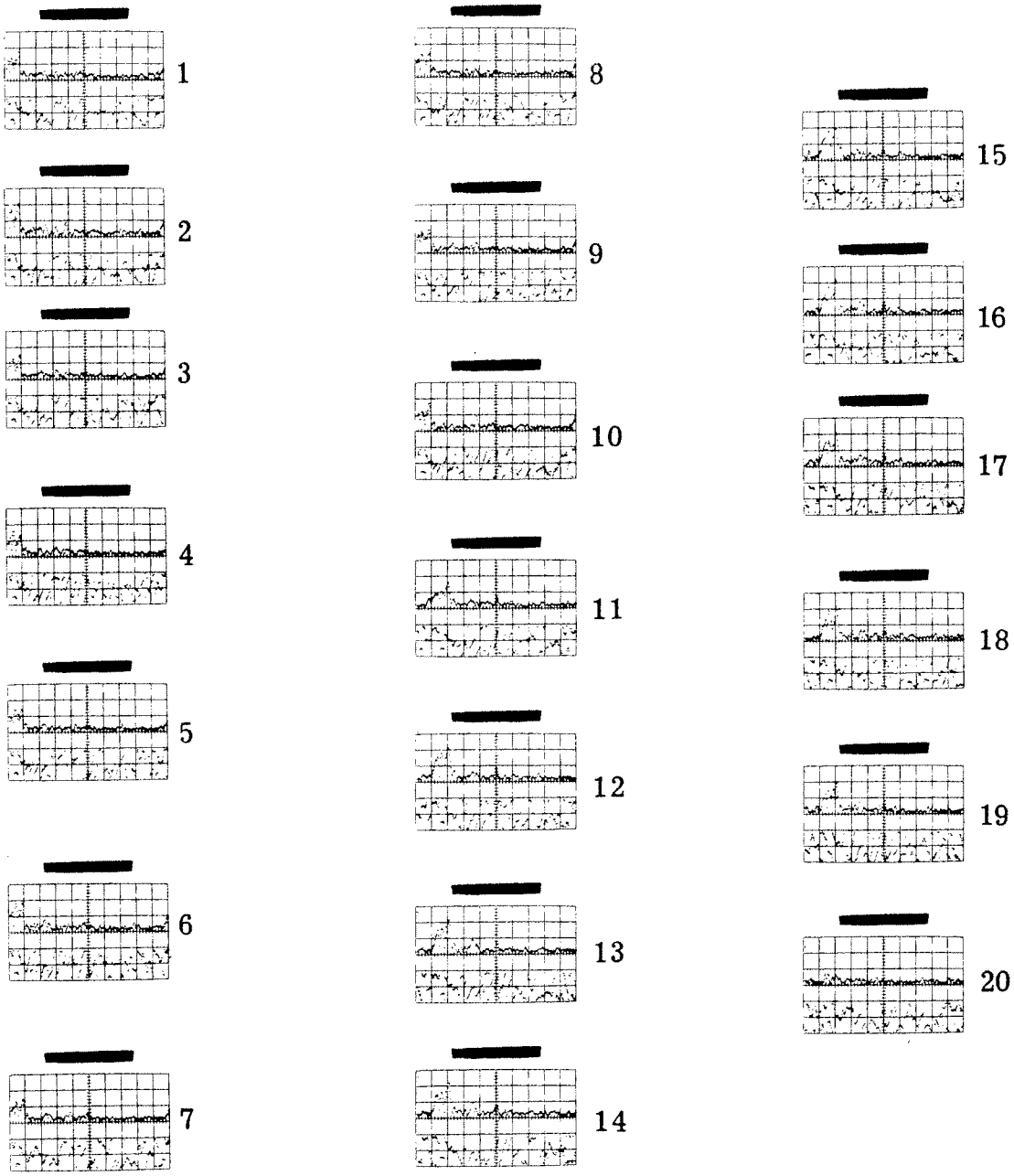

File IX. BMSEQ, 3 February 1965, 20:30-20:35 h. reception shallow. R = 1V/cm, att = 7 db, RS = 10

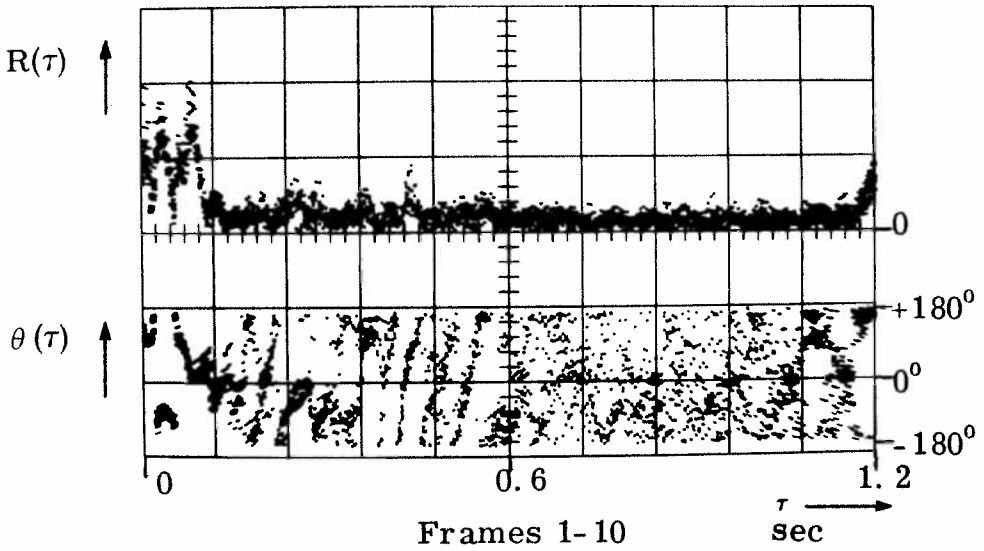

Frames 1-10

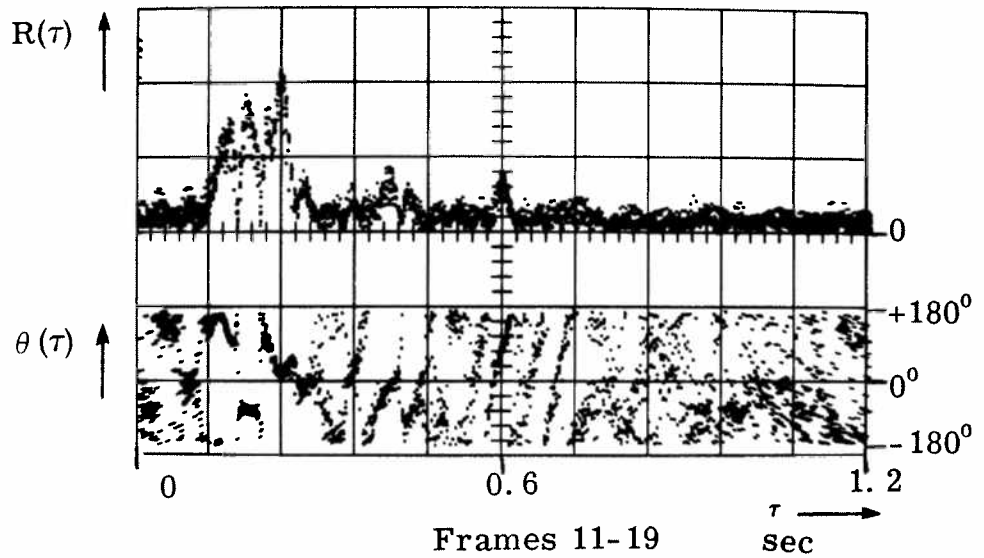

Frames 11-19

File IX

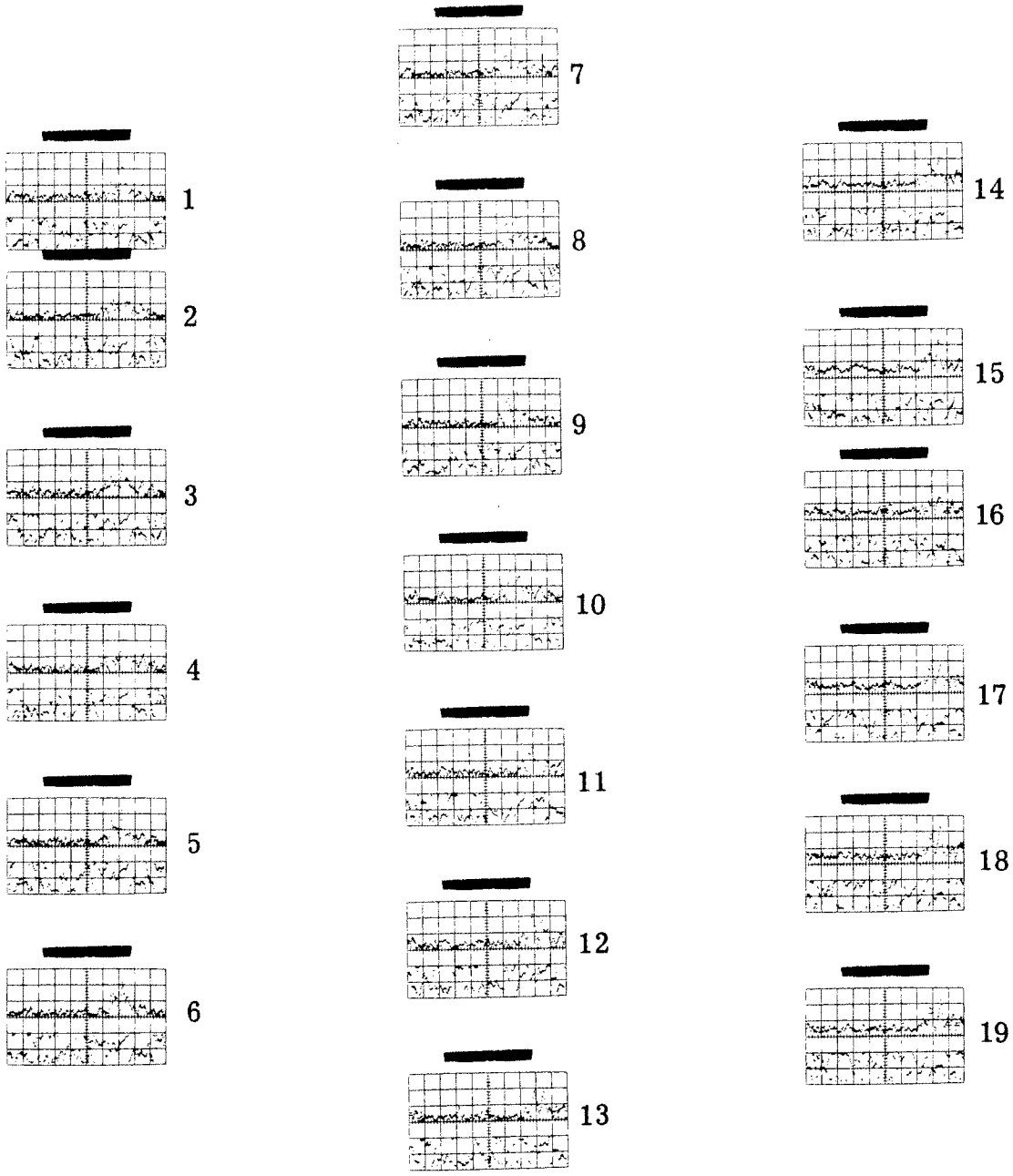

File X. BMSEQ, 3 February 1965, 21:00-21:05 h. reception deep. R = 0.5 V/cm, att = 0 db, RS = 10.

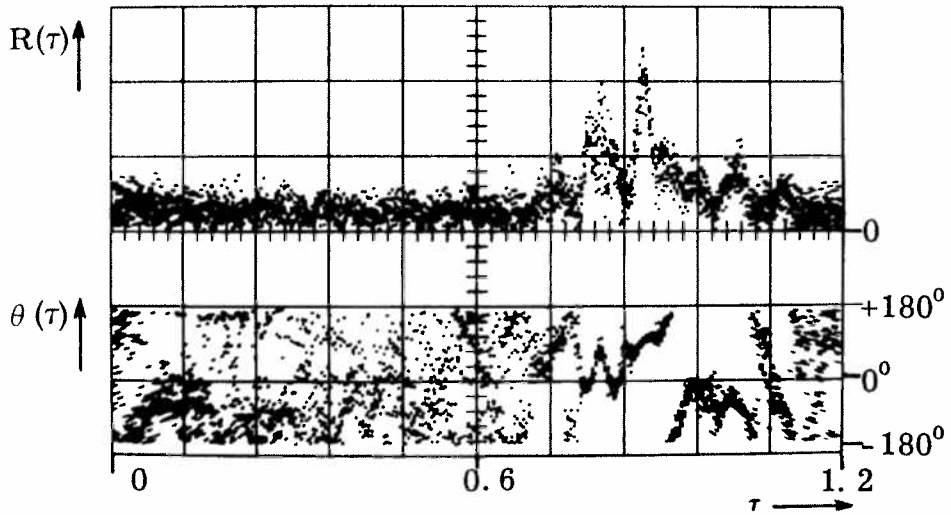

Frames 1-10

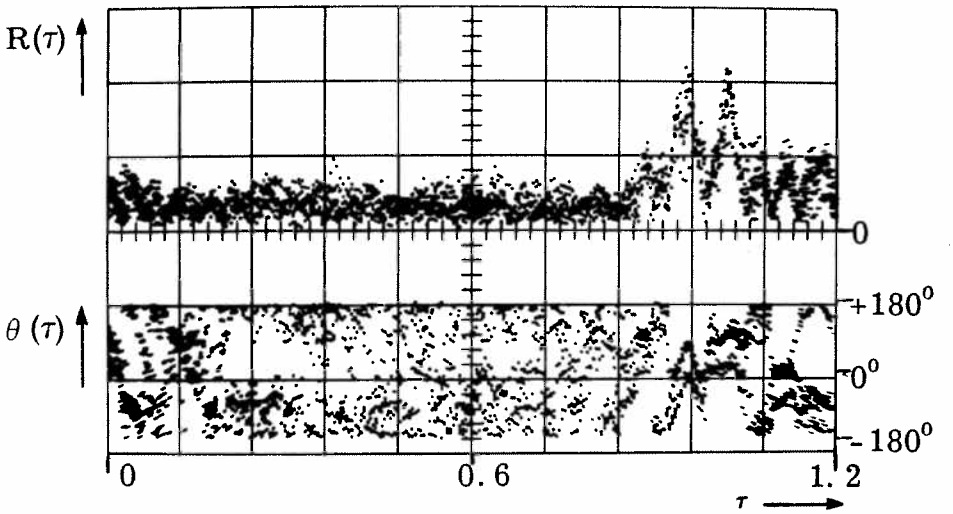

Frames 11-19

File X

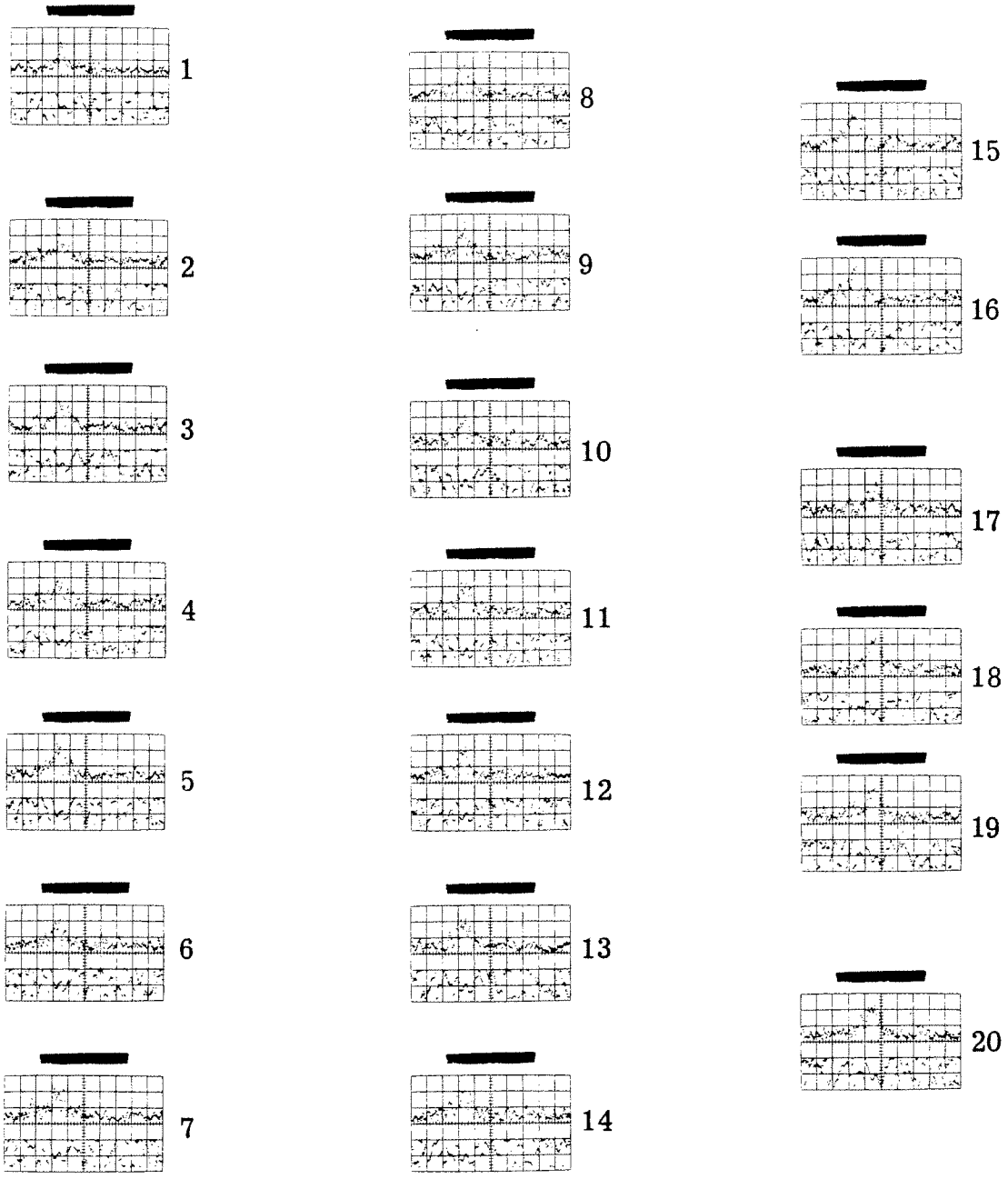

File XI. BMSEQ, 4 February 1965, 10:00-10:05 h. reception deep. R = 0.5 V/cm, att = 0 db, RS = 10.

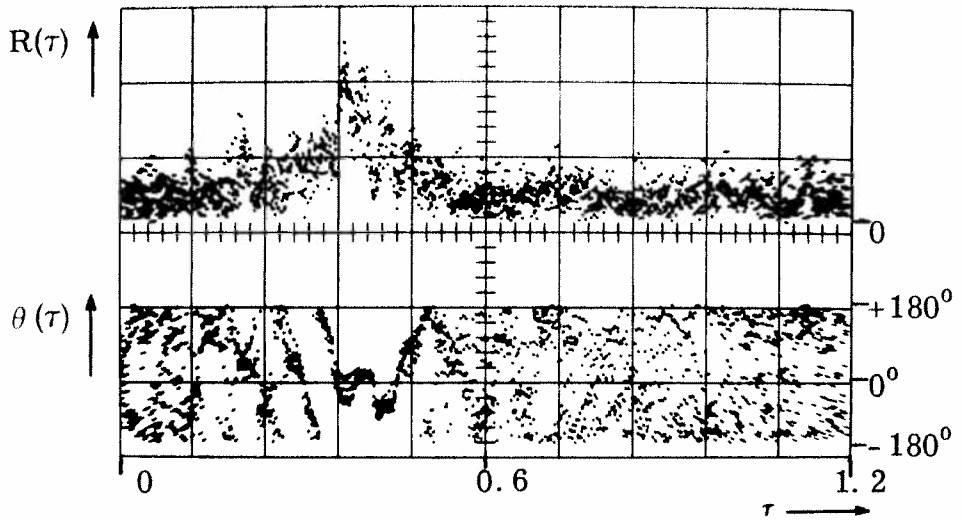

Frames 1-8

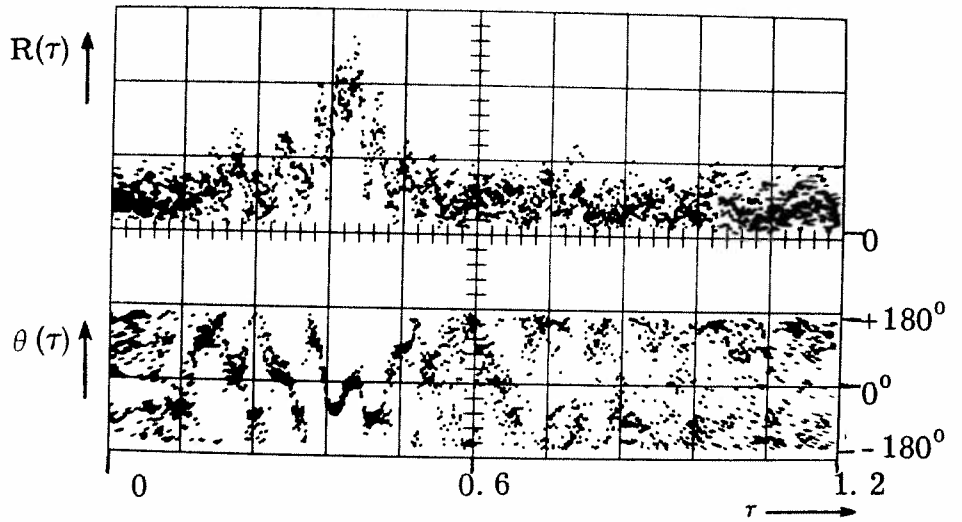

Frames 9-16

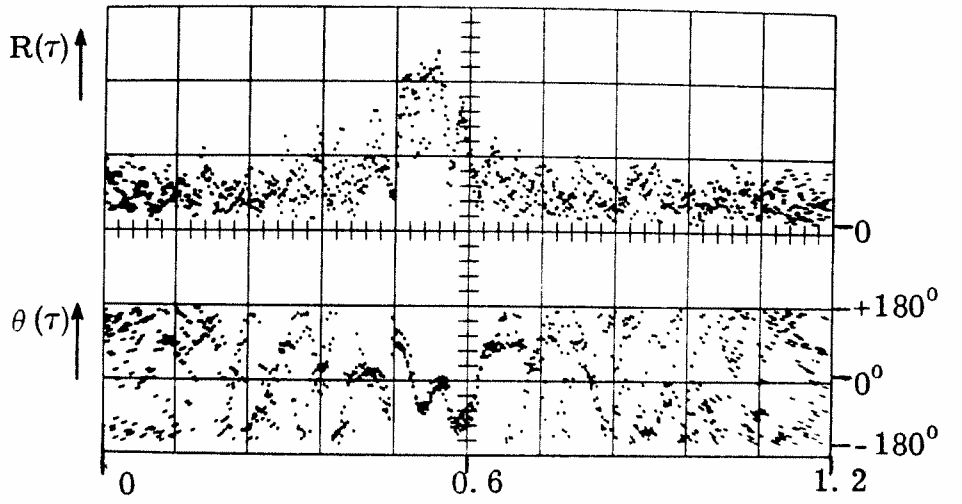

Frames 17-20

File XI

APPENDIX B

CW Analysis Results

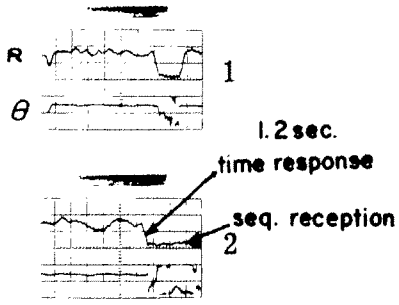

I. 15:45 h.

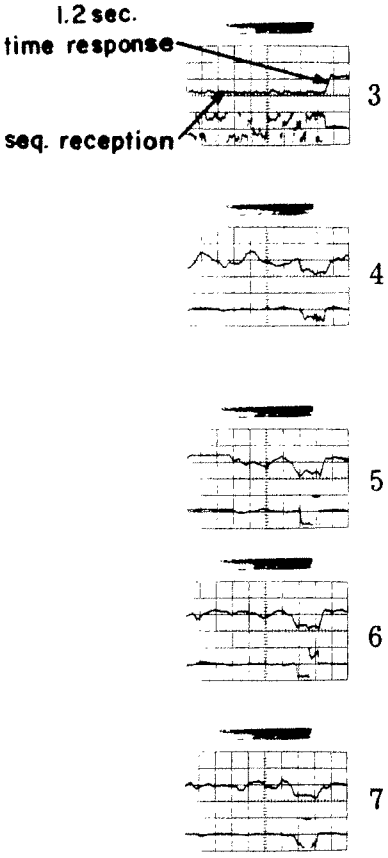

I. 15:50 h.

R = 0.5 V/cm,
att = 4 db.

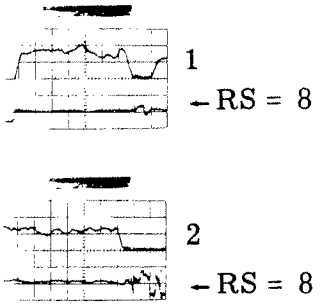

III. 17:30 h.

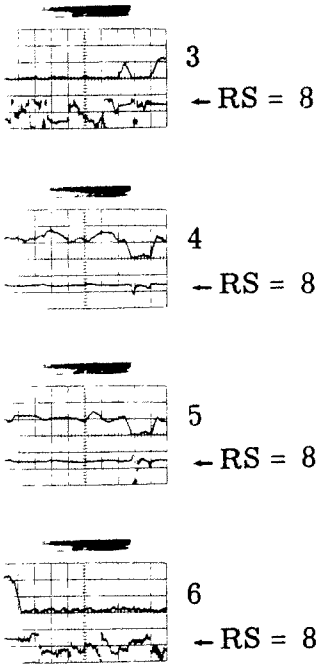

III. 17:35 h.,
IV. 18:00 h.

R = 2 V/cm,
att = 0 db.

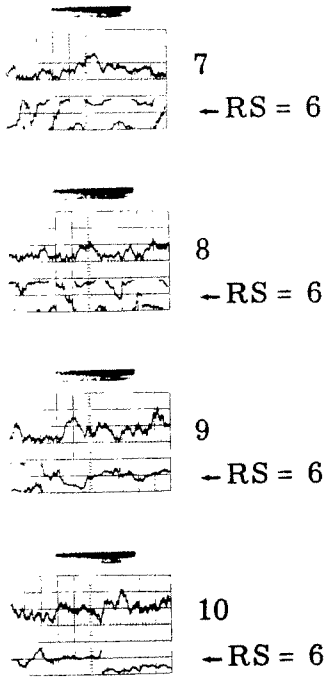

IV. 18:05 h.,
V. 18:30 h.

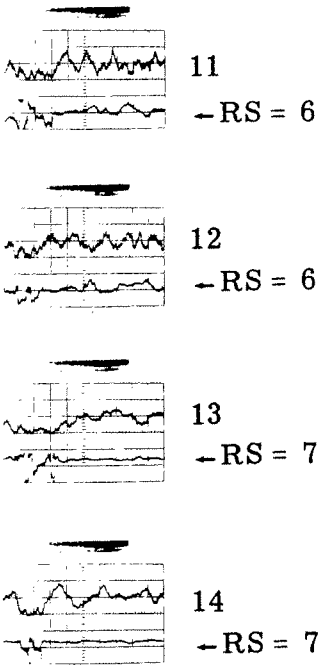

V. 18:35 h.,
VI. 19:00 h.

R = 2 V/cm,
att = 0 db.

CW 25/5, 3 February 1965, deep phone,
RS = 10 unless otherwise indicated.

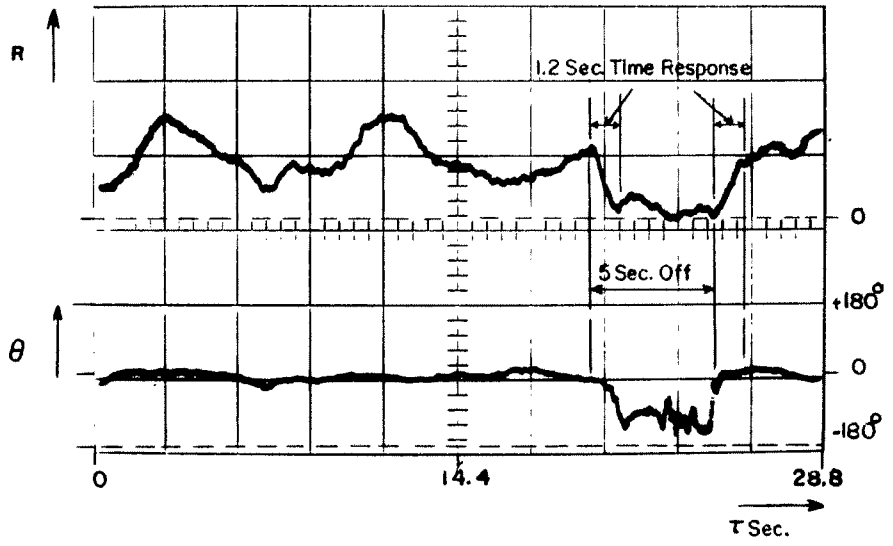

Frame 4

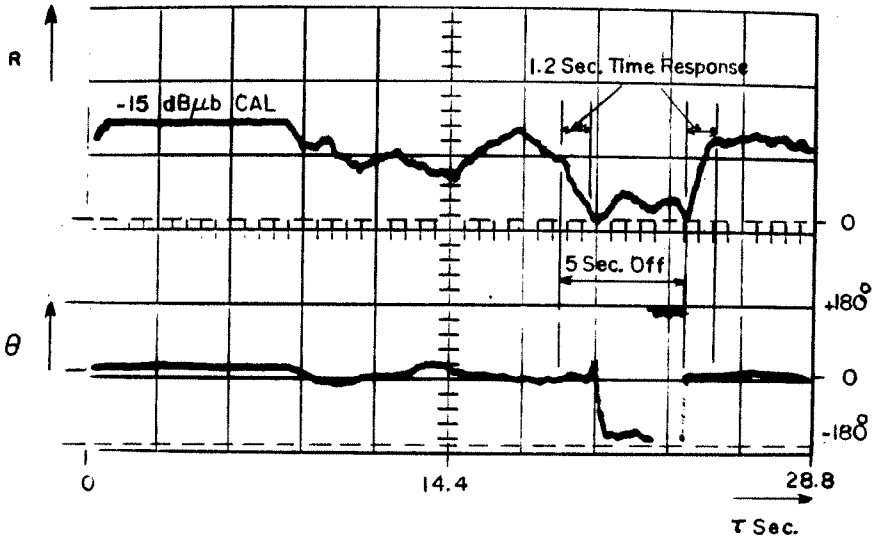

Frame 5

CW 25/5, File I

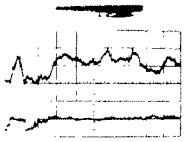

15
←RS = 7

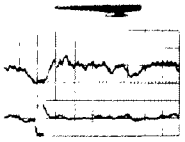

16
←RS = 7

VI. 19:05 h.,
0 db, 2 V/cm.

1

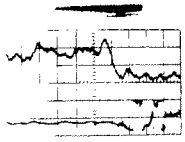

2

VII. 19:30 h.,
0 db, 0. 2 V/cm.

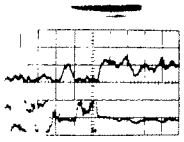

1

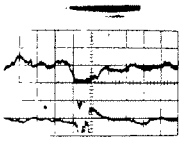

2

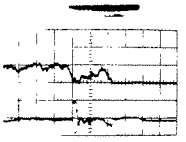

3

VIII. 20:05 h.,
0 db, 0. 2 V/cm.

3 February 1965

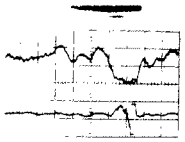

1

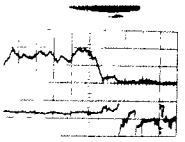

2

X. 21:00 h.,
0 db, 0. 2 V/cm.

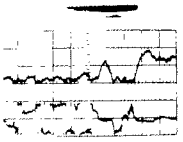

3

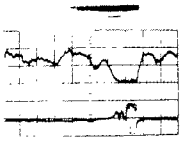

4

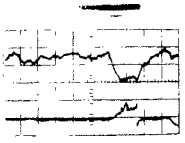

5

X. 21:05 h.,
0 db, 0. 2 V/cm.

3 February 1965

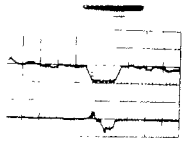

1

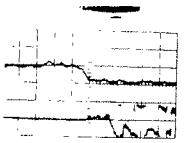

2

XI. 10:00 h.,
0 db, 0. 5 V/cm.

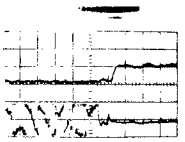

3

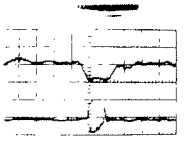

4

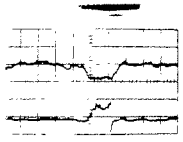

5

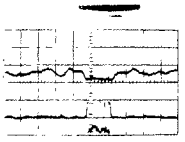

6

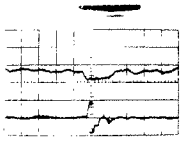

7

XI. 10:05 h.,
0 db, 0. 5 V/cm.
4 February 1965

CW 25/5, deep phone, RS = 10 unless otherwise indicated.

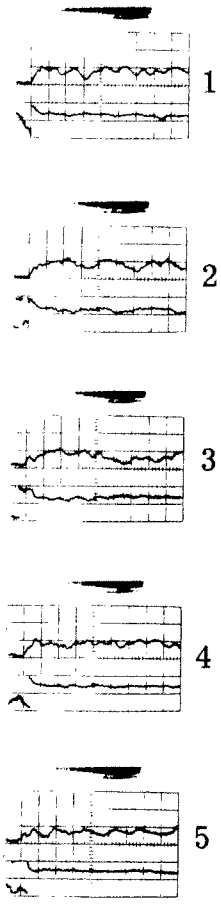

II. 15:55 h.

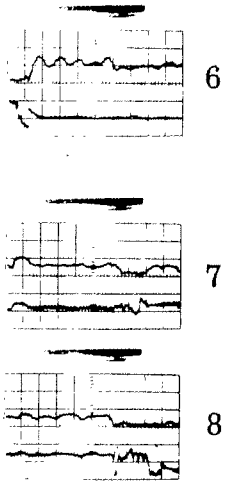

II. 15:55 h.,
IX. 20:30 h.

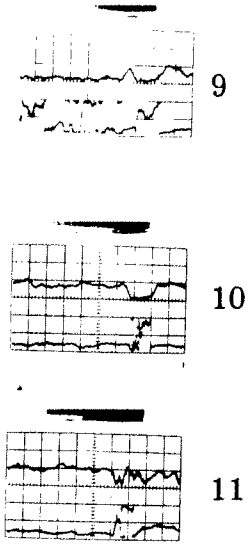

IX. 20:30 h.

CW 25/5, 3 February 1965, shallow phone, att = 7 db, RS = 10
R = 0.5 V/cm.

APPENDIX C

MIMI Sound Speed vs Depth Profiles

(From IMS Memorandum for File of 7 April, 1965: "Monthly Sound Speed Profiles").

Figure 1 shows the sound speed vs depth profiles as computed from temperature and salinity vs depth data taken on 22 February, 1963, at eight different stations along the $25^{o}40'$ N Latitude in the Straits of Florida. The station locations are given in Fig. 2. Assuming some annual recurrence of the environmental data, these are, in relation with the MIMI experiment of 3 and 4 February 1965, the most significant profiles available at present.

On the horizontal axis are given the station identifications and their geographical locations expressed as West Longitudes. The vertical axis plots the depth in meters. The sound speeds are plotted horizontally on a linear scale as indicated separately in the graph and along each profile. The sound speed 1540 m/sec is taken as an "origin" for each profile, each "origin" coinciding with the station locations, marked by a small triangle. The two dotted lines connect points of equal sound speed for 1520 m/sec and 1500 m/sec.

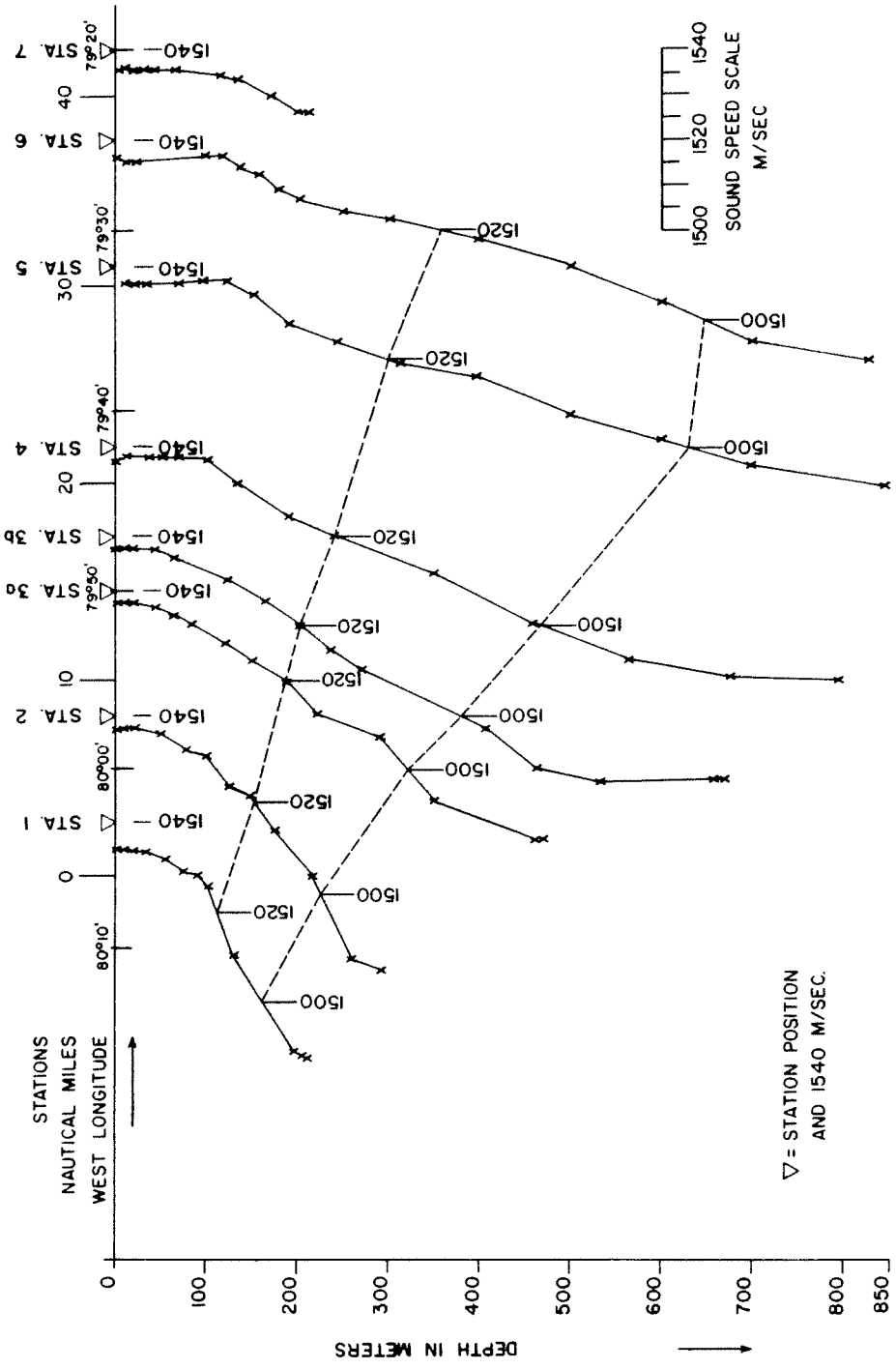

Fig. C. 1. MIMI Sound-speed depth profiles of 22 February, 1963

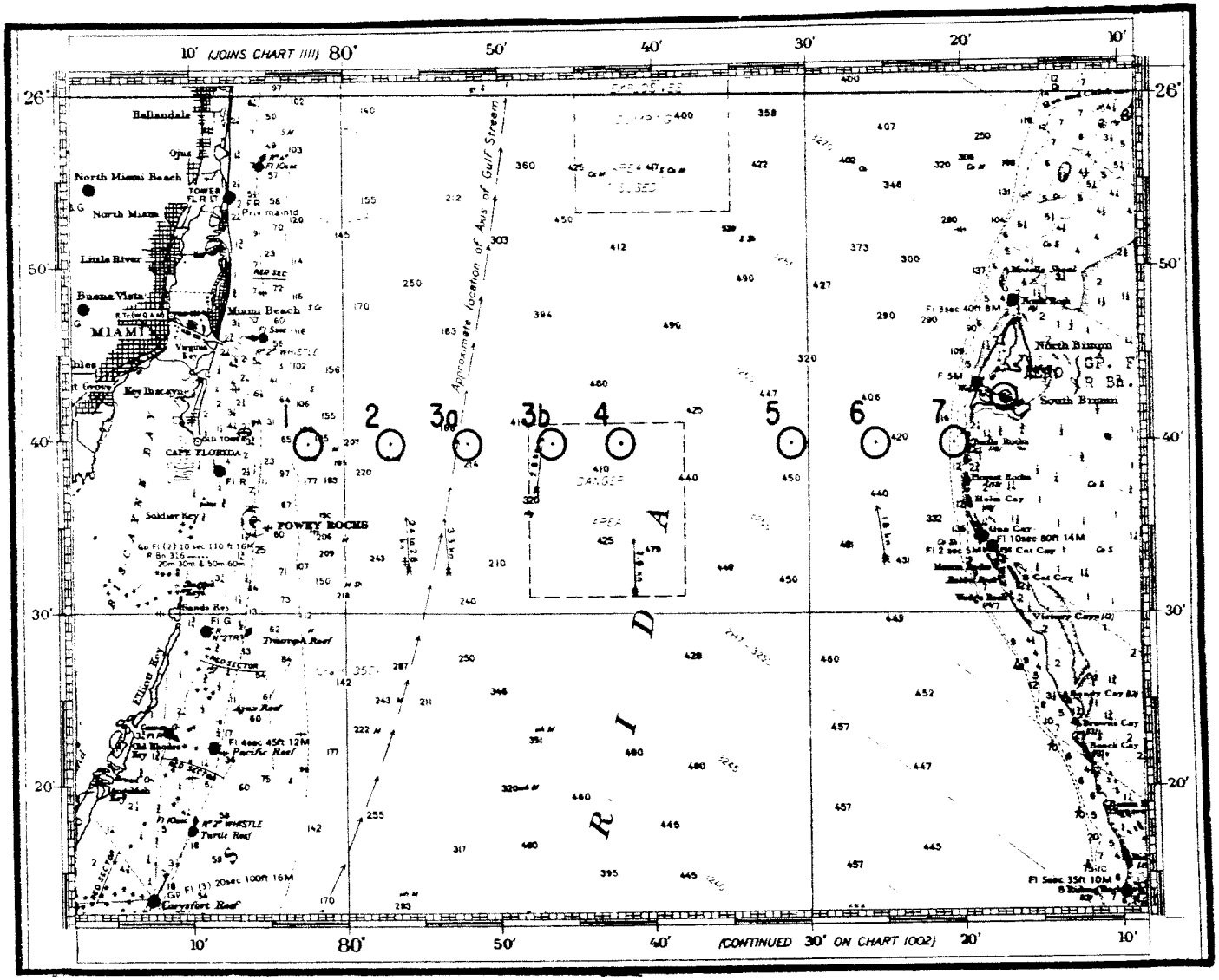

Fig. C. 2. Locations of 1962-63 Stations

REFERENCES

1. J. C. Steinberg and T. G. Birdsall, "Underwater Sound Propagation in the Straits of Florida," The Journal of the Acoustical Society of America, Vol. 39, No. 2, pp. 301-315, February 1966.

2. Proceedings of the November 1965 U. S. Navy Underwater Sound Symposium.

3. Y. W. Lee, Statistical Theory of Communication, J. Wiley and Sons, New York, London, 1964.

4. S. W. Colomb, L. D. Baumert, M. F. Easterling, J. J. Stifler, A. J. Viterbi, Digital Communications, Prentice-Hall, New Jersey, 1964.

DISTRIBUTION

	No. of Copies
Office of Naval Research (Code 468) Navy Department Washington, D. C. 20360	2
Director, Naval Research Laboratory Technical Information Division Washington, D. C. 20360	6
Director Office of Naval Research Branch Office 1030 East Green Street Pasadena California 91101	1
Office of Naval Research San Francisco Annex 1076 Mission Street San Francisco, California 94103	1
Office of Naval Research New York Annex 207 West 24th Street New York, New York 10011	1
Director Office of Naval Research Branch Office 219 South Dearborn Street Chicago, Illinois 60604	1
Commanding Officer Office of Naval Research Branch Office Box 39 FPO New York 09510	8
Commander, Naval Ordnance Laboratory Acoustics Division White Oak, Silver Spring, Maryland 20910	1
Commanding Officer and Director Naval Electronics Laboratory San Diego, California 92152	1
Chief Scientist Navy Underwater Sound Reference Div. Post Office Box 8337 Orlando, Florida 38200	1
Defense Documentation Center Cameron Station Alexandria, Virginia	20
Commanding Officer and Director Navy Underwater Sound Laboratory Fort Trumball New London, Connecticut 06321	1
Commanding Officer Naval Air Development Center Johnsville, Warminster, Pennsylvania	1
Commanding Officer and Director David Taylor Model Basin Washington, D. C. 2007	1
Superintendent Naval Postgraduate School Monterery, California 93940 Attn: Prof. L. E. Kinsler	1
Commanding Officer Navy Mine Defense Laboratory Panama City, Florida 32402	1
Superintendent Naval Academy Annapolis, Maryland 21402	1
Commander Naval Ordnance Systems Command Code ORD-0302 Navy Department Washington, D. C. 20360	1
Commander Naval Ship Systems Command Code SHIPS-03043 Navy Department Washington, D. C. 20360	1
Commander Naval Ship Systems Command Code SHIPS-1630 Navy Department Washington, D. C. 20360	1
Commander Naval Ordnance Test Station Pasadena Annex 3203 E. Foothill Boulevard Pasadena, California 91107	1

DISTRIBUTION (Cont.)

	No. of Copies
Dr. Melvin J. Jacobson Rensselaer Polytechnic Institute Troy, New York 12181	1
Dr. Charles Stutt General Electric Company P. O. Box 1088 Schnectady, New York 12301	1
Dr. J. V. Bouyoucos General Dynamics/Electronics 1400 N. Goodman Street P. O. Box 226 Rochester, New York 14609	1
Mr. J. Bernstein EDO Corporation College Point, New York 11356	1
Dr. T. G. Birdsall Cooley Electronics Laboratory The University of Michigan Ann Arbor, Michigan 49105	1
Dr. John Steinberg Institute of Marine Science The University of Miami Miami, Florida 33149	1
Mr. William Stalford Bendix Corporation Bendix-Pacific Division North Hollywood, California 91605	1
Dr. H. S. Hayre The University of Houston Cullen Boulevard Houston, Texas 77004	1
Dr. Robert R. Brockhurst Woods Hole Oceanographic Inst. Woods Hole, Massachusetts	1
Cooley Electronics Laboratory The University of Michigan Ann Arbor, Michigan	50
Director Office of Naval Research Branch Office 495 Summer Street Boston, Massachusetts 02210	1
Dr. Stephen Wolff Johns Hopkins University Baltimore, Maryland 21218	1
Dr. M. A. Basin Litton Industries 8000 Woodley Avenue Van Nuys, California 91409	1
Dr. Albert Nuttall Litton Systems, Inc. 335 Bear Hill Road Waltham, Massachusetts 02154	1
Dr. Philip Stocklin Box 360 Raytheon Company Newport, Rhode Island 02841	1
Dr. H. W. Marsh Raytheon Company P. O. Box 128 New London, Connecticut 06321	1
Mr. Ken Preston Perkin-Elmer Corporation Electro-Optical Division Norwalk, Connecticut 06852	1
Mr. Tom Barnard Texas Instruments Incorporated 100 Exchange Park North Dallas, Texas 75222	1
Mr. John Swets Bolt, Beranek and Newman 50 Moulton Street Cambridge 38, Massachusetts	1
Mr. F. Briggson Office of Naval Research Representative 121 Cooley Building The University of Michigan Ann Arbor, Michigan	1

UNCLASSIFIED
Security Classification

DOCUMENT CONTROL DATA - R&D
(Security classification of title, body of abstract and indexing annotation must be entered when the overall report is classified)

1. ORIGINATING ACTIVITY *(Corporate author)*
Cooley Electronics Laboratory
The University of Michigan
Ann Arbor, Michigan

2a. REPORT SECURITY CLASSIFICATION
UNCLASSIFIED

2b GROUP

3. REPORT TITLE
Underwater Sound Propagation in the Straits of Florida:
The Mimi Experiment of 3 and 4 February 1965

4. DESCRIPTIVE NOTES *(Type of report and inclusive dates)*
Technical Report No. 183-3674-12-T

5. AUTHOR(S) *(Last name, first name, initial)*
Unger, Rudolf
Veenkant, Raymond

6. REPORT DATE	7a. TOTAL NO. OF PAGES	7b. NO. OF REFS
May 1967	92	4

8a. CONTRACT OR GRANT NO.	9a. ORIGINATOR'S REPORT NUMBER(S)
Nonr-1224 (36)	3674-12-T
b. PROJECT NO.	
c.	9b. OTHER REPORT NO(S) *(Any other numbers that may be assigned this report)*
d.	TR 183

10. AVAILABILITY/LIMITATION NOTICES

11. SUPPLEMENTARY NOTES

12. SPONSORING MILITARY ACTIVITY
Office of Naval Research
Acoustic Branch, Code 468
Washington, D.C. 20360

13. ABSTRACT

An experiment was conducted on 3 and 4 February 1965 as a part of the study of underwater sound propagation in the Straits of Florida, called Project MIMI. A special pseudo-random modulation of a 420 Hz carrier was used to probe one-way multipath propagation. The non-modulated carrier was used for continuous-wave analysis. This report describes the experiments and the data processing, and presents the results of these analyses in photographical form.

DD FORM 1 JAN 64 1473

UNCLASSIFIED
Security Classification

14 KEY WORDS	LINK A		LINK B		LINK C	
	ROLE	WT	ROLE	WT	ROLE	WT

INSTRUCTIONS

1. ORIGINATING ACTIVITY: Enter the name and address of the contractor, subcontractor, grantee, Department of Defense activity or other organization *(corporate author)* issuing the report.

2*a*. REPORT SECURITY CLASSIFICATION: Enter the overall security classification of the report. Indicate whether "Restricted Data" is included. Marking is to be in accordance with appropriate security regulations.

2*b*. GROUP: Automatic downgrading is specified in DoD Directive 5200.10 and Armed Forces Industrial Manual. Enter the group number. Also, when applicable, show that optional markings have been used for Group 3 and Group 4 as authorized.

3. REPORT TITLE: Enter the complete report title in all capital letters. Titles in all cases should be unclassified. If a meaningful title cannot be selected without classification, show title classification in all capitals in parenthesis immediately following the title.

4. DESCRIPTIVE NOTES: If appropriate, enter the type of report, e.g., interim, progress, summary, annual, or final. Give the inclusive dates when a specific reporting period is covered.

5. AUTHOR(S): Enter the name(s) of author(s) as shown on or in the report. Enter last name, first name, middle initial. If military, show rank and branch of service. The name of the principal author is an absolute minimum requirement.

6. REPORT DATE: Enter the date of the report as day, month, year; or month, year. If more than one date appears on the report, use date of publication.

7*a*. TOTAL NUMBER OF PAGES: The total page count should follow normal pagination procedures, i.e., enter the number of pages containing information.

7*b*. NUMBER OF REFERENCES: Enter the total number of references cited in the report.

8*a*. CONTRACT OR GRANT NUMBER: If appropriate, enter the applicable number of the contract or grant under which the report was written.

8*b*, 8*c*, & 8*d*. PROJECT NUMBER: Enter the appropriate military department identification, such as project number, subproject number, system numbers, task number, etc.

9*a*. ORIGINATOR'S REPORT NUMBER(S): Enter the official report number by which the document will be identified and controlled by the originating activity. This number must be unique to this report.

9*b*. OTHER REPORT NUMBER(S): If the report has been assigned any other report numbers *(either by the originator or by the sponsor)*, also enter this number(s).

10. AVAILABILITY/LIMITATION NOTICES: Enter any limitations on further dissemination of the report, other than those imposed by security classification, using standard statements such as:

(1) "Qualified requesters may obtain copies of this report from DDC."

(2) "Foreign announcement and dissemination of this report by DDC is not authorized."

(3) "U. S. Government agencies may obtain copies of this report directly from DDC. Other qualified DDC users shall request through _____."

(4) "U. S. military agencies may obtain copies of this report directly from DDC. Other qualified users shall request through _____."

(5) "All distribution of this report is controlled. Qualified DDC users shall request through _____."

If the report has been furnished to the Office of Technical Services, Department of Commerce, for sale to the public, indicate this fact and enter the price, if known.

11. SUPPLEMENTARY NOTES: Use for additional explanatory notes.

12. SPONSORING MILITARY ACTIVITY: Enter the name of the departmental project office or laboratory sponsoring *(paying for)* the research and development. Include address.

13. ABSTRACT: Enter an abstract giving a brief and factual summary of the document indicative of the report, even though it may also appear elsewhere in the body of the technical report. If additional space is required, a continuation sheet shall be attached.

It is highly desirable that the abstract of classified reports be unclassified. Each paragraph of the abstract shall end with an indication of the military security classification of the information in the paragraph, represented as *(TS)*, *(S)*, *(C)*, or *(U)*

There is no limitation on the length of the abstract. However, the suggested length is from 150 to 225 words.

14. KEY WORDS: Key words are technically meaningful terms or short phrases that characterize a report and may be used as index entries for cataloging the report. Key words must be selected so that no security classification is required. Identifiers, such as equipment model designation, trade name, military project code name, geographic location, may be used as key words but will be followed by an indication of technical context. The assignment of links, rules, and weights is optional.